

Friedrich-Schiller-Universität Jena  
Physikalisch-Astronomische Fakultät  
Theoretisch-Physikalisches Institut



---

seit 1558

# Impact of higher dimensional operators on lower Higgs mass bounds in a Higgs-Yukawa system

Masterarbeit

zur Erlangung des  
akademischen Grades eines  
Master of Science (M.Sc.) im Studiengang Physik

vorgelegt von  
Matthias Warschinke  
geboren am 28. Mai 1991 in Weimar

1. Gutachter: Prof. Dr. Holger Gies (Friedrich-Schiller-Universität Jena)
2. Gutachter: Dr. Luca Zambelli (Friedrich-Schiller-Universität Jena)

*eingereicht am 01.10.2015*

This is an updated version of the original thesis. The essential content however has not been modified. If the reader finds any sort of mistakes I would appreciate sending an eMail to `matthias.warschinke@uni-jena.de`.

## Abstract

In this thesis we consider a Higgs-Yukawa system consisting of a self-interacting scalar field (Higgs field) that couples to a fermion (top quark) through a Yukawa interaction term. We study this system in the framework of the functional renormalization group and we use the Wetterich equation in order to describe its flow. The main goal is to directly derive Higgs mass bounds from the flow of this system. The non-perturbative nature of the Wetterich equation allows us to test a wide range of bare parameters and to investigate mechanisms that could decrease the Higgs mass bound. We confirm the results of [13], [14], [11] where it was shown that lower (and upper) Higgs mass bounds arise as a result from the flow of the effective potential itself, without any additional assumptions. We also confirm the fact that by taking deviations from the in perturbation theory commonly used  $\varphi^4$ -type UV potential into account, the Higgs mass can be further decreased. Similar to this investigation we consider a generalized Yukawa coupling  $H(\varphi)\bar{\psi}\psi$  in order to test the influence of the higher Yukawa interactions  $\mathfrak{h}_j\varphi^{2j+1}\bar{\psi}\psi$  ( $j > 0$ ) on the Higgs mass. We find that it is indeed possible to generate flows that result in even smaller Higgs masses. In the last chapter we extend the toy model by including the strong sector in order to describe the flow of the Yukawa interaction more accurately and we derive the corresponding new flow equations.

# Contents

<b>1</b>	<b>Introduction</b>	<b>7</b>
<b>2</b>	<b>Theoretical foundations</b>	<b>10</b>
2.1	Quantum Field Theory . . . . .	10
2.2	Renormalization and Functional Renormalization Group . . . . .	13
2.2.1	Wilsonian approach . . . . .	13
2.2.2	Some further notation . . . . .	14
2.2.3	The Wetterich equation . . . . .	17
2.3	Spontaneous symmetry breaking . . . . .	23
<b>3</b>	<b>Our toy model</b>	<b>26</b>
<b>4</b>	<b>Flow equations</b>	<b>30</b>
4.1	The fluctuation matrix . . . . .	30
4.2	The generalized Yukawa coupling . . . . .	32
4.3	The effective potential . . . . .	38
4.4	The anomalous dimensions . . . . .	39
<b>5</b>	<b>Numerical analysis</b>	<b>42</b>
5.1	Rewriting the flow equations . . . . .	42
5.2	Choosing the regulator functions . . . . .	43
5.3	Truncation of the effective potential and the generalized Yukawa coupling	47
5.3.1	Symmetric phase . . . . .	47
5.3.2	Spontaneously broken phase . . . . .	48
5.4	Our task . . . . .	49
5.5	Results and discussion . . . . .	50
5.5.1	A simple truncation . . . . .	50
5.5.2	Higher truncations . . . . .	54
5.5.3	Lower Higgs mass bound induced by $u_2$ . . . . .	56
5.5.4	Lower Higgs mass bound induced by $\mathfrak{h}_1$ . . . . .	58
<b>6</b>	<b>Extending the toy model</b>	<b>64</b>
6.1	Extended fluctuation matrix . . . . .	65
6.2	Extended flow equations . . . . .	68
6.2.1	Extended flow of the generalized Yukawa coupling . . . . .	68
6.2.2	Extended flow of the effective potential . . . . .	71
6.2.3	Extended flow of the anomalous dimensions . . . . .	72

<b>7 Summary and Outlook</b>	<b>77</b>
<b>Appendices</b>	<b>79</b>
<b>A Threshold functions</b>	<b>80</b>
<b>B Threshold functions for the Litim regulator</b>	<b>81</b>
<b>List of Figures</b>	<b>82</b>
<b>Bibliography</b>	<b>83</b>

# 1 Introduction

One of the biggest successes in the physics of the past century is the development of the Standard Model. It describes all so far discovered elementary particles and three of the four known fundamental interactions among them, the electromagnetic, the weak and the strong interaction. Many experiments confirmed the predictions of the Standard Model to high accuracy and also led to the discovery of many more particles. One central problem in the development of the Standard Model was to explain how the gauge bosons of the local gauge theories (or to be more precise, the gauge bosons of the weak interaction) and the fermions acquire their masses, since the introduction of corresponding mass terms violates the invariance under gauge transformations. A possible solution was proposed by Higgs, Kibble, Guralnik, Hagen, Englert and Brout in 1964 and became famous under the name Higgs mechanism ([1], [2], [3], [4]). By introducing a scalar field, the so-called Higgs field, the fermions and the gauge bosons of the weak interaction obtain their masses through spontaneous symmetry breaking within the newly introduced Higgs sector. This idea accompanies with the emergence of a new particle, the Higgs boson. It took further 50 years, until 2012, when the Higgs boson was finally verified at the LHC [5] and thus confirmed the Higgs mechanism to be an appropriate way to describe the mass generating within the Standard Model.

Despite its huge success, the Standard Model still exhibits some inconsistencies. First of all it does not contain the fourth fundamental interaction, the gravitation. However, at least at the Planck scale at around  $10^{19}$  GeV, the effects of gravitation become of the same order of magnitude as the other interactions and thus cannot be neglected. Furthermore, perturbative calculations hint at the existence of Landau poles of the electroweak interaction and the scalar self-interaction at finite momenta. All these are arguments for considering the Standard Model as an effective theory, emerging from a more fundamental theory. The natural question that arises now is up to which scale the Standard Model is valid. At best, the Standard Model is valid up to the Planck scale, but there is a possibility that new physics already appears at scales much closer to the IR. One way to approach this question is to investigate the scalar effective potential, deriving mass bounds for the Higgs boson. It turns out that the lower mass bound depends on the chosen cut-off, i.e. the scale up to which one assumes the theory to be valid. As soon as the measured Higgs mass falls below the derived lower Higgs mass bound, the theory is no longer valid at the corresponding cut-off.

The first approach to deriving lower Higgs mass bounds was by assuming that the effective potential might become unstable.

---

It was commonly believed that the one-loop contributions from the Higgs boson and the top quark destabilize the effective potential in the sense that if the top Yukawa coupling is much stronger than the  $\varphi^4$ -coupling of the Higgs field, the effective potential might no longer be bounded from below for large Higgs amplitudes. In other words, if the Higgs mass is too small compared to the top quark mass, the effective potential has no longer an absolute minimum. The Higgs mass bounds then were obtained by demanding the potential to be at least meta-stable, imposing that the (unstable) vacuum is sufficiently long-lived, with a lifetime comparable to the age of the universe. This way, by perturbative calculations, stability criteria were derived and thus corresponding lower Higgs mass bounds that were connected to the mass of the top quark ([6], [7], [8]). However, depending on different parameters such as the mentioned top mass, the experimental value of the Higgs mass is close to or even violates these mass bounds. Therefore, this instability approach was put into question.

Correspondingly, lattice calculations [9] for example did not show any instabilities at all, in [10] it was even shown that for a simplified model, the Higgs-Yukawa model, the instabilities of the effective potential only occur when the renormalized perturbation theory results are extended to areas where the approximation is no longer valid. Hence, new investigations of Higgs mass bounds are desirable.

In this thesis we will consider the Higgs-Yukawa model<sup>1</sup>. For different bare couplings at a given cut-off  $\Lambda$  we will compute the resulting Higgs masses, trying to find the combinations which yield the lowest mass. At first sight, this seems to contradict the common viewpoint that IR observables should be independent of details of the UV theory. However, the Higgs mass bound should not be regarded as a pure IR quantity. Usually it is expressed in terms of the UV cut-off  $\Lambda$ . If we want to investigate this dependence, we necessarily have to make some statements about the theory near the cut-off, for example concerning the UV regularization. Hence, the scheme-dependence of the Higgs mass bound becomes to some extent physical [11]. In the course of our analysis we also have to cover the case of large bare couplings and thus we face a non-perturbative problem. Accordingly, the framework of the functional renormalization group (FRG) delivers appropriate tools. We will calculate the flow of the appearing couplings according to an exact FRG equation, the Wetterich equation [12], and test the influence of different UV bare actions on the Higgs mass bound. Similar investigations already have been done in [13], [14]. In [13] it was shown that by allowing arbitrary bare couplings but demanding to reproduce the correct IR physics<sup>2</sup>, the RG flow restricts the possible Higgs masses to a finite window, providing us with upper and lower bounds for it, without any additional restrictions or instability assumptions. In [14] these investigations have been extended by considering deviations from the in perturbative calculations usually used quartic scalar potential. The author showed that in this case the lower Higgs mass bound could be further decreased. The main purpose of this thesis is to further extend the toy model by taking additional operators into account, namely a generalized Yukawa interaction of the form  $H(\varphi)\bar{\psi}\psi$  instead of  $h\varphi\bar{\psi}\psi$ .

---

<sup>1</sup>Why this is an appropriate simplification of the Standard Model will be discussed in chapter 3.

<sup>2</sup>That is to reproduce the correct vacuum expectation value of the Higgs field and the top mass.

---

In chapter 2 we recall some basic results of quantum field theory (QFT). Beside a general introduction we will explain the Wilsonian approach to the FRG and present the important steps of the derivation of the Wetterich equation, which will be the starting point for all of our calculations. Finally we give a short introduction to the Higgs mechanism. The content of this chapter is mostly standard text book knowledge.

Chapter 3 deals with the question why for our purposes the simple Higgs-Yukawa model is an appropriate simplification of the Standard Model. This discussion has already been held in e.g. [13], we will recall the important steps.

In chapter 4 we will derive the necessary flow equations of the effective potential, the generalized Yukawa coupling  $H(\varphi)$  and the anomalous dimensions of the fields.

The approximate solution of the corresponding set of equations will be performed in chapter 5. First they are rewritten in renormalized and dimensionless quantities and afterwards we apply some further approximations. The simplified equations are solved numerically with *Wolfram Mathematica*. Subsequently, we briefly discuss the results.

The last chapter is dedicated to a last extension of the toy model. We will take the  $SU(N_C)$  gauge symmetry of the Standard Model into account, because the strong coupling  $g_3$  has a significant impact on the top Yukawa coupling, as we will see in chapter 3. Hence, after introducing a Yang-Mills term as well as corresponding gauge fixing and ghost terms, we will derive the new flow equations of the quantities mentioned above.

We end with a summary and an outlook to possible future investigations.

## 2 Theoretical foundations

The content of this chapter is standard textbook knowledge and thus inspired by for example [15], [16], [17] or by reviews such as [18].

### 2.1 Quantum Field Theory

In QFT, all important physical quantities like cross sections can be calculated by so-called  $n$ -point Green's functions, where  $n$  denotes the number of involved particles or fields. Formally, these functions are defined as the vacuum expectation value of the time ordered product of these fields in the Heisenberg picture. In the path integral formalism, this expectation value is equivalent to integrating over all possible field configurations, weighted by the classical action,

$$\langle \varphi(x_1) \cdots \varphi(x_n) \rangle \equiv \langle \Omega | T(\hat{\varphi}(x_1) \cdots \hat{\varphi}(x_n)) | \Omega \rangle = \mathcal{N} \int \mathcal{D}\varphi \varphi(x_1) \cdots \varphi(x_n) e^{iS[\varphi]}. \quad (2.1.1)$$

Note that we have operators on the left hand side, but usual functions in the integrand of the path integral. The normalization constant  $\mathcal{N}$  is fixed by the condition  $\langle \mathbb{1} \rangle = 1$ . The path integral measure can be considered as

$$\int \mathcal{D}\varphi = \prod_{\substack{\vec{x} \in \mathbb{R}^{d-1}, \\ t \in (-\infty, \infty)}} d\varphi(\vec{x}, t). \quad (2.1.2)$$

To make the exponent in equation (2.1.1) real, we perform a so-called Wick rotation. By transforming  $x_0 \mapsto -ix_0$  and  $\vec{x} \mapsto \vec{x}$ , we effectively change over to the Euclidean metric, changing the exponent from  $iS[\varphi]$  to  $-S[\varphi]$ . Consequently, the Clifford Algebra reads  $\{\gamma_\mu, \gamma_\nu\} = 2\delta_{\mu\nu}$ .

Now the Green's functions can be calculated with the help of the generating functional  $Z[J]$ , given by

$$Z[J] = \int \mathcal{D}\varphi e^{-S + \int_x J\varphi}, \quad (2.1.3)$$

where we have used the short hand notation  $\int_x J\varphi = \int d^d x J(x)\varphi(x)$ .

Then we obtain the n-point functions just by taking the derivative of  $Z[J]$  with respect to the source  $J$ ,

$$\langle \varphi(x_1) \cdots \varphi(x_n) \rangle = \frac{1}{Z[0]} \frac{\delta^n}{\delta J(x_1) \cdots \delta J(x_n)} Z[J] \Big|_{J=0}. \quad (2.1.4)$$

However, there are more effective ways to store the physics than using the generating functional  $Z$ , since it also produces unconnected terms like  $\langle \varphi(x_1) \rangle \cdots \langle \varphi(x_n) \rangle$ , which do not contain any new physical information. Therefore, we consider the Schwinger functional  $W[J] = \log Z[J]$ . Now the derivatives only yield the connected terms,

$$\langle \varphi(x_1) \cdots \varphi(x_n) \rangle_{conn} = \frac{\delta^n}{\delta J(x_1) \cdots \delta J(x_n)} W[J] \Big|_{J=0}. \quad (2.1.5)$$

To see how this works, let us consider the simple case of 2-point functions:

$$\begin{aligned} \frac{\delta^2 W[J]}{\delta J(x_1) \delta J(x_2)} \Big|_{J=0} &= \left( \frac{\delta}{\delta J(x_1)} \left( \frac{1}{Z[J]} \int \mathcal{D}\varphi \varphi(x_2) e^{-S + \int_x J\varphi} \right) \right) \Big|_{J=0} \\ &= \left( \frac{1}{Z[J]} \int \mathcal{D}\varphi \varphi(x_1) \varphi(x_2) e^{-S + \int_x J\varphi} \right) \Big|_{J=0} \\ &\quad - \left( \frac{1}{Z[J]} \int \mathcal{D}\varphi \varphi(x_2) e^{-S + \int_x J\varphi} \frac{1}{Z[J]} \int \mathcal{D}\varphi \varphi(x_1) e^{-S + \int_x J\varphi} \right) \Big|_{J=0} \\ &= \langle \varphi(x_1) \varphi(x_2) \rangle - \langle \varphi(x_1) \rangle \langle \varphi(x_2) \rangle \\ &= \langle \varphi(x_1) \varphi(x_2) \rangle_{conn}. \end{aligned}$$

Similar calculations for all  $n \geq 2$  can be obtained.

If we are able to explicitly calculate  $Z[J]$  or  $W[J]$ , we can regard our theory as solved, because then we have access to all Green's functions and therefore, as mentioned above, to all other physical quantities.

But still, the Schwinger functional is not the most elegant way to store our information of the theory. This would be the effective action  $\Gamma$ . First, we introduce the classical field  $\phi(x)$  as the (connected) vacuum expectation value of the field operator  $\hat{\varphi}(x)$  in the presence of a source  $J$ , hence

$$\phi(x) := \langle \varphi(x) \rangle_{conn}^J = \frac{\delta W[J]}{\delta J(x)}. \quad (2.1.6)$$

The effective action is then defined as the Legendre transformed function of the Schwinger functional with respect to the variables  $J$  and  $\phi$ ,

$$\Gamma[\phi] = \sup_J \left\{ -W[J] + \int_x J\phi \right\}. \quad (2.1.7)$$

We will skip the supremum and just keep in mind that  $J = J_{sup}$ . Now the variation with respect to the classical field yields

$$\begin{aligned} \frac{\delta\Gamma}{\delta\phi(x)} &= - \int_y \underbrace{\frac{\delta W}{\delta J(y)}}_{\phi(y)} \frac{\delta J(y)}{\delta\phi(x)} + \int_y \phi(y) \frac{J(y)}{\phi(x)} + \int_y \delta(x-y) J(y) \\ &= J(x). \end{aligned} \quad (2.1.8)$$

Equation (2.1.8) can be viewed as the quantum equation of motion of the vacuum expectation value in presence of a source  $J$ .

It is also possible to derive an equation of the effective action. Starting from the generating functional  $Z[J]$  we obtain

$$Z[J] = \int \mathcal{D}\varphi e^{-S[\varphi] + \int_x J\varphi} = e^{W[J]} = e^{-\Gamma[\phi] + \int_x J\phi},$$

which is equivalent to

$$e^{-\Gamma[\phi]} = \int \mathcal{D}\varphi e^{-S[\varphi] + \int_x J(\varphi - \phi)}.$$

By performing a shift of the variable  $\varphi \mapsto \varphi + \phi$ , which according to equation (2.1.2) leaves the path integral measure invariant, we obtain

$$e^{-\Gamma[\phi]} = \int \mathcal{D}\varphi e^{-S[\varphi + \phi] + \int_x J\varphi} = \int \mathcal{D}\varphi e^{-S[\varphi + \phi] + \int_x \frac{\delta\Gamma}{\delta\phi}\varphi}. \quad (2.1.9)$$

Equation (2.1.9) represents a functional diffeo-integral equation for  $\Gamma$ , which is hard to solve. The common perturbative approach is to expand the action  $S$  in the exponent of the integrand, yielding a Gaussian integral.

$$\begin{aligned} S[\varphi + \phi] &= S[\phi] + \int_x \frac{\delta S}{\delta\varphi(x)} \varphi(x) + \frac{1}{2} \int_x \int_y \frac{\delta^2 S}{\delta\varphi(x)\delta\varphi(y)} \varphi(x)\varphi(y) + \mathcal{O}(\varphi^3) \\ &\equiv S + S^{(1)}\varphi + \frac{1}{2}S^{(2)}\varphi\varphi + \mathcal{O}(\varphi^3). \end{aligned}$$

If we only consider the 1-loop approximation, we can neglect the term  $\left(\frac{\delta\Gamma}{\delta\phi} - \frac{\delta S}{\delta\varphi}\right)\varphi$  as well and find

$$e^{-\Gamma[\phi]} = e^{-S[\phi]} \int \mathcal{D}\varphi e^{-\frac{1}{2}S^{(2)}\varphi\varphi}.$$

Now we can solve the Gaussian type integral, take the logarithm and after applying the identity  $\log \det^{-\frac{1}{2}} = -\frac{1}{2} \text{Tr} \log$  we finally get

$$\Gamma[\phi] = S[\phi] + \frac{1}{2} \text{Tr} \log S^{(2)}. \quad (2.1.10)$$

However, in this thesis we will take a different approach, namely by applying the ideas of the renormalization group (RG) to QFT.

## 2.2 Renormalization and Functional Renormalization Group

### 2.2.1 Wilsonian approach

Whenever one starts to calculate the n-point Green's functions of a given theory, one will recognize that divergences can appear. The reason are high-energy quantum fluctuations, i.e. fluctuations on high momentum scales. Therefore, we have to use a technique called regularization to get rid of these infinities. A simple way to do so is to introduce a UV cut-off  $\Lambda$ , which restricts us only to fluctuations with  $|p| \leq \Lambda$ . At this point we see another reason why it was important to perform the Wick rotation. In Minkowski space, the condition above would also hold for momenta with both large timelike and large spacelike components. In the Euclidean space however,  $|p| \leq \Lambda$  really implies small components of the momentum. We denote the regularization by writing the path integral measure as follows:

$$\int_{\Lambda} \mathcal{D}\varphi = \int \prod_{|p| \leq \Lambda} d\varphi(p).$$

Of course, our divergences are now encoded in the parameter  $\Lambda$ . Taking the limit  $\Lambda \rightarrow \infty$ , they will appear again. In order to avoid this phenomenon one has to apply the technique of renormalization. The goal is to introduce new parameters in such a way that the results become independent of  $\Lambda$  and hence remain finite when sending  $\Lambda$  to infinity again. This can be done for example by adding so-called counter terms to the original Lagrangian, which compensate the occurring divergences<sup>1</sup>.

However, we will use a different point of view. Just from the beginning we claim that our considered theory is just an effective theory in a sense that it is only valid up to the scale  $\Lambda$ . Hence, if we try to construct the corresponding effective action, fluctuations on a higher scale will not be taken into account.

Now Wilson introduced the idea to "integrate out" the fluctuations (momentum-) shell by shell, unlike in perturbation theory, where the fluctuations are treated the same way on all scales by the bare quantities [19], [20]. Let  $\delta\Lambda$  denote the thickness of such a shell and let us decompose the field as follows

$$\varphi(p) = \bar{\varphi}(p)\Theta[(\Lambda - \delta\Lambda)^2 - p^2] + \tilde{\varphi}(p)(\Theta[\Lambda^2 - p^2] - \Theta[(\Lambda - \delta\Lambda)^2 - p^2]).$$

While  $\bar{\varphi}(p)$  carries the modes with small momenta and is often referred to as soft mode,  $\tilde{\varphi}(p)$  carries the modes with larger momenta and is called hard mode.

---

<sup>1</sup>To be more accurate, the bare couplings are split into renormalized parts and counter term parts.

We can perform the shell integration, considering the regularized generating functional

$$\begin{aligned}
 Z[J] &= \int_{\Lambda} \mathcal{D}\varphi e^{-S[\varphi] + \int J\varphi} \\
 &= \int_{\Lambda - \delta\Lambda} \mathcal{D}\bar{\varphi} \int_{\Lambda - \delta\Lambda \leq |p| \leq \Lambda} \mathcal{D}\tilde{\varphi} e^{-S[\bar{\varphi} + \tilde{\varphi}] + \int J(\bar{\varphi} + \tilde{\varphi})} \\
 &=: \int_{\Lambda - \delta\Lambda} \mathcal{D}\bar{\varphi} e^{-S_{Wilson}[\bar{\varphi}] + \int J_{Wilson}\bar{\varphi}}.
 \end{aligned}$$

Here  $S_{Wilson}$  corresponds to a theory that is valid up to the scale  $\Lambda - \delta\Lambda$ , containing all the information of the high energy fluctuations of the hard modes. Therefore, the hard modes affect the dynamics of the soft modes. In general, the new couplings in  $S_{Wilson}$  will be different from those in the original action. It is even possible that the high energy fluctuations will generate completely new interactions which did not even appear before, as well as some other interactions might die out. One should think of all possible interactions to be represented by their couplings and consider these to be coordinates of an infinite dimensional coordinate system. Then each point in this coordinate system would represent a different action, i.e. a different theory. In this sense, the space spanned by the couplings could be referred to as theory space. The integration of the hard modes with  $\Lambda - \delta\Lambda \leq |p| \leq \Lambda$  (= RG transformation step) corresponds to moving from one point in theory space to another. If we let the thickness of each shell tend to be infinitely small and iteratively perform these RG steps, we generate a smooth trajectory (= flow) of the action in the theory space. An elegant mathematical equation that describes the flow of the corresponding effective action  $\Gamma$  is given by the Wetterich equation and will be derived in subsection 2.2.3.

### 2.2.2 Some further notation

Before we start with the actual derivation of the Wetterich equation let us first introduce some notation and conventions. First we define the Fourier transformation:

$$\varphi(x) = \int \frac{d^d p}{(2\pi)^d} \varphi(p) e^{ipx} \equiv \int_p \varphi(p) e^{ipx}, \quad \varphi(p) = \int d^d x \varphi(x) e^{-ipx} \equiv \int_x \varphi(x) e^{-ipx}.$$

Concerning the anti-spinors of fermionic fields be aware of the complex conjugation,

$$\bar{\psi}(x) = \int_p \bar{\psi}(p) e^{-ipx}, \quad \bar{\psi}(p) = \int_x \bar{\psi}(x) e^{ipx}.$$

By these definitions we have

$$\frac{\delta\varphi(x)}{\delta\varphi(y)} = \delta(x - y), \quad \frac{\delta\varphi(p)}{\delta\varphi(q)} = (2\pi)^d \delta(p - q) \equiv \delta_{p,q},$$

and the same rules for spinors.

No matter how many and what kind of fields the considered theory is made of, the Wetterich equation always looks the same if one combines all fields in an adept way. Since our toy model will contain one bosonic field and one fermionic field, as we will discuss in chapter 3, we will restrict ourselves to this case in the following lines. First we define a vector containing all the fields <sup>2</sup>,

$$\Phi^a(p) := \begin{pmatrix} \varphi(p) \\ \psi(p) \\ \bar{\psi}^T(-p) \end{pmatrix},$$

where  $a = 1, 2, 3$  denotes the index in the field space. For the path integral measure we use the short hand notation

$$\int \mathcal{D}\Phi \equiv \int \mathcal{D}\varphi \mathcal{D}\psi \mathcal{D}\bar{\psi}.$$

The field vector  $\Phi$  motivates the introduction of the source vector

$$J^a(p) = \begin{pmatrix} j(p) \\ \bar{\eta}^T(-p) \\ \eta(p) \end{pmatrix}.$$

One should notice that since we operate in the path integral formalism, all fermionic fields as well as the corresponding source fields are Grassmann valued fields. Therefore, their components are anti-commutating numbers, according to their spin statistics. This yields some subtleties when working with the quantities defined above. For example consider the quantity  $\Phi^T J$ , which clearly is a scalar. Therefore, we should be able to transpose it, getting the same number again:

$$\begin{aligned} (\Phi^T J)^T &= (\varphi\varphi + \psi^T \bar{\eta}^T + \bar{\psi}\eta)^T \\ &= (\varphi\varphi - \bar{\eta}\psi - \eta^T \bar{\psi}^T) \\ &\neq J^T \Phi. \end{aligned}$$

---

<sup>2</sup>The reason why we define the field this way is to write the source term in our effective action in a convenient way, as we will see later.

To obtain the expression  $J^T \Phi$ , we have to change the sign of the second and third term, i.e. the sign in the fermionic sectors. This is exactly due to spin statistics. To remind ourselves of this fact we insert a factor  $(-1)^s$ , with  $s = 0$  in bosonic sectors and  $s = 1$  in fermionic sectors. Then we can write

$$(\Phi^T J)^T = (-1)^s J^T \Phi.$$

Whenever we change the order of multiplying such objects (for example when transposing a product), we have to insert this statistic factor.

Of course we can also define linear operators, acting on the field space as well as the momentum space. Such objects carry two field indices as well as two momentum indices. The multiplication is then defined as

$$(A\Phi)^a(p) = \int_q A^{ab}(p, q) \Phi_b(q),$$

or the product of two such operators

$$(AB)^{ab}(p, q) = \int_{p'} A^{ac}(p, p') B_c^b(p', q).$$

Finally, we introduce the so-called super trace. Its definition is to take the trace over all existing types of indices. In our case this would be integrating over the continuous momentum indices, taking the sum over the field indices (where we have to consider the statistic factor as well) and finally taking the Dirac trace in the fermionic sectors, since these objects live in the  $d_\gamma$ -dimensional Dirac space<sup>3</sup>. Thus, in our specific case of one bosonic sector and two fermionic sectors we have

$$\text{STr } A = \int_p A^{11}(p, p) - \text{Tr}_\gamma (A^{22}(p, p) + A^{33}(p, p)).$$

As mentioned above, more fields can be easily included by extending the field and source vector, respectively.

After all these definitions we can now begin with the actual derivation of the Wetterich equation.

---

<sup>3</sup> $d_\gamma = 2^{\lfloor d/2 \rfloor}$  is the dimension of the Clifford-Algebra in fundamental representation in a  $d$ -dimensional space time.

### 2.2.3 The Wetterich equation

The derivation of the Wetterich equation is widely known and presented in many papers, for example in the original work of Wetterich [12] or in various reviews such as [18], [21], [22]. Inspired by these templates, we will recall the important steps of the derivation. Let us first introduce a RG scale parameter  $k$ , denoting the momentum scale up to which the high energy modes have been integrated out. Now we can specify the starting and end point of the theory space trajectory. We demand

$$\lim_{k \rightarrow \Lambda} \Gamma_k = S, \quad \lim_{k \rightarrow 0} \Gamma_k = \Gamma,$$

where  $S$  is the microscopic action that has to be quantized and  $\Gamma$  is the full quantum effective action, including all fluctuations. As a next step, we define the UV and IR regularized functional

$$Z_k[J] = \int_{\Lambda} \mathcal{D}\Phi e^{-S[\Phi] + \int J^T \Phi - \Delta S_k[\Phi]}, \quad (2.2.1)$$

where we added a so-called regulator term to the exponent. It is given by

$$\begin{aligned} \Delta S_k[\Phi] &= \frac{1}{2} \int_q \varphi(-q) R_{kB}(q) \varphi(+q) + \int_q \bar{\psi}(q) R_{kF}(q) \psi(q) \\ &= \frac{1}{2} \int_q \Phi^T(-q) R_k(q) \Phi(q), \end{aligned} \quad (2.2.2)$$

where<sup>4</sup>

$$R_k(q) = \begin{pmatrix} R_{kB}(q) & 0 & 0 \\ 0 & 0 & -R_{kF}^T(-q) \\ 0 & R_{kF}(q) & 0 \end{pmatrix}. \quad (2.2.3)$$

The indices B and F denote the bosonic and fermionic regulator functions respectively. Since the regulator term is quadratic in the fields, it can be viewed as a scale dependent mass term of the fields. The regulator functions are required to satisfy the following relations:

$$\begin{aligned} \lim_{\frac{q^2}{k^2} \rightarrow 0} R_k &> 0 \\ \lim_{\frac{k^2}{q^2} \rightarrow 0} R_k &= 0 \\ \lim_{k^2 \rightarrow \Lambda^2 \rightarrow \infty} R_k &= \infty. \end{aligned} \quad (2.2.4)$$

---

<sup>4</sup>The regulator is diagonal in the momentum indices,  $R_k(p, q) = \delta_{p,q} R_k(p)$ .

The first condition implements the IR regularization. For example, if  $R_k$  is proportional to  $k^2$  for  $q^2 \ll k^2$ , the regulator equips the IR modes with a mass proportional to  $k$  and therefore suppresses them. The second condition ensures that we recover the standard generating functional  $Z$  (respectively the full quantum effective action  $\Gamma$ ) in the limit  $k \rightarrow 0$ . The last condition justifies the use of the saddle point approximation in the limit  $k^2 \rightarrow \Lambda^2 \rightarrow \infty$ , which returns the microscopic action  $S^5$ . Furthermore, it is convenient to rewrite the regulator functions in the following form<sup>6</sup>

$$R_{kB}(p) = Z_{\varphi,k} p^2 r_{kB} \left( \frac{p^2}{k^2} \right); \quad R_{kF}(p) = -Z_{\psi,k} \not{p} r_{kF} \left( \frac{p^2}{k^2} \right),$$

with dimensionless shape functions  $r_i(y)$  and the dimensionless argument  $y = \frac{p^2}{k^2}$ . Since we defined appropriate boundary conditions, we now consider the actual trajectory of the effective average action  $\Gamma_k$ . First we determine the behaviour of the IR regularized Schwinger functional  $W_k = \log Z_k$  under changes of the scale  $k$ . But instead of using derivatives with respect to  $k$ , we introduce the dimensionless RG time

$$t = \log \frac{k}{\Lambda}, \quad \partial_t = k \frac{d}{dk}.$$

Let us see how this operates on the Schwinger functional if we keep the source  $J$  fixed:

$$\begin{aligned} \partial_t W_k[J] \Big|_J &= -\frac{1}{Z_k} \int_{\Lambda} \mathcal{D}\Phi \partial_t (\Delta S_k[\Phi]) e^{-S[\Phi] + \int J^T \Phi - \Delta S_k[\Phi]} \\ &\stackrel{(2.2.2)}{=} -\frac{1}{2} \int_q (\partial_t R_k)^{ab}(q) \underbrace{\frac{1}{Z_k} \int_{\Lambda} \mathcal{D}\Phi \Phi_a^T(-q) \Phi_b(q) e^{-S[\Phi] + \int J^T \Phi - \Delta S_k[\Phi]}}_{\langle \Phi_a^T(-q) \Phi_b(q) \rangle^J} \\ &= -\frac{1}{2} \int_q \partial_t R_{kB}(q) \langle \varphi(-q) \varphi(q) \rangle^J - \int_q \partial_t R_{kF}(q) \langle \bar{\psi}(q) \psi(q) \rangle^J. \end{aligned}$$

By adding zeros

$$\begin{aligned} 0 &= \langle \varphi(-q) \rangle^J \langle \varphi(q) \rangle^J - \langle \varphi(-q) \rangle^J \langle \varphi(q) \rangle^J \\ 0 &= \langle \bar{\psi}(q) \rangle^J \langle \psi(q) \rangle^J - \langle \bar{\psi}(q) \rangle^J \langle \psi(q) \rangle^J \end{aligned}$$

we can rewrite the expression above as following,

$$\begin{aligned} \partial_t W_k[J] \Big|_J &= -\frac{1}{2} \int_q \text{Tr} (\partial_t R_k(q) G_k(q, q)) \\ &\quad - \frac{1}{2} \int_q \partial_t R_{kB}(q) \langle \varphi(-q) \rangle^J \langle \varphi(q) \rangle^J - \int_q \partial_t R_{kF}(q) \langle \bar{\psi}(q) \rangle^J \langle \psi(q) \rangle^J, \quad (2.2.5) \end{aligned}$$

---

<sup>5</sup>For details see [21]

<sup>6</sup>In fact, this is already a special choice, see further comments at the end of this subsection or in section 5.2.

where we introduced the full connected propagator  $G_k$

$$G_{k,ab}(p, p) := \langle \Phi_a^T(-p) \Phi_b(p) \rangle^J - \langle \Phi_a^T(-p) \rangle^J \langle \Phi_b(p) \rangle^J = \frac{\overrightarrow{\delta}}{\delta J^{T,b}(-p)} W_k \frac{\overleftarrow{\delta}}{\delta J^a(p)}.$$

The last two terms in the equation for  $\partial_t W_k[J] \Big|_J$  just yield the scale derivative of the full regulator term, where the argument is now the vacuum expectation value of the field,

$$\begin{aligned} \frac{1}{2} \int_q \partial_t R_{kB}(q) \langle \varphi(-q) \rangle^J \langle \varphi(q) \rangle^J - \int_q \partial_t R_{kF}(q) \langle \bar{\psi}(q) \rangle^J \langle \psi(q) \rangle^J \\ = \frac{1}{2} \int_q \langle \Phi_a^T(-q) \rangle^J (\partial_t R_k)^{ab}(q) \langle \Phi_b(q) \rangle^J \\ = \partial_t \Delta S_k[\langle \Phi \rangle^J]. \end{aligned}$$

Thus, we finally find

$$\partial_t W_k[J] \Big|_J = -\frac{1}{2} \int_q \text{Tr}(\partial_t R_k(q) G_k(q, q)) - \partial_t \Delta S_k[\langle \Phi \rangle^J]. \quad (2.2.6)$$

Motivated by this, we define a macroscopic field<sup>7</sup>

$$\phi(x) \equiv \begin{pmatrix} \varphi(x) \\ \psi(x) \\ \bar{\psi}^T(x) \end{pmatrix} := \langle \Phi(x) \rangle_{conn}^J = \frac{\overrightarrow{\delta}}{\delta J^T(x)} W_k[J] \quad (2.2.7)$$

and introduce a modified effective average action as the Legendre transformation modified by the regulator term,

$$\Gamma_k[\phi] = \sup_J \left\{ -W_k[J] + \int J^T \phi \right\} - \Delta S_k[\phi]. \quad (2.2.8)$$

As before, for every given macroscopic configuration  $\phi$  exists a source field  $J = J_{sup}$  which maximizes the expression in the curly brackets. Because  $W_k$  depends on  $k$ ,  $J_{sup}$  will do so as well. From now on we skip the supremum and the subscript of  $J_{sup}$  again. Since the first term in the definition of  $\Gamma_k$  is a Legendre transformation and thus convex, any non-convexity results from the regulator term.

Let us consider the new equation of motion for the macroscopic field:

$$\begin{aligned} \frac{\overrightarrow{\delta}}{\delta \phi^T(x)} \Gamma_k[\phi] &= - \int_y \frac{\delta J^T(y)}{\delta \phi^T(x)} \underbrace{\frac{\overrightarrow{\delta}}{\delta J^T(y)} W_k[J]}_{\phi(y)} + \int_y \frac{\delta J^T(y)}{\delta \phi^T(x)} \phi(y) \\ &\quad + (-1)^s \int_y \frac{\delta \phi^T(y)}{\delta \phi^T(x)} J(y) - \frac{\overrightarrow{\delta}}{\delta \phi^T(x)} \Delta S_k[\phi] \\ &= (-1)^s J(x) - \frac{\overrightarrow{\delta}}{\delta \phi^T(x)} \Delta S_k[\phi]. \end{aligned}$$

---

<sup>7</sup>Note that we now use the variables  $\varphi, \psi$  and  $\bar{\psi}$  for the macroscopic fields.

In position space, the functional derivative of  $\Delta S_k$  reads

$$\begin{aligned} \frac{\overrightarrow{\delta}}{\delta\phi^T(x)} \frac{1}{2} \int_{y,z} \phi^T(y) R_k(z-y) \phi(z) &= \int_z R_k(z-x) \phi(z) \\ &\equiv (R_k\phi)(x). \end{aligned}$$

Thus, the equation of motion is given by

$$\frac{\overrightarrow{\delta}}{\delta\phi^T(x)} \Gamma_k[\phi] = (-1)^s J(x) - (R_k\phi)(x) \quad (2.2.9)$$

and in momentum space

$$\frac{\overrightarrow{\delta}}{\delta\phi^T(-p)} \Gamma_k[\phi] = (-1)^s J(p) - R_k(p)\phi(p). \quad (2.2.10)$$

Our next goal is to compute the behaviour of the effective average action under a change of the RG scale, while we keep the macroscopic field configuration fixed. It is necessary to find a relation between the connected propagator and the effective average action to be able to express the corresponding differential equation in terms of  $\Gamma_k$  itself. For this purpose, let us introduce the so-called fluctuation matrix as the second variation of  $\Gamma_k$ ,

$$\begin{aligned} \Gamma_k^{(2)}(p, q) &:= \frac{\overrightarrow{\delta}}{\delta\phi^T(-p)} \Gamma_k[\phi] \frac{\overleftarrow{\delta}}{\delta\phi(q)} \\ &= \begin{pmatrix} \frac{\overrightarrow{\delta}}{\delta\varphi(-p)} \\ \frac{\overrightarrow{\delta}}{\delta\psi^T(-p)} \\ \frac{\overrightarrow{\delta}}{\delta\psi(p)} \end{pmatrix} \Gamma_k[\phi] \begin{pmatrix} \frac{\overleftarrow{\delta}}{\delta\varphi(q)} & \frac{\overleftarrow{\delta}}{\delta\psi(q)} & \frac{\overleftarrow{\delta}}{\delta\psi^T(-q)} \end{pmatrix}. \end{aligned} \quad (2.2.11)$$

We refer to this matrix as a  $3 \times 3$  matrix (according to what we call field indices), but keep in mind that it has the following sub-structure,

$$\Gamma_k^{(2)} = \begin{pmatrix} (1 \times 1) & (1 \times d_\gamma) & (1 \times d_\gamma) \\ (d_\gamma \times 1) & (d_\gamma \times d_\gamma) & (d_\gamma \times d_\gamma) \\ (d_\gamma \times 1) & (d_\gamma \times d_\gamma) & (d_\gamma \times d_\gamma) \end{pmatrix}.$$

Then from equation (2.2.10) we get

$$\Gamma_k^{(2)}(p, q) = (-1)^s J(p) \frac{\overleftarrow{\delta}}{\delta\phi(q)} - R_k(p) \delta_{p,q}. \quad (2.2.12)$$

It is now possible to derive the relation we are looking for:

$$\begin{aligned}
 \delta_{p,q} = J(p) \frac{\overleftarrow{\delta}}{\delta J(q)} &= \int_{q'} \left( J(p) \frac{\overleftarrow{\delta}}{\delta \phi(q')} \right) \left( \phi(q') \frac{\overleftarrow{\delta}}{\delta J(q)} \right) \\
 &\stackrel{(2.2.12)}{=} \int_{q'} (-1)^s \left( \Gamma_k^{(2)}(p, q') + R_k(p) \delta_{p,q'} \right) \left( \phi(q') \frac{\overleftarrow{\delta}}{\delta J(q)} \right) \\
 &\stackrel{(2.2.7)}{=} \int_{q'} (-1)^s \left( \Gamma_k^{(2)}(p, q') + R_k(p) \delta_{p,q'} \right) G_k(q', q),
 \end{aligned}$$

or in operator notation

$$\mathbb{1} = (-1)^s (\Gamma_k^{(2)} + R_k) G_k. \tag{2.2.13}$$

This enables us to write down the Wetterich equation:

$$\begin{aligned}
 \partial_t \Gamma_k[\phi] \Big|_{\phi} &= -\partial_t W_k \Big|_{\phi} + \int_y \partial_t J^T(y) \phi(y) - \partial_t \Delta S_k[\phi] \\
 &= -\partial_t W_k \Big|_J - \partial_t \Delta S_k[\phi] \\
 &\stackrel{(2.2.6)}{=} \frac{1}{2} \int_q \text{Tr} (\partial_t R_k(q) G_k(q, q)) \\
 &\stackrel{(2.2.13)}{=} \frac{(-1)^s}{2} \int_{p,q} \text{Tr} \left( \partial_t R_k(p) \delta_{p,q} \left( \Gamma_k^{(2)} + R_k \right)^{-1}(p, q) \right) \\
 &= \frac{1}{2} \text{STr} \left[ \frac{\partial_t R_k}{\Gamma_k^{(2)} + R_k} \right]. \tag{2.2.14}
 \end{aligned}$$

The Wetterich equation (2.2.14) is a pure differential equation of the effective action, we got rid of any functional integrals. Furthermore, it has a one-loop structure (compare with equation (2.1.10)), but it is exact since the full propagator  $\Gamma_k^{(2)}$  appears in the denominator. As mentioned above, the regulator term in the denominator guarantees the IR regularization, since it behaves like a scale dependent mass term. Its scale derivative in the numerator however expresses the Wilsonian idea of integrating out momentum shell by momentum shell, because it is peaked around  $p^2 \approx k^2$ , as shown in figure 2.1.

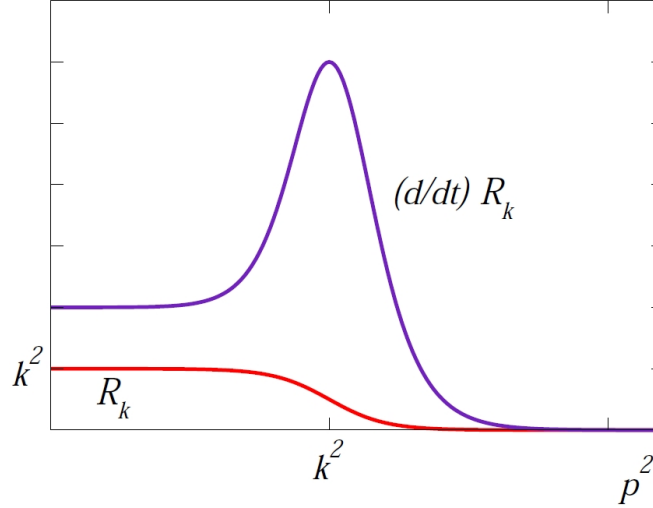


FIGURE 2.1: Typical shape of the regulator (red) and its scale derivative (purple). Quoted from [18]

In this sense the UV regularization is implemented as well. The solution to the Wetterich equation corresponds to the trajectory of the scale dependent effective action with fixed starting point ( $\Gamma_\Lambda = S$ ) and fixed endpoint, i.e. the full quantum effective action. The trajectory itself also depends on the choice of the regulator<sup>8</sup>. As already mentioned above, all operators that satisfy the symmetries of the theory can be excited during the flow. Hence, we will have to truncate the effective action when performing actual calculations, taking only a finite number of operators into account. Due to this we might end up in some distance to the actual quantum effective action. The quality of the convergence depends on the truncation as well as on the regulator.

---

<sup>8</sup>See section 5.2 for further comments.

## 2.3 Spontaneous symmetry breaking

To understand the basic principle, let us consider a simple  $\varphi^4$ -theory, where  $\varphi$  is a real scalar field. Furthermore, the Lagrangian shall be invariant under  $\mathbb{Z}_2$  transformations. Thus, the Lagrangian in Euclidean spacetime reads

$$\mathcal{L} = \frac{1}{2}\partial_\mu\varphi\partial^\mu\varphi + \frac{1}{2}\mu^2\varphi^2 + \frac{\lambda}{8}\varphi^4 \equiv \frac{1}{2}\partial_\mu\varphi\partial^\mu\varphi + V(\varphi), \quad (2.3.1)$$

where  $\lambda > 0$  has to hold since we demand the potential to be bounded from below. The shape of the potential is determined by the parameters  $\mu$  and  $\lambda$  and thus the ground state of the system, since it corresponds to the minimum of the potential. Let us consider homogeneous field configurations. Then, in case of  $\mu^2 > 0$ , there only exists a single minimum at  $\varphi_0 \equiv v = 0$ . If  $\mu^2 < 0$  holds we have two physically equivalent minima at

$$\varphi_0 = \pm v = \pm\sqrt{-\frac{2\mu^2}{\lambda}},$$

The two phases are illustrated in figure 2.2.

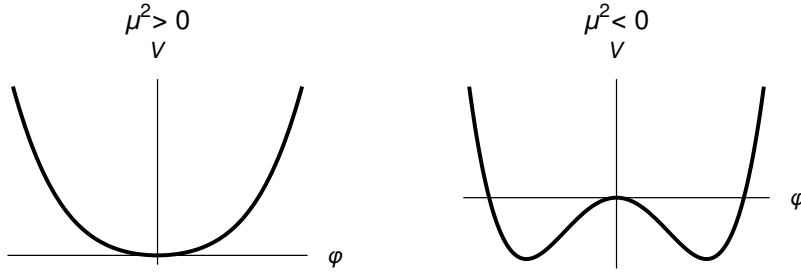


FIGURE 2.2: (Left) System in symmetric phase. (Right) System in broken phase.

In the latter case the system will choose one of these two minima to be the ground state. In case that the field configuration is  $\varphi = 0$ , i.e. the unstable extremum, small fluctuations will drive the system into a stable field configuration at  $\varphi = \pm v$ . However, since  $v \neq 0$  holds, the ground state violates the original  $\mathbb{Z}_2$  symmetry of the Lagrangian. We say the theory is spontaneously broken. To decide whether a system is in the broken phase or not, we simply have to investigate if the vacuum expectation value  $v$  vanishes.

As a next step, we introduce a priori massless fermions to our model. They shall interact with the scalar field via a Yukawa interaction  $h\varphi\bar{\psi}\psi$ . But if we now decompose the scalar field into its vacuum expectation value and fluctuations around it,

$$\varphi(x) = v + \sigma(x), \quad \langle \sigma(x) \rangle = 0,$$

the interaction term reads

$$h\varphi\bar{\psi}\psi = hv\bar{\psi}\psi + h\sigma\bar{\psi}\psi.$$

If the system is in the spontaneously broken phase, i.e.  $v \neq 0$ , the left term can be interpreted as a fermionic mass term with  $m = hv$ . Although we introduced a priori massless fermions, they received a mass via spontaneous symmetry breaking. The mass of the scalar field itself is given by the curvature of the scalar potential at the ground state.

#### The Higgs mechanism in the Standard Model

The original purpose of introducing the Higgs sector within the Standard Model was different from the suggestions above. The interactions of the Standard Model are described by gauge theories. As a consequence, fermionic mass terms are forbidden because they would violate the gauge invariance of the Lagrangian. This is not a problem for the theories of quantum electrodynamics (QED) and quantum chromodynamics (QCD), because their gauge bosons (photons and gluons) are known to be massless. In case of the weak sector however, experiments showed that the three corresponding gauge bosons ( $W^\pm$  and  $Z$  bosons) do have a mass, which are in addition much larger than the masses of most of the other elementary particles. To explain this circumstance, the Higgs mechanism was proposed ([1], [2], [3], [4]). Furthermore, since the gauge group of the (electro)weak sector<sup>9</sup> is  $SU(2)_L \times U(1)_Y$  [23], [24], the Higgs field was originally introduced as a complex scalar doublet rather than a single scalar field. Hence, we have four physical degrees of freedom. The breaking of this symmetry is different from the example above as well. The consequences of spontaneous symmetry breaking depend on the nature of the symmetry that becomes broken. If the symmetry is a global continuous symmetry, the Goldstone theorem predicts the appearance of massless particles, the so-called Goldstone bosons. In our example the Lagrangian was invariant under a discrete symmetry. Thus, no Goldstone boson appeared. The more interesting case is the breaking of local gauge symmetries like the ones of the Standard Model. However, the proof of the Goldstone theorem only holds for global symmetries. Nevertheless there exist no Goldstone bosons in the Standard Model due to the local gauge symmetries. In the Standard Model the degrees of freedom of the Higgs doublet split into one massive scalar field, the Higgs boson, and three so-called would-be Goldstone bosons. The latter ones are "eaten" by the gauge bosons and provide them their masses. In general, the mechanism works as follows. Let  $G$  be the gauge group. Then after symmetry breaking the ground state still might be invariant under a subgroup of  $G$ , the so-called stability group  $H$ .

---

<sup>9</sup>In the Standard Model, the electromagnetic interaction and the weak interaction are combined to the electroweak sector.

Furthermore, let  $n$  be the number of involved (real) scalar fields.

Then  $n - (\dim G - \dim H)$  of these fields remain as massive Higgs fields. Consequently  $(\dim G - \dim H)$  would-be Goldstone bosons appear, which are eaten by gauge bosons, providing them with their masses. Hence,  $\dim H$  gauge bosons remain massless. In the case of the Standard Model we have the four-dimensional gauge group  $G = SU(2)_L \times U(1)_Y$  that becomes spontaneously broken. After symmetry breaking the ground state remains invariant under the one-dimensional electromagnetic gauge group  $H = U(1)_{e.m.}$ . As mentioned above, we have  $n = 4$  physical degrees of freedom. Thus, we end up with one massive scalar field (the Higgs boson), three massive gauge bosons ( $W^\pm$  and  $Z$ ) and one massless gauge boson (the photon). In a similar way the fermions receive their masses via a Yukawa interaction with the Higgs doublet.

### 3 Our toy model

In this chapter we want to introduce the toy model we are going to work with. Let us first write down our ansatz for the effective effective action and discuss it afterwards:

$$\Gamma_k[\phi] = \int_x \left[ U_k(\varphi^2) + \frac{Z_{\varphi,k}}{2} \partial_\mu \varphi \partial^\mu \varphi + Z_{\psi,k} \bar{\psi} i \not{\partial} \psi + i H_k(\varphi) \bar{\psi} \psi \right], \quad H_k(\varphi) = \varphi h_k(\varphi^2) \tag{3.0.1}$$

The toy model consists of a real scalar field  $\varphi$  and a fermion, which represent the Higgs field and the top quark respectively. We allow arbitrary self-interactions of the scalar field, given by the effective potential  $U_k$  and we also introduce a generalized Yukawa coupling  $H_k(\varphi)$ <sup>1</sup>. Note that we impose a  $\mathbb{Z}_2$  symmetry on  $U_k$  and  $h_k$ . The discussion why this is an appropriate simplification of the Standard Model has already been held in [13], [25], we are going to recall the important steps.

The original Standard Model is of course much more complex than our toy model. For example, as already mentioned, the Higgs field is a complex doublet in the Standard Model. Beside self-interaction terms it couples with the gauge bosons of the electroweak interaction through the couplings  $g(U(1))$  and  $g'(SU(2))$ , implementing the masses of  $W^\pm$  and  $Z$  bosons via the Higgs mechanism. The same holds for the fermions, here the couplings are of the Yukawa type  $h_f$ . The main interest of this work focusses on calculating Higgs masses and therefore on the effective potential  $U_k$ . To justify the ansatz we thus have to answer two questions: Why is the dominant influence of the other sectors on the scalar sector only given by the top quark and why are we allowed to reduce the complex Higgs doublet to a real scalar field with a  $\mathbb{Z}_2$  symmetry?

To support our arguments we will use some results of perturbation theory. We are conscious of the fact that the couplings of the strong interaction sector increase in the IR, denying the application of perturbative methods.

---

<sup>1</sup>If we choose  $h(\varphi^2)$  to be constant, we obtain the original Yukawa coupling.

---

But indeed, this happens on a scale lower than the one of electroweak symmetry breaking, so that the IR flow should not have a significant impact on the flow of the effective potential, since it should already have been frozen out. Because the  $SU(2)$  coupling  $g'$  is smaller than the strong coupling  $g_3(SU(3))$  in the IR, the same argument holds, too. Furthermore, the Yukawa couplings can be considered to be in the perturbative regime as well, if we have a look at the experimental data<sup>2</sup>: In the IR the vacuum expectation value of the Higgs field is given by 246 GeV and the top mass is measured to be 173 GeV. Hence, the strongest Yukawa coupling, i.e. the coupling of the top quark, would have an IR value of  $h_{top} \approx \frac{173}{246} = 0.70$ , which is still smaller than one. Only the scalar sector might turn out to be non-perturbative, especially since we are going to test the parameter space over a wide range, including strong bare couplings. This could influence the other sectors as well, it might even be possible that they are all driven into a non-perturbative regime. This again would render the neglect of their influence on the scalar sector unjustified. Although, if such strong dynamics would play an important role in the Standard Model, their qualitative effects should be observable within the scope of our toy model as well.

Let us start with the RG improved perturbation theory result for the effective potential of the Standard Model up to one-loop-order ([27], [28], [29])

$$\begin{aligned}
U = & -\frac{1}{2}m^2(t)\phi^2(t) + \frac{1}{8}\lambda(t)\phi^4(t) \\
& + \sum_{i=1}^5 \frac{n_i}{64\pi^2} M_i(\phi)^4 \left[ \log \frac{M_i^2(\phi)}{\mu^2(t)} - c_i \right] + \Omega(t), \tag{3.0.2}
\end{aligned}$$

whereas

$$M_i^2(\phi) = \kappa_i \phi^2(t) - \kappa'_i$$

and

$$\begin{aligned}
n_1 = 6, & \quad \kappa_1 = \frac{1}{4}g^2(t), & \quad \kappa'_1 = 0, & \quad c_1 = \frac{5}{6} \\
n_2 = 3, & \quad \kappa_2 = \frac{1}{4}[g^2(t) + g'^2(t)], & \quad \kappa'_2 = 0, & \quad c_2 = \frac{5}{6} \\
n_3 = -12, & \quad \kappa_3 = \frac{1}{2}h_{top}^2(t), & \quad \kappa'_3 = 0, & \quad c_3 = \frac{3}{2} \\
n_4 = 1, & \quad \kappa_4 = \frac{3}{2}\lambda(t), & \quad \kappa'_4 = m^2(t), & \quad c_4 = \frac{3}{2} \\
n_5 = 3, & \quad \kappa_5 = \frac{1}{2}\lambda(t), & \quad \kappa'_5 = m^2(t), & \quad c_5 = \frac{3}{2}.
\end{aligned}$$

---

<sup>2</sup>All experimental data are quoted from [26].

---

$M_i$  contains the masses of the particles, i.e.  $M_i = (m_W, m_Z, m_{top}, m_{Higgs}, m_{Goldstone})$ .  $m^2(t)$  and  $\lambda(t)$  are the couplings of the quartic Standard Model potential. Finally,  $\Omega(t)$  is the cosmological constant, which is irrelevant for our considerations, since we are interested in the Higgs mass. The Higgs mass is related to the curvature of the potential and thus independent of  $\Omega(t)$ . Among the fermions the top quark is by far the heaviest and therefore the corresponding Yukawa coupling  $h_{top}(t)$  the strongest. Hence, we already neglected all the other fermions (quarks and leptons) in equation (3.0.2). Furthermore, the couplings  $g$  and  $g'$  of the electroweak interaction are known to be much smaller than the top Yukawa coupling and the  $SU(3)$  coupling  $g_3$  in the IR. Although  $g$  is increasing with momentum, both  $g$  and  $g'$  are smaller than  $g_3$  and  $h_{top}$  at least up to the GUT scale at around  $10^{16}$  GeV. Thus, we are able to disregard all terms with  $i = 1, 2$  in equation (3.0.2) as well as in the  $\beta$ -functions of the remaining couplings. Among the remaining couplings, the  $\beta$ -function of  $h_{top}$  contains contributions from the strong and electroweak sector and thus would be the last connection to the sectors we neglected so far. Hence, we have to investigate whether a neglect of these contributions to the  $\beta$ -function of  $h_{top}$  can be justified as well. From [27] we know that at one-loop level the  $\beta$ -function reads

$$\partial_t h_{top} = \frac{1}{16\pi^2} \left( \frac{9}{2} h_{top}^3 - 8g_3^2 h_{top} - \frac{9}{4} g^2 h_{top} - \frac{17}{12} g'^2 h_{top} \right). \quad (3.0.3)$$

As discussed above, the electroweak contributions can be ignored. The problem is the strong interaction term. Using  $h_{top} \approx 0.70$  we get  $\frac{9}{2} h_{top}^3 \approx 1.57$ . Comparing this to the strong interaction term (with  $\alpha_s(m_Z) = \frac{g_3^2}{4\pi} = 0.118$  we obtain  $8g_3^2 h_{top} \approx 8.30$ ) we see that its neglect is in fact a rough approximation. Because we are mainly interested in the qualitative behaviour of the Higgs mass and the effective potential respectively, we can nevertheless omit this term as well.

The last step is the reduction of the complex Higgs doublet to a single real scalar Higgs field. Since we dropped the electroweak sector, we lost its corresponding local gauge invariance, including the gauge bosons. The spontaneous breaking of the remaining global symmetry would lead to massless Goldstone bosons, which however cannot be "eaten" by the (missing) gauge bosons. This problem has to be solved and at the same time we have to imitate one key property of the Standard Model, that is we have to set up our toy model in a way that mass terms for the fermions are forbidden. Motivated by the Standard Model itself, where it is indeed possible to express the scalar potential just via one single scalar field by making use of the gauge invariance, we approximate the scalar sector by one real scalar field. This theory does not possess any continuous symmetries and thus the problem of the Goldstone bosons vanishes.

---

To make sure that no fermionic mass terms are allowed, we demand our theory to be invariant under chiral transformations,

$$\psi \rightarrow e^{i\gamma_5 \frac{\pi}{2}} \psi, \quad \bar{\psi} \rightarrow \bar{\psi} e^{i\gamma_5 \frac{\pi}{2}}.$$

Due to this transformation, a mass term would behave like  $\bar{\psi}\psi \rightarrow -\bar{\psi}\psi$  and thus violate the symmetry. However, this would also hold for Yukawa type interactions. To solve this problem we additionally impose a discrete  $\mathbb{Z}_2$ -symmetry on the scalar field, which then compensates the minus sign. For this reason, the scalar potential has to have the form  $U_k = U_k(\varphi^2)$  and the generalized Yukawa coupling has to satisfy  $H_k(\varphi) = \varphi h_k(\varphi^2)$ . Hence, we find the proposed truncation (3.0.1).

## 4 Flow equations

In this chapter we want to derive the flow equations corresponding to our toy model.

### 4.1 The fluctuation matrix

As a first ingredient of the Wetterich equation (2.2.14) we calculate the fluctuation matrix of our model, that is

$$\Gamma_k^{(2)}(p, q) = \begin{pmatrix} \overrightarrow{\delta} \\ \frac{\delta\varphi(-p)}{\delta\overrightarrow{\delta}} \\ \frac{\delta\psi^T(-p)}{\delta\overrightarrow{\delta}} \\ \frac{\delta\psi(p)}{\delta\overrightarrow{\delta}} \end{pmatrix} \Gamma_k[\phi] \begin{pmatrix} \overleftarrow{\delta} & \overleftarrow{\delta} & \overleftarrow{\delta} \\ \frac{\delta\varphi(q)}{\delta\overleftarrow{\delta}} & \frac{\delta\psi(q)}{\delta\overleftarrow{\delta}} & \frac{\delta\psi^T(-q)}{\delta\overleftarrow{\delta}} \end{pmatrix}.$$

We consider the action in momentum space (at least kinetic terms)<sup>1</sup>,

$$\Gamma_k[\phi] = \int_x U_k(\varphi) + \int_q \frac{Z_{\varphi,k}}{2} q^2 \varphi(q) \varphi(-q) - \int_q Z_{\psi,k} \bar{\psi}(q) \not{q} \psi(q) + i \int_x H_k(\varphi) \bar{\psi}(x) \psi(x),$$

and compute the (1,3) element as an example:

$$\frac{\overrightarrow{\delta}}{\delta\varphi(-p)} \Gamma_k \frac{\overleftarrow{\delta}}{\delta\psi^T(-q)} = i \int_x H'_k(\varphi) \frac{\delta\varphi(x)}{\delta\varphi(-p)} \bar{\psi}(x) \psi(x) \frac{\overleftarrow{\delta}}{\delta\psi^T(-q)}.$$

To perform the derivative acting from the right, we have to transpose the product  $\bar{\psi}\psi$ , which yields a minus sign since both fields are Grassmann valued:

$$\frac{\overrightarrow{\delta}}{\delta\varphi(-p)} \Gamma_k \frac{\overleftarrow{\delta}}{\delta\psi^T(-q)} = -i \int_x H'_k(\varphi) \frac{\delta\varphi(x)}{\delta\varphi(-p)} \psi^T(x) \frac{\bar{\psi}^T(x)}{\bar{\psi}^T(-q)}.$$

Finally, by using our conventions concerning the Fourier transformation we get

$$\frac{\overrightarrow{\delta}}{\delta\varphi(-p)} \Gamma_k \frac{\overleftarrow{\delta}}{\delta\bar{\psi}^T(-q)} = -i \int_x H'_k(\varphi) \psi^T(x) e^{-i(p-q)}.$$

---

<sup>1</sup>We will write  $U_k(\varphi)$  instead of  $U_k(\varphi^2)$  again to not get confused with the derivatives with respect to  $\varphi$  that are going to appear.

## 4.1 The fluctuation matrix

The other entries can be calculated similarly, the final result becomes

$$\Gamma_k^{(2)}(p, q) = \begin{pmatrix} Z_{\varphi, k} p^2 \delta_{p, q} + \int_x U_k''(\varphi) e^{-i(p-q)x} + & i \int_x H_k'(\varphi) \bar{\psi}(x) e^{-i(p-q)x} & -i \int_x H_k'(\varphi) \psi^T(x) e^{-i(p-q)x} \\ i \int_x H_k''(\varphi) e^{-i(p-q)x} \bar{\psi}(x) \psi(x) & 0 & -Z_{\psi, k} \not{p}^T \delta_{p, q} - i \int_x H_k(\varphi) e^{-i(p-q)x} \\ -i \int_x H_k'(\varphi) \bar{\psi}^T(x) e^{-i(p-q)x} & -Z_{\psi, k} \not{p} \delta_{p, q} + i \int_x H_k(\varphi) e^{-i(p-q)x} & 0 \\ i \int_x H_k'(\varphi) \psi(x) e^{-i(p-q)x} & & \end{pmatrix}, \quad (4.1.1)$$

where primes denote derivatives with respect to  $\varphi$ . We will now add the regulator term  $R_k$ . By defining the quantities <sup>2</sup>

$$P(q) = q^2(1 + r_{kB}(q)), \quad P_F(q) = q^2(1 + r_{kF}(q))^2$$

we thus get

$$\left( \Gamma_k^{(2)} + R_k \right) (p, q) = \begin{pmatrix} Z_{\varphi, k} P(p) \delta_{p, q} + \int_x U_k''(\varphi) e^{-i(p-q)x} + & i \int_x H_k'(\varphi) \bar{\psi}(x) e^{-i(p-q)x} & -i \int_x H_k'(\varphi) \psi^T(x) e^{-i(p-q)x} \\ i \int_x H_k''(\varphi) e^{-i(p-q)x} \bar{\psi}(x) \psi(x) & 0 & -Z_{\psi, k} \not{p}^T (1 + r_{kF}) \delta_{p, q} \\ -i \int_x H_k'(\varphi) \bar{\psi}^T(x) e^{-i(p-q)x} & -Z_{\psi, k} \not{p} (1 + r_{kF}) \delta_{p, q} & -i \int_x H_k(\varphi) e^{-i(p-q)x} \\ i \int_x H_k'(\varphi) \psi(x) e^{-i(p-q)x} & + i \int_x H_k(\varphi) e^{-i(p-q)x} & 0 \end{pmatrix}. \quad (4.1.2)$$

Furthermore, we will see later that some of the projection rules include setting the fields to constants. Thus, we also write down the expression above for this case <sup>3</sup>:

$$\left( \Gamma_k^{(2)} + R_k \right) \Big|_{\varphi = \text{const}} (p, q) = \delta_{p, q} \times \begin{pmatrix} Z_{\varphi, k} P(p) + U_k''(\varphi) & i H_k'(\varphi) \bar{\psi} & -i H_k'(\varphi) \psi^T \\ + i H_k''(\varphi) \bar{\psi} \psi & 0 & -Z_{\psi, k} \not{p}^T (1 + r_{kF}) - i H_k(\varphi) \\ -i H_k'(\varphi) \bar{\psi}^T & -Z_{\psi, k} \not{p} (1 + r_{kF}) \delta_{p, q} + i H_k(\varphi) & 0 \\ i H_k'(\varphi) \psi & & \end{pmatrix}. \quad (4.1.3)$$

<sup>2</sup>Actually,  $P_F$  will appear later in the inverse expression.

<sup>3</sup>Setting the fields to constants means that we can perform the position space integrals, which together with the exponential functions just yield factors  $\delta_{p, q}$ .

## 4.2 The generalized Yukawa coupling

The flow of a field-dependent generalized Yukawa coupling has already been studied in different physical contexts, e.g. linked to gravitation [31],[30] or to QCD [32]. In [33] the authors investigated exactly the same system as in this thesis but with respect to the search of Gaussian fixed points and critical behaviour. Nevertheless, the latter work will be appropriate for comparing the derived flow equations.

The first step to compute the flow of any quantity is to find a projection rule which extracts it from the effective average action. In the case of the generalized Yukawa coupling we have

$$\delta_0 H_k(\varphi_0) \mathbb{1}_{d_\gamma} = \frac{1}{i} \frac{\overrightarrow{\delta}}{\delta \bar{\psi}} \Gamma_k \frac{\overleftarrow{\delta}}{\delta \psi} \Big|_{\substack{\varphi = \varphi_0 = const \\ \psi = \bar{\psi} = 0}},$$

where  $\delta_0$  is an infinite volume factor, emerging from the integration over the full space-time. Since the Wetterich equation (2.2.14) already describes how  $\Gamma_k$  evolves with the RG time, we immediately get the flow equation of  $H_k$ ,

$$\delta_0 \partial_t H_k(\varphi_0) \mathbb{1}_{d_\gamma} = \frac{1}{i} \frac{\overrightarrow{\delta}}{\delta \bar{\psi}} \frac{1}{2} \text{STr} \left[ \frac{\partial_t R_k}{\Gamma_k^{(2)} + R_k} \right] \frac{\overleftarrow{\delta}}{\delta \psi} \Big|_{\substack{\varphi = \varphi_0 = const \\ \psi = \bar{\psi} = 0}}. \quad (4.2.1)$$

From now on we skip the subscript on  $\varphi_0$ . Our task is to compute the right hand side of equation (4.2.1). We will not do this straightforwardly but apply some technical tricks that will simplify our calculations. We want to rewrite the argument of the super trace by introducing an alternative scale derivative:

$$\tilde{\partial}_t := \sum_{i=\varphi,\psi} \int_x \frac{\partial_t (Z_{i,k} r_i(x))}{Z_{i,k}} \frac{\delta}{\delta r_i(x)} \quad (4.2.2)$$

Here we have  $r_\varphi \equiv r_{kB}$  and  $r_\psi \equiv r_{kF}$ . This derivative acts only on the regulator parts. Thus, we immediately have

$$\frac{\partial_t R_k}{\Gamma_k^{(2)} + R_k} = \tilde{\partial}_t \log[\Gamma_k^{(2)} + R_k]. \quad (4.2.3)$$

Now we want to use the fact that terms which do not contain any fermionic fluctuations (that is  $\psi$  or  $\bar{\psi}$  fields) will vanish under the projection. Hence, we decompose

$$\Gamma_k^{(2)} + R_k = \Gamma_{\varphi,k}^{(2)} + \Delta \Gamma_k^{(2)} + R_k,$$

where  $\Gamma_{\varphi,k}^{(2)} + R_k$  contains the terms that do not include any fermionic fluctuations and the regulator, while  $\Delta \Gamma_k^{(2)}$  includes the remaining terms that involve fermions.

This enables us to rewrite the super trace as following

$$\begin{aligned} \text{STr} \left[ \frac{\partial_t R_k}{\Gamma_k^{(2)} + R_k} \right] &= \text{STr} \tilde{\partial}_t \log[\Gamma_k^{(2)} + R_k] \\ &= \text{STr} \tilde{\partial}_t \log[\Gamma_{\varphi,k}^{(2)} + R_k] + \text{STr} \left[ \tilde{\partial}_t \log \left( 1 + \frac{\Delta\Gamma_k^{(2)}}{\Gamma_{\varphi,k}^{(2)} + R_k} \right) \right]. \end{aligned} \quad (4.2.4)$$

The first summand will vanish due to the projection, because it is independent of fermionic fields and thus vanishes when applying the field derivatives. Concerning the remaining term, we can apply another trick: Since after the functional field derivatives  $\frac{\overrightarrow{\delta}}{\delta\psi}$  and  $\frac{\overleftarrow{\delta}}{\delta\bar{\psi}}$  the fermionic fields are set to zero anyway, we can set  $\psi$  and  $\bar{\psi}$  to constants right from the beginning, so that the functional derivatives actually become simple partial derivatives. This also implies that we can use version (4.1.3) of the fluctuation matrix. The quantities introduced above then read as following

$$\Delta\Gamma_k^{(2)}(p, q) = \delta_{p,q} \times \begin{pmatrix} iH_k'' \bar{\psi} \psi & iH_k' \bar{\psi} & -iH_k' \psi^T \\ -iH_k' \bar{\psi}^T & 0 & 0 \\ iH_k' \psi & 0 & 0 \end{pmatrix}, \quad (4.2.5)$$

$$\begin{aligned} & \left( \Gamma_{\varphi,k}^{(2)} + R_k \right) (p, q) = \delta_{p,q} \times \\ & \begin{pmatrix} Z_{\varphi,k} P(p) + U_k'' & 0 & 0 \\ 0 & 0 & -Z_{\psi,k} \not{p}^T (1 + r_{kF}) - iH_k \\ 0 & -Z_{\psi,k} \not{p} (1 + r_{kF}) + iH_k & 0 \end{pmatrix}. \end{aligned} \quad (4.2.6)$$

We now introduce the "full inverse propagators"

$$\xi_\varphi(q) = Z_{\varphi,k} P(q) + U_k''(\varphi), \quad \xi_\psi(q) = Z_{\psi,k}^2 P_F(q) + H_k^2(\varphi).$$

Then the inverse of the expression above can be written as

$$\left( \Gamma_{\varphi,k}^{(2)} + R_k \right)^{-1} (p, q) = \delta_{p,q} \times \begin{pmatrix} \frac{1}{\xi_\varphi(p)} & 0 & 0 \\ 0 & 0 & -\frac{Z_{\psi,k}(1+r_{kF})}{\xi_\psi(p)} \not{p} - \frac{iH_k}{\xi_\psi(p)} \\ 0 & -\frac{Z_{\psi,k}(1+r_{kF})}{\xi_\psi(p)} \not{p}^T + \frac{iH_k}{\xi_\psi(p)} & 0 \end{pmatrix} \quad (4.2.7)$$

and we are able to perform the matrix multiplication

$$\begin{aligned}
 \frac{\Delta\Gamma_k^{(2)}}{\Gamma_{\varphi,k}^{(2)} + R_k}(p, q) &= \int_{p'} \left( \Gamma_{\varphi,k}^{(2)} + R_k \right)^{-1} (p, p') \Delta\Gamma_k^{(2)}(p', q) \\
 &= \delta_{p,q} iH'_k \times \\
 &\quad \begin{pmatrix} \frac{iH''_k \bar{\psi} \psi}{iH'_k \xi_\varphi} & \frac{\bar{\psi}}{\xi_\varphi} & -\frac{\psi^T}{\xi_\varphi} \\ \frac{-Z_{\psi,k}(1+r_{kF})\not{p} - iH_k}{\xi_\psi} \psi & 0 & 0 \\ \frac{Z_{\psi,k}(1+r_{kF})\not{p}^T - iH_k}{\xi_\psi} \bar{\psi}^T & 0 & 0 \end{pmatrix}. \tag{4.2.8}
 \end{aligned}$$

As we have already discussed, we reduced the flow equation to

$$\delta_0 \partial_t H(\varphi) \mathbb{1}_{d_\gamma} = \frac{1}{i} \frac{\overrightarrow{\delta}}{\delta \bar{\psi}} \frac{1}{2} \text{STr} \left[ \bar{\partial}_t \log \left( 1 + \frac{\Delta\Gamma_k^{(2)}}{\Gamma_{\varphi,k}^{(2)} + R_k} \right) \right] \frac{\overleftarrow{\delta}}{\delta \psi} \Big|_{\varphi = \text{const}} \Big|_{\psi = \bar{\psi} = 0}. \tag{4.2.9}$$

Of course, we can change the order of accomplishing the different steps of calculation. We will first compute the super trace, then perform the field derivatives and finally compute the modified scale derivative. Setting the fermionic fields to zero also implies that the only terms of  $\log \left( 1 + \frac{\Delta\Gamma_k^{(2)}}{\Gamma_{\varphi,k}^{(2)} + R_k} \right)$  that will contribute according to the projection are those containing exactly one  $\psi$  and one  $\bar{\psi}$  field. Therefore, we expand the logarithm into a power series,  $\log(1+x) = \sum \frac{(-1)^{k+1}}{k} x^k$ . Since we already know that each non-zero entry of the matrix (4.2.8) contains at least one of the mentioned fields, the only orders that contribute to the flow equation are the first and the second orders. Let us start with the first order contributions. Performing the first part of taking the super trace (that is summing over the diagonal field indices) yields

$$\delta_{p,q} iH'_k \frac{iH''_k \bar{\psi} \psi}{iH'_k \xi_\varphi} = \delta_{p,q} \frac{iH''_k \bar{\psi} \psi}{\xi_\varphi}.$$

The next step is to sum ( $\hat{=}$  integrate) over the diagonal momentum indices, which includes setting  $p = q$ :

$$\delta_0 \int_p \frac{iH''_k \bar{\psi} \psi}{\xi_\varphi}.$$

We see that the factor  $\delta_0$  appears as well as on the left hand side of equation (4.2.9). As mentioned before, it is formally infinite. But if one puts our theory in a box with finite length  $L$ , this factor is nothing but the volume of this box and therefore finite as well. Now we can cut the factor on both sides of the equation and take the limit  $L \rightarrow \infty$  again. Furthermore, the field derivatives cause the term  $\bar{\psi} \psi$  to disappear,

$$\frac{\overrightarrow{\delta}}{\delta \bar{\psi}} \bar{\psi} \psi \frac{\overleftarrow{\delta}}{\delta \psi} = \mathbb{1}_{d_\gamma}.$$

The Dirac identity means that we obtain  $d_\gamma$  copies of the flow equation, just like we saw on the left hand side of the projection rule. Thus, we can skip this factor.

## 4.2 The generalized Yukawa coupling

Now we are only left with executing the modified scale derivative

$$\begin{aligned}\tilde{\partial}_t \delta_0 \int_p \frac{iH_k''}{\xi_\varphi} &= \delta_0 iH_k'' \int_p \int_x \frac{(-1)}{\xi_\varphi^2} p^2 Z_{\varphi,k} \frac{\delta r_{kB}(p)}{\delta r_{kB}(x)} \frac{\partial_t(Z_{\varphi,k} r_{kB}(x))}{Z_{\varphi,k}} \\ &= -i\delta_0 H_k'' \int_p p^2 \frac{\partial_t(Z_{\varphi,k} r_{kB}(p))}{\xi_\varphi^2}.\end{aligned}\quad (4.2.10)$$

Up to coefficients resulting from the projection rule and the log-expansion, this is our first contribution to the flow equation of  $H_k$ . Let us now consider the second order contributions. First of all we have to compute the square of  $\frac{\Delta\Gamma_k^{(2)}}{\Gamma_{\varphi,k}^{(2)} + R_k}$ . Because the (1,1) entry already contains  $\psi$  as well as  $\bar{\psi}$ , we can effectively set it to zero when calculating the square. The interesting parts then read

$$\begin{aligned}\left(\frac{\Delta\Gamma_k^{(2)}}{\Gamma_{\varphi,k}^{(2)} + R_k}\right)^2(p,q) &\approx -(H_k')^2 \delta_{p,q} \times \\ &\begin{pmatrix} -\frac{Z_{\psi,k}(1+r_{kF})}{\xi_\varphi \xi_\psi} (\bar{\psi} \not{p} \psi + \psi^T \not{p}^T \bar{\psi}^T) & 0 & 0 \\ -\frac{2iH_k}{\xi_\varphi \xi_\psi} \bar{\psi} \not{p} \psi & -\frac{Z_{\psi,k}(1+r_{kF}) \not{p} + iH_k}{\xi_\varphi \xi_\psi} \psi \bar{\psi} & 0 \\ 0 & 0 & -\frac{Z_{\psi,k}(1+r_{kF}) \not{p}^T - iH_k}{\xi_\varphi \xi_\psi} \bar{\psi}^T \psi^T \end{pmatrix}.\end{aligned}\quad (4.2.11)$$

In the (1,1) element the terms containing the slashed momenta will cancel each other, because

$$\bar{\psi} \not{p} \psi + \psi^T \not{p}^T \bar{\psi}^T = \bar{\psi} \not{p} \psi - \bar{\psi} \not{p} \psi = 0,$$

where we used that transposing the second scalar yields a minus sign since we changed the order between the fermionic fields. This leaves us only with the term  $-\frac{2iH_k}{\xi_\varphi \xi_\psi} \bar{\psi} \not{p} \psi$  in the (1,1) element, which makes the further calculations in this sector similar to the steps above. We thus state only the final result (including the  $-\frac{1}{2}$  from the log-expansion):

$$i\delta_0 H_k (H_k')^2 \int_p \frac{p^2 \partial_t(Z_{\varphi,k} r_{kB})}{\xi_\varphi^2 \xi_\psi} + \frac{2p^2 Z_{\psi,k} (1+r_{kF}) \partial_t(Z_{\psi,k} r_{kF})}{\xi_\varphi \xi_\psi^2}.\quad (4.2.12)$$

## 4.2 The generalized Yukawa coupling

---

Let us now consider the fermionic sectors. Note that we have to take a factor  $(-1)$  in front of each term into account, according to our definition of the super trace, as well as we have to take the trace over the Dirac indices. Still the terms with slashed momenta cancel:

$$\begin{aligned}\mathrm{Tr}_\gamma(\not{p}\psi\bar{\psi}) + \mathrm{Tr}_\gamma(\not{p}^T\bar{\psi}^T\psi^T) &= \mathrm{Tr}_\gamma(\not{p}\psi\bar{\psi}) - \mathrm{Tr}_\gamma(\psi\bar{\psi}\not{p}) \\ &= \mathrm{Tr}_\gamma(\not{p}\psi\bar{\psi}) - \mathrm{Tr}_\gamma(\not{p}\psi\bar{\psi}) \\ &= 0.\end{aligned}$$

In the second step we used the cyclicity of the trace, but because we did not change the order between  $\psi$  and  $\bar{\psi}$  no extra minus occurs. Furthermore, since

$$\mathrm{Tr}_\gamma(\bar{\psi}^T\psi^T) = -\mathrm{Tr}_\gamma(\psi\bar{\psi}),$$

the (2, 2) and (3, 3) entry yield the same contribution. By setting  $p = q$  and by integrating over  $p$  we get (including the  $-\frac{1}{2}$  from the log-expansion and the  $(-1)$  due to spin statistics)

$$(-1) \left(-\frac{1}{2}\right) \delta_0(-1)(H'_k)^2 \int_p \left(-\frac{2iH_k}{\xi_\varphi\xi_\psi}\right) \mathrm{Tr}_\gamma(\psi\bar{\psi}). \quad (4.2.13)$$

Performing the field derivatives as earlier gives

$$-i\delta_0 d_\gamma H_k (H'_k)^2 \int_p \frac{1}{\xi_\varphi\xi_\psi} \mathbb{1}_{d_\gamma}, \quad (4.2.14)$$

where we can skip the factor  $\mathbb{1}_{d_\gamma}$  again. It is straightforward to compute the modified scale derivative, which leads to

$$i\delta_0 H_k (H'_k)^2 \int_p \frac{p^2 \partial_t(Z_{\varphi,k} r_{kB})}{\xi_\varphi^2 \xi_\psi} + \frac{2Z_{\psi,k} p^2 (1 + r_{kF}) \partial_t(Z_{\psi,k} r_{kF})}{\xi_\varphi \xi_\psi^2}. \quad (4.2.15)$$

Now we can write down the full flow equation by collecting all these terms and by including the missing coefficients. We finally find

$$\begin{aligned} \partial_t H_k(\varphi) = & -\frac{1}{2} \int_p \frac{p^2 H_k''(\varphi) \partial_t(Z_{\varphi,k} r_{kB}(p))}{\xi_\varphi^2(p)} \\ & + \frac{1}{2} \int_p H_k(\varphi) H_k'^2(\varphi) \left\{ \frac{2p^2 \partial_t(Z_{\varphi,k} r_{kB}(p))}{\xi_\varphi^2(p) \xi_\psi(p)} + \frac{4Z_{\psi,k} p^2 (1 + r_{kF}(p)) \partial_t(Z_{\psi,k} r_{kF}(p))}{\xi_\varphi(p) \xi_\psi^2(p)} \right\}. \end{aligned} \quad (4.2.16)$$

It is convenient to express the result in terms of the so-called threshold functions. Their definition is given in appendix A. In terms of these threshold functions the expression above reads

$$\begin{aligned} \partial_t H_k(\varphi) = & -2H_k''(\varphi) Z_{\varphi,k}^{-1} v_d k^{d-2} l_1^d \left[ Z_{\varphi,k}^{-1} k^{-2} U_k''(\varphi); \eta_\varphi \right] \\ & + 4v_d k^{d-4} Z_{\varphi,k}^{-1} Z_{\psi,k}^{-2} H_k(\varphi) H_k'^2(\varphi) l_{1,1}^{(FB)d} \left[ Z_{\psi,k}^{-2} k^{-2} H_k^2(\varphi), Z_{\varphi,k}^{-1} k^{-2} U_k''(\varphi); \eta_\psi, \eta_\phi \right], \end{aligned} \quad (4.2.17)$$

where  $\frac{1}{v_d} = 2^{d+1} \pi^{\frac{d}{2}} \Gamma(\frac{d}{2})$ . This fully agrees with the flow equation derived in [33], where the authors also considered the  $\mathbb{Z}_2$ -symmetric Higgs-Yukawa model at zero temperature. However, they are discussing the system for a continuous number of fermion degrees  $X_f = d_\gamma N_f$ , where  $N_f$  is the number of fermions. In this thesis we so far considered the  $N_f = 1$  case. Comparing this result with former works on the Higgs-Yukawa system including only the standard Yukawa interaction  $\mathfrak{h}_0 \varphi \bar{\psi} \psi$  (see [13], [14] or the corresponding joined work [11]) we find that especially the term  $\sim H_k''$  will be interesting because in the former truncation  $H(\varphi) = \mathfrak{h}_0 \varphi$  it did not appear at all. In the same manner the combination  $H_k H_k'^2$  corresponds to the inclusion of new terms. By taking them into account we hope that we can further decrease the lower Higgs mass bounds.

### 4.3 The effective potential

A first consideration of the flow of the effective potential can for example be found in [12]. To extract the of the potential from the flow of the full effective action we use the projection according to [13]

$$\delta_0 U_k(\varphi_0) = \Gamma_k \left| \begin{array}{l} \varphi = \varphi_0 = \text{const} \\ \psi = \bar{\psi} = 0 \end{array} \right.$$

and therefore the flow equation reads (we skip the subscript on  $\varphi$  as usual)

$$\delta_0 \partial_t U_k(\varphi) = \frac{1}{2} \text{STr} \left[ \frac{\partial_t R_k}{\Gamma_k^{(2)} + R_k} \right] \left| \begin{array}{l} \varphi = \text{const} \\ \psi = \bar{\psi} = 0 \end{array} \right. \quad (4.3.1)$$

This projection is much simpler than in the case of  $H_k$ , because we do not have to apply any field derivatives. We are even allowed to set  $\psi$  and  $\bar{\psi}$  to zero right from the beginning, which simplifies the fluctuation matrix (4.1.3) significantly. We do not have to make use of the trick involving the modified scale derivative either, it is possible to straightforwardly compute  $\frac{\partial_t R_k}{\Gamma_k^{(2)} + R_k}$  and take the super trace. We find

$$\partial_t U_k(\varphi) = \frac{1}{2} \int_p \frac{p^2 \partial_t (Z_{\varphi,k} r_{kB}(p))}{\xi_\varphi(p)} - d_\gamma \int_p \frac{p^2 Z_{\psi,k} (1 + r_{kF}(p)) \partial_t (Z_{\psi,k} r_{kF}(p))}{\xi_\psi(p)}, \quad (4.3.2)$$

or again expressed in terms of threshold functions

$$\partial_t U_k(\varphi) = 2v_d k^d l_0^d \left[ Z_{\varphi,k}^{-1} k^{-2} U_k''(\varphi); \eta_\varphi \right] - 2d_\gamma v_d k^d l_0^{(F)d} \left[ Z_{\psi,k}^{-2} k^{-2} H_k^2; \eta_\psi \right]. \quad (4.3.3)$$

Again our result matches with the flow equation derived in [33]. If we compare it with the former results corresponding to the standard Yukawa coupling [13], [14], [11] we find that, as expected, no additional terms appear in the flow of the effective potential. The only difference in the flow equation is that in the denominator of the fermionic contribution (second term of equation (4.3.2)) we have  $\xi_\psi(q) = Z_{\psi,k}^2 P_F(q) + H_k^2(\varphi)$  instead of  $Z_{\psi,k}^2 P_F(q) + \varphi^2 \mathfrak{h}_0^2$ . Hence, our result is consistent with the old one because we easily recover it by choosing  $H(\varphi) = \mathfrak{h}_0 \varphi$ . The fact that we only have to substitute  $h_k^2 \varphi^2 \rightarrow H_k^2$  goes hand in hand with the calculations essentially being the same in both cases. Thus, we decided to only state the final result, the detailed calculations can be found in [13], [14].

## 4.4 The anomalous dimensions

In this section we deal with the flow of the field renormalizations  $Z_{\psi,k}$  and  $Z_{\varphi,k}$ . Let us start with the scalar field renormalization. The projection rule is given by [13]

$$\delta_0 Z_{\varphi,k} = \frac{1}{2d} \eta^{\rho\sigma} \partial_{q^\rho} \partial_{q^\sigma} \frac{\delta}{\delta\sigma(q)} \frac{\delta}{\delta\sigma(p')} \Gamma_k \Bigg|_{\substack{\sigma=0 \\ \psi=\bar{\psi}=0 \\ p'=-q \\ p'=-q=0}}. \quad (4.4.1)$$

We introduced the fluctuation of the scalar field around the vacuum expectation value,  $\sigma = \varphi - v$ . The reason why we only set  $\sigma$  to zero instead of the entire field  $\varphi$  is that in the spontaneously broken, regime we explicitly have a non-vanishing vacuum expectation value (which itself will be a scale dependent quantity, too). Therefore, it is important to take operators of the form  $v_k^n \partial_\mu \sigma \partial^\mu \sigma$  into account when calculating the flow of  $Z_{\varphi,k}$ . Furthermore, unlike the cases of  $H_k$  and  $U_k$ , we have to leave at least the fluctuation around the vacuum expectation value with some momentum. After performing the field derivatives we have to set  $p' = -q$  and then we can take the momentum derivatives. As a last step  $q$  (respectively  $-p'$ ) is set to zero. Because it is somewhat more complicated, let us quickly check the projection rule. The only term of the effective action we have to consider is the kinetic term of the scalar field:

$$\begin{aligned} & \frac{1}{2d} \eta^{\rho\sigma} \partial_{q^\rho} \partial_{q^\sigma} \frac{\delta}{\delta\sigma(q)} \frac{\delta}{\delta\sigma(p')} \int_p \frac{1}{2} Z_{\varphi,k} p^\lambda p_\lambda \varphi(p) \varphi(-p) \\ &= \frac{1}{2d} \eta^{\rho\sigma} \partial_{q^\rho} \partial_{q^\sigma} \int_p \frac{1}{2} Z_{\varphi,k} p^\lambda p_\lambda \frac{\delta}{\delta\sigma(q)} (\delta_{p,p'} \varphi(-p) + \varphi(p) \delta_{-p,p'}) \\ &= \frac{1}{2d} \eta^{\rho\sigma} \partial_{q^\rho} \partial_{q^\sigma} \int_p \frac{1}{2} Z_{\varphi,k} p^\lambda p_\lambda (\delta_{p,p'} \delta_{-p,q} + \delta_{p,q} \delta_{-p,p'}) \\ &= \frac{1}{2d} Z_{\varphi,k} \eta^{\rho\sigma} \partial_{q^\rho} \partial_{q^\sigma} (\delta_{-q,p'} q^\lambda q^\lambda) \end{aligned}$$

Now we set  $p' = -q$  and perform the momentum derivatives, which indeed yields  $\delta_0 Z_{\varphi,k}$ . According to this we see that the derivation of the flow equation will be much more technical, since one has to be very careful of how to treat the momenta. However, just like in the case of  $U_k$ , the fluctuation matrix becomes simpler because the fermionic fields are set to zero. We expect that no new terms will occur in comparison to the old truncation, because any new fluctuation terms involving  $H_k$  vanish under the projection  $\bar{\psi} = \psi = 0$ . Indeed we reproduce the old results up to natural substitutions like  $h_k^2 v_k^2 \rightarrow H_k^2(v_k)$  or  $h_k^2 \rightarrow H_k^2(v_k)$ . The reason why these functions are evaluated at the vacuum expectation value is just due to setting  $\sigma$  to zero. Furthermore, there occurs a term containing the third derivative of the scalar potential. It arises because during the calculations we expand the effective potential into a power series about the vacuum expectation value in order to properly perform the field derivatives with respect to  $\sigma$ .

Furthermore, we have to apply the trick involving the expansion of the logarithm again and finally make use of the fact that only terms containing exactly two fields  $\sigma$  will contribute according to the projection rule. Because the fluctuation matrix already includes second derivatives of the effective potential (see (4.1.1)) we end up with third derivatives. For detailed calculations we refer to [13], [14], because again the result is the same up to the substitutions mentioned in the case of  $U_k$ . Consequently, we just state the final result

$$\begin{aligned} \partial_t Z_{\varphi,k} = & \frac{1}{d} \int_p \tilde{\partial}_t \left\{ p^2 \left( \partial_{p^2} \frac{U_k^{(3)}(v_k)}{\xi_\varphi(p)} \right)^2 \right\} \\ & + \frac{2d_\gamma}{d} H_k'^2(v_k) \int_p \tilde{\partial}_t \left\{ p^4 \left( \partial_{p^2} \frac{Z_{\psi,k}(1+r_{kF}(p))}{\xi_\psi(p)} \right)^2 \right\} \\ & - \frac{2d_\gamma}{d} H_k'^2(v_k) \int_p \tilde{\partial}_t \left\{ p^2 \left( \partial_{p^2} \frac{H_k(v_k)}{\xi_\psi(p)} \right)^2 \right\}. \end{aligned} \quad (4.4.2)$$

In case of the field renormalizations it is more convenient not to perform the modified scale derivative right now, it will be done later when we start with the numerical analysis. In terms of the threshold functions we obtain<sup>4</sup>

$$\begin{aligned} \partial_t Z_{\varphi,k} = & -\frac{4}{d} v_d k^{d-6} \left( U_k^{(3)} \right)^2 Z_{\varphi,k}^{-2} m_{2,2}^d \left[ Z_{\varphi,k}^{-1} k^{-2} U_k''(v_k), Z_{\varphi,k}^{-1} k^{-2} U_k''(v_k); \eta_\varphi \right] \\ & - \frac{8}{d} d_\gamma v_d k^{d-4} H_k'^2(v_k) Z_{\psi,k}^{-2} m_4^{(F)d} \left[ Z_{\psi,k}^{-2} k^{-2} H_k^2(v_k); \eta_\varphi \right] \\ & + \frac{8}{d} d_\gamma v_d k^{d-6} H_k'^2(v_k) H_k^2(v_k) Z_{\psi,k}^{-4} m_2^{(F)d} \left[ Z_{\psi,k}^{-2} k^{-2} H_k^2(v_k); \eta_\psi \right]. \end{aligned} \quad (4.4.3)$$

The flow of  $Z_{\varphi,k}$  agrees with the result derived in [33]. As mentioned before, the flow in the former truncation [13], [14] is reproduced for the choice  $H_k = \mathfrak{h}_0 \varphi$ . For a general choice however, the combinations of  $H_k$  and  $H_k'$  will generate new contributions. The discussion we held on  $Z_{\varphi,k}$  is also valid for  $Z_{\psi,k}$ . Hence, we consequently just state the corresponding projection rule [13] and the final result for the flow equation. The projection reads

$$\delta_0 Z_{\psi,k} = -\frac{1}{dd_\gamma} \text{Tr}_\gamma \gamma^\mu \partial_{p'^\mu} \frac{\overrightarrow{\delta}}{\delta \bar{\psi}(p')} \Gamma_k \frac{\overleftarrow{\delta}}{\delta \psi(q)} \Bigg|_{\substack{\sigma = 0 \\ \psi = \bar{\psi} = 0 \\ q = p' \\ q = p' = 0}}, \quad (4.4.4)$$

<sup>4</sup>A short comment on why there suddenly appear derivatives with respect to  $p^2$ : Actually, the functions  $\xi_\psi$  and  $\xi_\phi$  are functions of  $p^2$  rather than  $p$ , because the functions  $P = p^2 \left( 1 + r_{kB} \left( \frac{p^2}{k^2} \right) \right)$  and  $P_F = p^2 \left( 1 + r_{kF} \left( \frac{p^2}{k^2} \right) \right)^2$  depend on  $p^2$ . During the calculations terms like  $p^\sigma \partial_{p^\sigma} u(p^2)$  appear, which can be rewritten as  $2p^2 \partial_{p^2} u(p^2)$ .

and for the flow equation we get

$$\partial_t Z_{\psi,k} = -\frac{2}{d} H_k'^2(v_k) \tilde{\partial}_t \int_p \frac{Z_{\psi,k}(1+r_{kF}(p))}{\xi_{\psi}(p)} p^2 \partial_{p^2} \frac{1}{\xi_{\varphi}(p)}. \quad (4.4.5)$$

Expressed in terms of the threshold functions we finally obtain

$$\partial_t Z_{\psi,k} = -\frac{8}{d} H_k'^2(v_k) v_d k^{d-4} Z_{\psi,k}^{-1} Z_{\varphi,k}^{-1} m_{1,2}^{(FB)d} \left[ Z_{\psi,k}^{-2} k^{-2} H_k^2(v_k), Z_{\varphi,k}^{-1} k^{-2} U_k''(v_k); \eta_{\psi}, \eta_{\varphi} \right]. \quad (4.4.6)$$

The result matches with [33] and the choice  $H_k = \mathfrak{h}_0 \varphi$  reproduces the former results of [13], [14]. In general, the pre-factor  $H_k'^2$  in front of the threshold function will generate new terms.

There is one more interesting feature concerning these flow equations. In the next chapter we will see that if we switch over to dimensionless quantities and after choosing our specific regulator functions we can transform the coupled differential equations (4.4.2) and (4.4.5) into an algebraic system by introducing the anomalous field dimensions  $\eta_{\varphi,k} = -\partial_t \log Z_{\varphi,k}$  and  $\eta_{\psi,k} = -\partial_t \log Z_{\psi,k}$ .

# 5 Numerical analysis

## 5.1 Rewriting the flow equations

Before we can start a proper numerical analysis of the flow equations, it is convenient to rewrite them using dimensionless quantities. A simple power counting of the mass dimension of the fields yields

$$[\varphi] = \frac{d-2}{2}, \quad [\psi] = \frac{d-1}{2}.$$

We thus introduce the renormalized and dimensionless field variables

$$\tilde{\varphi} = Z_{\varphi,k}^{\frac{1}{2}} k^{\frac{2-d}{2}} \varphi, \quad \tilde{\psi} = Z_{\psi,k}^{\frac{1}{2}} k^{\frac{1-d}{2}} \psi,$$

as well as the dimensionless effective potential and the dimensionless generalized Yukawa coupling

$$\tilde{U}_k = k^{-d} U_k, \quad \tilde{H}_k = Z_{\psi,k}^{-1} k^{-1} H_k.$$

Before we move on we finally want to treat the effective potential as a function of  $\varphi^2$  or more conveniently of  $\rho = \frac{1}{2}\varphi^2$ . Thus, in the following all field derivatives of the effective potential are defined with respect to  $\rho$  or its dimensionless counterpart. Furthermore, we also caused a "dimensional" flow, because the pre-factors of the quantities are now scale dependent, too. We obtain

$$\begin{aligned} \partial_t \tilde{U}_k(\tilde{\rho}) &= -d \tilde{U}_k + (d-2 + \eta_{\varphi,k}) \tilde{\rho} \tilde{U}'_k(\tilde{\rho}) + k^{-d} \partial_t U_k, \quad \tilde{\rho} = \frac{1}{2} \tilde{\varphi}^2 \\ \partial_t \tilde{H}_k(\tilde{\varphi}) &= (\eta_{\psi,k} - 1) \tilde{H}_k + \left( \frac{d}{2} - 1 + \frac{\eta_{\varphi,k}}{2} \right) \tilde{\varphi} \tilde{H}'_k(\tilde{\varphi}) + k^{-1} Z_{\psi,k}^{-1} \partial_t H_k. \end{aligned}$$

The expressions for  $\partial_t U_k$  and  $\partial_t H_k$  can be read off from equation (4.3.2) and from equation (4.2.16) respectively. We only have to rewrite them in our new variables as well. For example, in equation (4.3.2) we have

$$\begin{aligned} \xi_{\varphi}(p) &= Z_{\varphi,k} P(p) + \frac{d^2}{d\varphi^2} U_k(\varphi) \\ &= Z_{\varphi,k} P(p) + Z_{\varphi,k} k^2 \left( 2\tilde{\rho} \tilde{U}''_k(\tilde{\rho}) + \tilde{U}'_k(\tilde{\rho}) \right). \end{aligned}$$

Performing similar calculations for the other terms and introducing

$$\begin{aligned}\mathcal{D}[\tilde{U}_k](\tilde{\rho}) &= \tilde{\rho} \left( 3\tilde{U}_k''(\tilde{\rho}) + 2\tilde{\rho}\tilde{U}_k'''(\tilde{\rho}) \right)^2 \\ \omega_u(\tilde{\rho}) &= 2\tilde{\rho}\tilde{U}_k''(\tilde{\rho}) + \tilde{U}_k'(\tilde{\rho}) \\ \tilde{\kappa}_k &= \frac{1}{2}\tilde{v}_k^2\end{aligned}$$

we finally find

$$\begin{aligned}\partial_t \tilde{U}_k(\tilde{\rho}) &= -d\tilde{U}_k + (d-2 + \eta_{\varphi,k})\tilde{\rho}\tilde{U}_k'(\tilde{\rho}) + 2v_d l_0^d \left[ \omega_u(\tilde{\rho}); \eta_\varphi \right] - 2d_\gamma v_d l_0^{(F)d} \left[ \tilde{H}_k^2(\tilde{\varphi}); \eta_\psi \right] \\ \partial_t \tilde{H}_k(\tilde{\varphi}) &= (\eta_{\psi,k} - 1)\tilde{H}_k + \left( \frac{d}{2} - 1 + \frac{\eta_{\varphi,k}}{2} \right) \tilde{\varphi}\tilde{H}_k'(\tilde{\varphi}) - 2\tilde{H}_k''(\tilde{\varphi})v_d l_1^d \left[ \omega_u(\tilde{\rho}); \eta_\varphi \right] \\ &\quad + 4v_d \tilde{H}_k(\tilde{\varphi})\tilde{H}_k'^2(\tilde{\varphi})l_{1,1}^{(FB)d} \left[ \tilde{H}_k^2(\tilde{\varphi}), \omega_u(\tilde{\rho}); \eta_\psi, \eta_\phi \right] \\ \partial_t Z_{\psi,k} &= -\frac{8}{d}\tilde{H}_k'^2(\tilde{v}_k)v_d Z_{\psi,k} m_{1,2}^{(FB)d} \left[ \tilde{H}_k^2(\tilde{v}_k), \omega_u(\tilde{\kappa}_k); \eta_\psi, \eta_\varphi \right] \\ \partial_t Z_{\varphi,k} &= -\frac{4}{d}v_d Z_{\varphi,k} \mathcal{D}[\tilde{U}_k](\tilde{\kappa}_k) m_{2,2}^d \left[ \omega_u(\tilde{\kappa}_k), \omega_u(\tilde{\kappa}_k); \eta_\varphi \right] \\ &\quad - \frac{8}{d}d_\gamma v_d Z_{\varphi,k} \tilde{H}_k'^2(\tilde{v}_k) m_4^{(F)d} \left[ \tilde{H}_k^2(\tilde{v}_k); \eta_\varphi \right] \\ &\quad + \frac{8}{d}d_\gamma v_d Z_{\varphi,k} \tilde{H}_k'^2(\tilde{v}_k)\tilde{H}_k^2(\tilde{v}_k) m_2^{(F)d} \left[ \tilde{H}_k^2(\tilde{v}_k); \eta_\psi \right].\end{aligned}\tag{5.1.1}$$

The flow equations of the  $Z_i$  can be multiplied by a factor  $-Z_{i,k}^{-1}$ , which yields the anomalous dimensions  $\eta_{i,k}$  on the left hand side of the equations. Remember the fact that concerning  $\tilde{U}_k$  primes denote derivatives with respect to  $\tilde{\rho}$ , whereas concerning  $\tilde{H}_k$ , primes still denote derivatives with respect to  $\tilde{\varphi}$ . Because we will only deal with the dimensionless quantities in this chapter, we furthermore skip the tilde again, if nothing else is stated.

## 5.2 Choosing the regulator functions

The next step is to choose specific regulator functions so that we can finally perform the remaining momentum integrals encoded in the threshold functions. There are various possibilities to choose regulator functions that satisfy the conditions (2.2.5). However, since the choice of the regulator functions affects the flow of the effective action, one should ensure that the flow remains as stable as possible and converges fast towards the physical theory. The corresponding optimization of the regulator functions has already been investigated a lot (see e.g. [22], [34], [35]). It turned out that choosing the following "Litim regulator" is reasonable

$$\begin{aligned}R_{kB} &= Z_{\varphi,k} p^2 r_{kB} \stackrel{choice}{=} Z_{\varphi,k} (k^2 - p^2) \Theta[k^2 - p^2] \\ R_{kF} &= -Z_{\psi,k} p r_{kF}, \quad (1 + r_{kF})^2 \stackrel{choice}{=} 1 + r_{kB},\end{aligned}\tag{5.2.1}$$

## 5.2 Choosing the regulator functions

---

where  $r_{kB} = \left(\frac{k^2}{p^2} - 1\right) \Theta[k^2 - p^2]$  according to the first equation. Another advantage of this regulator choice is the fact that the integrals can be performed analytically. Let us consider the threshold function  $l_1^d[\omega_u(\rho); \eta_\varphi]$  in the flow equation of  $H_k$  as an example. It reads

$$l_1^d[\omega_u(\rho); \eta_\varphi] = \frac{1}{4} v_d^{-1} k^{2-d} \int_q \frac{\partial_t R_{kB}}{Z_{\varphi,k}(P(p) + k^2 \omega_u(\rho))^2}.$$

By using

$$P(p) = p^2(1 + r_{kB}) = p^2 \left(1 + \left(\frac{k^2}{p^2} - 1\right) \Theta[k^2 - p^2]\right)$$

and

$$\begin{aligned} Z_{\varphi,k}^{-1} \partial_t R_{kB} &= Z_{\varphi,k}^{-1} p^2 \partial_t (Z_{\varphi,k} r_{kB}) \\ &= -\eta_{\varphi,k} (k^2 - p^2) \Theta[k^2 - p^2] + 2k^2 \Theta[k^2 - p^2] + 2k^2 (k^2 - p^2) \delta(k^2 - p^2) \end{aligned}$$

we are left with<sup>1</sup>

$$\begin{aligned} &\frac{1}{4} v_d^{-1} k^{2-d} \int_p \frac{-\eta_{\varphi,k} (k^2 - p^2) \Theta[k^2 - p^2] + 2k^2 \Theta[k^2 - p^2]}{\left(p^2 \left(1 + \left(\frac{k^2}{p^2} - 1\right) \Theta[k^2 - p^2]\right) + k^2 \omega_u(\rho)\right)^2} \\ &= \frac{1}{4} v_d^{-1} k^{2-d} \frac{1}{(2\pi)^d} \text{Vol}(S^{d-1}) \int_0^k dp p^{d-1} \frac{-\eta_{\varphi,k} (k^2 - p^2) + 2k^2}{k^4 (1 + \omega_u(\rho))^2} \\ &= \frac{1}{4} v_d^{-1} k^{2-d} k^{d-2} \frac{2}{d(2\pi)^d} \text{Vol}(S^{d-1}) \frac{1}{(1 + \omega_u(\rho))^2} \left(1 - \frac{\eta_{\varphi,k}}{d+2}\right) \\ &= \frac{2}{d} \frac{1}{(1 + \omega_u(\rho))^2} \left(1 - \frac{\eta_{\varphi,k}}{d+2}\right), \end{aligned}$$

where  $\text{Vol}(S^{d-1})$  is the surface area of the  $(d-1)$ -sphere. This result agrees with [36]. The computation of the other threshold functions works similarly and does match with the threshold functions given in [36] as well.

---

<sup>1</sup>The term proportional to  $(k^2 - p^2) \delta(k^2 - p^2)$  does not contribute when we integrate over the full momentum space.

## 5.2 Choosing the regulator functions

---

Appendix B shows all appearing threshold functions after the application of the regulator. Eventually, the flow equations (5.1.1) read

$$\begin{aligned}
\partial_t U_k(\rho) &= -dU_k(\rho) + (d-2 + \eta_{\varphi,k})\rho U'_k(\rho) + \frac{4v_d}{d} \left[ \frac{1 - \frac{\eta_{\varphi,k}}{d+2}}{1 + \omega_u(\rho)} - d_\gamma \frac{1 - \frac{\eta_{\psi,k}}{d+1}}{1 + H_k^2(\varphi)} \right] \\
\partial_t H_k(\varphi) &= (\eta_{\psi,k} - 1)H_k(\varphi) + \left( \frac{d}{2} - 1 + \frac{\eta_{\varphi,k}}{2} \right) \varphi H'_k(\varphi) \\
&\quad - \frac{4v_d}{d} H_k''(\varphi) \frac{1}{(1 + \omega_u(\rho))^2} \left[ 1 - \frac{\eta_{\varphi,k}}{d+2} \right] \\
&\quad + \frac{8v_d}{d} H_k(\varphi) H_k'^2(\varphi) \frac{1}{1 + H_k^2} \frac{1}{(1 + \omega_u(\rho))^2} \left[ 1 - \frac{\eta_{\varphi,k}}{d+2} \right] \\
&\quad + \frac{8v_d}{d} H_k(\varphi) H_k'^2(\varphi) \frac{1}{(1 + H_k^2)^2} \frac{1}{1 + \omega_u(\rho)} \left[ 1 - \frac{\eta_{\psi,k}}{d+1} \right] \\
\eta_{\varphi,k} &= \frac{4v_d}{d} \mathcal{D}[U_k](\kappa_k) \frac{1}{(1 + \omega_u(\kappa_k))^4} \\
&\quad + \frac{8v_d}{d} d_\gamma H_k'^2(v_k) \left\{ \frac{1}{(1 + H_k^2(v_k))^4} + \frac{1 - \eta_{\psi,k}}{d-2} \frac{1}{(1 + H_k^2(v_k))^3} \right. \\
&\quad \left. - \left( \frac{1 - \eta_{\psi,k}}{2d-4} + \frac{1}{4} \right) \frac{1}{(1 + H_k^2(v_k))^2} \right\} \\
\eta_{\psi,k} &= \frac{8v_d}{d} H_k'^2(v_k) \left( 1 - \frac{\eta_{\varphi,k}}{d+1} \right) \frac{1}{(1 + H_k^2(v_k))^2} \frac{1}{(1 + \omega_u(\kappa_k))^2}. \tag{5.2.2}
\end{aligned}$$

Now the differential-algebraic nature of the equation system is obvious. The last two equations of the anomalous dimensions are purely algebraic, the solutions can then be inserted into the two remaining differential equations of  $H_k$  and  $U_k$ . However, there is still a little inconvenience: We mixed between the variables  $\varphi$  and  $\rho$ . It is not difficult to rewrite everything in terms of  $\rho$ . For example  $H_k^2(\varphi) = \varphi^2 h_k^2(\rho) = 2\rho h_k(\rho)$ . In the case of the flow equation of  $H_k$  there is a little subtlety: Here the rewriting causes the appearance of a global factor  $\varphi$ , e.g.

$$H_k''(\varphi) = \varphi(3\partial_\rho h_k + 2\rho\partial_\rho^2 h_k).$$

This global  $\varphi$  on the right hand side of the flow equation cancels with the  $\varphi$  on the left hand side,  $\partial_t H_k = \varphi \partial_t h_k$ , which leaves us with the flow equation of  $h_k(\rho)$ .

Hence, we finally find

$$\begin{aligned}
 \partial_t U_k(\rho) &= -d U_k(\rho) + (d-2 + \eta_{\varphi,k}) \rho U_k'(\rho) + \frac{4v_d}{d} \left[ \frac{1 - \frac{\eta_{\varphi,k}}{d+2}}{1 + \omega_u(\rho)} - d_\gamma \frac{1 - \frac{\eta_{\psi,k}}{d+1}}{1 + 2\rho h_k^2} \right] \\
 \partial_t h_k(\rho) &= (\eta_{\psi,k} - 1) h_k(\rho) + \left( \frac{d}{2} - 1 + \frac{\eta_{\varphi,k}}{2} \right) (h_k(\rho) + 2\rho h_k'(\rho)) \\
 &\quad - \frac{4v_d}{d} (3h_k'(\rho) + 2\rho h_k''(\rho)) \frac{1}{(1 + \omega_u(\rho))^2} \left[ 1 - \frac{\eta_{\varphi,k}}{d+2} \right] \\
 &\quad + \frac{8v_d}{d} h_k(\rho) (h_k(\rho) + 2\rho h_k'(\rho))^2 \frac{1}{1 + 2\rho h_k^2(\rho)} \frac{1}{(1 + \omega_u(\rho))^2} \left[ 1 - \frac{\eta_{\varphi,k}}{d+2} \right] \\
 &\quad + \frac{8v_d}{d} h_k(\rho) (h_k(\rho) + 2\rho h_k'(\rho))^2 \frac{1}{(1 + 2\rho h_k^2(\rho))^2} \frac{1}{1 + \omega_u(\rho)} \left[ 1 - \frac{\eta_{\psi,k}}{d+1} \right] \\
 \eta_{\varphi,k} &= \frac{4v_d}{d} \mathcal{D}[U_k](\kappa_k) \frac{1}{(1 + \omega_u(\kappa_k))^4} \\
 &\quad + \frac{8v_d}{d} d_\gamma (h_k(\kappa_k) + 2\kappa_k h_k'(\kappa_k))^2 \left\{ \frac{1}{(1 + 2\kappa_k h_k^2(\kappa_k))^4} \right. \\
 &\quad \left. + \frac{1 - \eta_{\psi,k}}{d-2} \frac{1}{(1 + 2\kappa_k h_k^2(\kappa_k))^3} - \left( \frac{1 - \eta_{\psi,k}}{2d-4} + \frac{1}{4} \right) \frac{1}{(1 + 2\kappa_k h_k^2(\kappa_k))^2} \right\} \\
 \eta_{\psi,k} &= \frac{8v_d}{d} (h_k(\kappa_k) + 2\kappa_k h_k'(\kappa_k))^2 \left( 1 - \frac{\eta_{\varphi,k}}{d+1} \right) \frac{1}{(1 + 2\kappa_k h_k^2(\kappa_k))^2} \frac{1}{(1 + \omega_u(\kappa_k))^2}.
 \end{aligned} \tag{5.2.3}$$

Now primes only denote derivatives with respect to  $\rho$ .

Before we go further a short comment on why it suffices to consider only one specific regulator, although we explained in subsection 2.2.3 that due to truncating our theory the IR physics (and thus possibly the Higgs mass bound as well) becomes dependent of the regulator. The point is that we fix our theory in the IR rather than the UV, because the UV values of the couplings are experimentally not accessible. If we consider a specific UV set-up that yields a corresponding Higgs mass, then of course, the usage of a different regulator with the same UV set-up might yield a different mass. However, we could just change the UV set-up in order to recover the original Higgs mass. In this sense, the Higgs mass bounds do not depend on the choice of the regulator as long as we adjust the bare couplings correctly. Since we are not interested in their actual value but only in the IR physics we are fine with using only the Litim regulator for our analysis.

## 5.3 Truncation of the effective potential and the generalized Yukawa coupling

We will now perform one last approximation, because the full equations (5.2.3) are still too complicated to be solved. Our ansatz will be to expand the effective potential and the generalized Yukawa coupling about the vacuum expectation value. We thus have to distinguish between the symmetric phase and the spontaneously broken phase. The latter one will be slightly more complicated, because the vacuum expectation value itself is scale dependent as well.

### 5.3.1 Symmetric phase

In the symmetric phase we expand about  $v_k = 0$ . Thus, our expansions read

$$U_k(\rho) = \sum_{i=1}^n \frac{u_i(t)}{i!} \rho^i, \quad h_k(\rho) = \sum_{j=0}^m \frac{\mathfrak{h}_j(t)}{j!} \rho^j.$$

Here  $n$  and  $m$  are the orders of the truncations of  $U_k$  and  $h_k$ , they correspond to the amount of operators that are taken into account. We will choose finite  $n$  and  $m$  and solve the flow of the couplings  $u_i$  and  $\mathfrak{h}_j$ . Their flow equations can be easily derived:

$$\begin{aligned} \partial_t u_i &= \partial_\rho^{(i)} (\partial_t U_k) \Big|_{\rho=0}, \quad i = 1, \dots, n \\ \partial_t \mathfrak{h}_j &= \partial_\rho^{(j)} \partial_t h_k \Big|_{\rho=0}, \quad j = 0, \dots, m. \end{aligned} \tag{5.3.1}$$

Together with the algebraic equation system of the anomalous dimensions<sup>2</sup> we obtain a differential-algebraic system which we can solve numerically.

As discussed in section 2.3, the system can switch from the symmetric phase to the spontaneously broken phase, which corresponds to the fact that the minimum of the effective potential moves away from  $\rho = 0$ . This suggests to expand  $U_k$  and  $h_k$  differently in the spontaneously broken phase.

---

<sup>2</sup>See last two equations of (5.2.3).

### 5.3.2 Spontaneously broken phase

In the spontaneously broken phase we expand about  $\kappa_k$ . Per construction  $U_k$  should have a minimum at  $\rho = \kappa_k$  and thus  $u_1 = 0$ . Therefore, our truncations read

$$U_k(\rho) = \sum_{i=2}^n \frac{u_i(t)}{i!} (\rho - \kappa_k)^i, \quad h_k(\rho) = \sum_{j=0}^m \frac{\mathfrak{h}_j(t)}{j!} (\rho - \kappa_k)^j.$$

Hence, the flow equations of the couplings become a bit more complicated

$$\begin{aligned} \partial_t u_i &= \partial_\rho^{(i)} (\partial_t U_k) \Big|_{\rho=\kappa_k} + \partial_t \kappa_k u_{i+1}, \quad i = 2, \dots, n \\ \partial_t \mathfrak{h}_j &= \partial_\rho^{(j)} (\partial_t h_k) \Big|_{\rho=\kappa_k} + \partial_t \kappa_k \mathfrak{h}_{j+1}, \quad j = 0, \dots, m, \end{aligned} \quad (5.3.2)$$

where  $\mathfrak{h}_{m+1} = u_{n+1} = 0$ . Furthermore, we have to calculate the flow of the minimum. By using the condition  $U'_k(\kappa_k) = 0$ , which implies  $\partial_t U'_k(\kappa_k) = 0$ , we obtain

$$\partial_t \kappa_k = -\frac{1}{u_2} \partial_\rho (\partial_t U_k) \Big|_{\rho=\kappa_k}. \quad (5.3.3)$$

From experiments we know that in the IR the system is situated within the spontaneously broken phase with a non-vanishing vacuum expectation value of 246 GeV. The IR physics corresponds to the limit  $t \rightarrow -\infty$  (or equivalently  $k \rightarrow 0$ ), however, the solutions show that the flows already freeze out at  $t = -20 \dots -5$ . As described in section 2.3, the Higgs mass is given by the curvature of the effective potential at the vacuum expectation value,

$$m_H = \lim_{k \rightarrow 0} \sqrt{\frac{d^2}{d\varphi^2} U_k(\varphi)} = \lim_{k \rightarrow 0} v_k \sqrt{u_2(k)}. \quad (5.3.4)$$

## 5.4 Our task

The main goal is to investigate the influence of the different couplings on the lower Higgs mass bound. The first step is to choose the initial conditions of the flow equations, i.e. the UV or bare values of the couplings. Then we start to integrate the flow equations numerically. However, we cannot allow arbitrary flows. As mentioned above we know from experiments that there is a non-vanishing vacuum expectation value of 246 GeV. Consequently, the UV parameters have to be chosen in a way that the system will be situated within the spontaneously broken phase in the limit  $k \rightarrow 0$ . Furthermore, according to section 2.3, the top mass is determined by  $m_{top} = v \mathfrak{h}_0$ . It is measured to be 173 GeV, hence we also have to make sure that  $\mathfrak{h}_0$  freezes out at  $\frac{173}{246}$ . Basically, there are two possibilities: We could start in the symmetric regime, using equations (5.3.1). Then we have to define a criterion that specifies when to switch to the broken phase. For example in the simplest possible truncation  $n = 2$  and  $m = 0$ , assuming that we start with positive  $u_1$  and  $u_2$ , the switching criterion would be that  $u_1$  becomes zero. From that point on the system is described by the equations (5.3.2) and (5.3.3)<sup>3</sup>. The values at the switching scale define the new initial values in the spontaneously broken phase. For this kind of flow the UV value of  $u_1$  is adjusted so that we generate the requested vacuum expectation value, while the correct IR top mass is ensured by the adjustment of the UV value of  $\mathfrak{h}_0$ . This process is called fine-tuning and is realised by two nested bisections. The UV values of the other couplings are free parameters in our investigation. Note that as long as the system is situated within the symmetric regime,  $\kappa_k$  has to be set to zero in the (algebraic) flow equations of  $\eta_{\varphi,k}$  and  $\eta_{\psi,k}$ .

The second possibility is to start directly in the broken phase. The role of  $u_1$  is then replaced by  $\kappa_k$ . Thus, at all scales, the flow is described by the equations (5.3.2) and (5.3.3). The correct IR values of the vacuum expectation value and the top mass are then ensured by the fine-tuning of the initial values of  $\kappa_k$  and  $\mathfrak{h}_0$ . The fine-tuning is again realised by nested bisections of these parameters and the UV values of the other couplings remain as free parameters.

Now we can test different truncations  $n$  and  $m$  to see which couplings affect the Higgs mass significantly. Furthermore, we are interested in how the actual numerical values of the UV parameters affect the Higgs mass. Beside this, the cut-off  $\Lambda$  also plays an important role. For a fixed UV set-up, the Higgs mass will differ between different cut-offs. The argumentation is now as following: From experiments we know the Higgs mass to be 125 GeV. If we observed that the lower Higgs mass bound at a specific cut-off  $\Lambda_{crit}$  is higher than the measured Higgs mass, this would mean that the Standard Model is no longer valid at this scale. However, since our toy model is just an approximation of the Standard Model, the results of this thesis are rather of qualitative than of quantitative value. Nevertheless, the idea described above clearly shows why it is interesting to find out how the different couplings might shift the lower Higgs mass bound.

<sup>3</sup>In principle, the flow could switch between the two phases several times. However, in case of the UV conditions considered in this thesis this has not been observed. Once the flow reached the broken phase (or if it started in the broken phase) it never switched back to the symmetric phase.

## 5.5 Results and discussion

### 5.5.1 A simple truncation

To understand the basic behaviour of the couplings let us first consider the simplest truncation  $n = 2$  and  $m = 0$ . Furthermore, we assume a four-dimensional spacetime, i.e.  $d = 4$  and  $d_\gamma = 4$ . The flow equations in the symmetric case then read

$$\begin{aligned}
 \partial_t u_1 &= u_1(\eta_{\varphi,k} - 2) - \frac{\mathfrak{h}_0^2(\eta_{\psi,k} - 5)}{20\pi^2} + \frac{u_2(\eta_{\varphi,k} - 6)}{64\pi^2(u_1 + 1)^2} \\
 \partial_t u_2 &= 2u_2(\eta_{\varphi,k} + 2) - 4u_2 + \frac{1}{5\pi^2}\mathfrak{h}_0^4(\eta_{\psi,k} - 5) - \frac{3}{32\pi^2}\frac{u_2^2(\eta_{\varphi,k} - 6)}{(u_1 + 1)^3} \\
 \partial_t \mathfrak{h}_0 &= \frac{\mathfrak{h}_0}{2}(\eta_{\varphi,k} + 2) + \mathfrak{h}_0(\eta_{\psi,k} - 1) - \frac{\mathfrak{h}_0^3(\eta_{\varphi,k} - 6)}{96\pi^2(u_1 + 1)^2} - \frac{\mathfrak{h}_0^3(\eta_{\psi,k} - 5)}{80\pi^2(u_1 + 1)} \\
 \eta_{\psi,k} &= \frac{\mathfrak{h}_0^2(1 - \frac{1}{5}\eta_{\varphi,k})}{16\pi^2(u_1 + 1)^2} \\
 \eta_{\varphi,k} &= \frac{\mathfrak{h}_0^2}{4\pi^2}\left(\frac{1}{2}(1 - \eta_{\psi,k}) + \frac{1}{4}(\eta_{\psi,k} - 1) + \frac{3}{4}\right)
 \end{aligned} \tag{5.5.1}$$

and in the spontaneously broken phase

$$\begin{aligned}
 \partial_t u_2 &= 2u_2(\eta_{\varphi,k} + 2) - 4u_2 + \frac{\mathfrak{h}_0^4(\eta_{\psi,k} - 5)}{5(2\mathfrak{h}_0^2\kappa_k + 1)^3} - \frac{3u_2^2(\eta_{\varphi,k} - 6)}{32(2u_2\kappa_k + 1)^3} \\
 \partial_t \mathfrak{h}_0 &= \frac{\mathfrak{h}_0}{2}(\eta_{\varphi,k} + 2) + \mathfrak{h}_0(\eta_{\psi,k} - 1) \\
 &\quad - \frac{\mathfrak{h}_0^3(\eta_{\varphi,k} - 6)}{96\pi^2(2\mathfrak{h}_0^2\kappa_k + 1)(2u_2\kappa_k + 1)^2} - \frac{\mathfrak{h}_0^3(\eta_{\psi,k} - 5)}{80\pi^2(2\mathfrak{h}_0^2\kappa_k + 1)^2(2u_2\kappa_k + 1)} \\
 \eta_{\psi,k} &= \frac{\mathfrak{h}_0^2(1 - \frac{1}{5}\eta_{\varphi,k})}{16\pi^2(2\mathfrak{h}_0^2\kappa_k + 1)(2u_2\kappa_k + 1)^2} \\
 \eta_{\varphi,k} &= \frac{\mathfrak{h}_0^6\kappa_k^2(\eta_{\psi,k} - 2)}{4\pi^2(2\mathfrak{h}_0^2\kappa_k + 1)^4} - \frac{\mathfrak{h}_0^2(\eta_{\psi,k} - 4)}{16\pi^2(2\mathfrak{h}_0^2\kappa_k + 1)^4} - \frac{3\mathfrak{h}_0^4\kappa_k}{4\pi^2(2\mathfrak{h}_0^2\kappa_k + 1)^4} + \frac{9u_2^2\kappa_k}{16\pi^2(2u_2\kappa_k + 1)^4} \\
 \partial_t \kappa_k &= -\kappa_k(\eta_{\varphi,k} + 2) - \frac{1}{u_2}\left(\frac{\mathfrak{h}_0^2(1 - \frac{1}{5}\eta_{\psi,k})}{4\pi^2(2\mathfrak{h}_0^2\kappa_k + 1)^2} - \frac{3u_2(1 - \frac{1}{6}\eta_{\varphi,k})}{32\pi^2(2u_2\kappa_k + 1)^2}\right).
 \end{aligned} \tag{5.5.2}$$

In this truncation only positive  $u_2(\Lambda)$  are allowed, since the UV potential has to be bounded from below. This criterion has also been chosen in several lattice simulations that included  $\varphi^4$ -type potentials. In [9] it is shown that considering the Higgs-Yukawa model with  $N_f = 8$  fermions coupling to the scalar field no instabilities of the effective potential occur. [37], [38] extended this model and took the doublet structure of the Higgs field into account, interacting with the top-bottom doublet. In [39] the effect of a potential fourth quark generation has been investigated. All these works have in common that the lower Higgs mass bounds were determined by  $u_2 = 0$ .

In our current simple truncation  $n = 2$  and  $m = 0$  we will also show that the lowest Higgs masses are achieved in the case of  $u_2 = 0$ . However, we will see later that by considering higher truncations the Higgs masses can be further decreased.

Since we restrict ourselves to  $u_2 \geq 0$  for now, we also have to start with positive  $u_1(\Lambda)$ . Otherwise  $U_\Lambda$  would already possess a minimum at  $\rho \neq 0$  and the system would not be situated within the symmetric phase. In our analysis we observed two basic facts about the different types of couplings: The couplings  $u_i$  push the system towards the symmetric phase. If their UV values are chosen too large, we cannot reach the broken phase, no matter which UV values of  $\mathfrak{h}_j$  are chosen. Consequently, the IR value of the vacuum expectation value decreases with increasing UV values of the  $u_i$ , because the longer (in terms of the RG time  $t$ ) the system flows within the symmetric phase the shorter it flows within the broken phase before the quantities freeze out. However, the vacuum expectation value (or better its corresponding quantity  $\kappa_k$ ) is built up in the broken phase. Hence, if the system does not flow sufficiently long within the spontaneously broken phase, we end up with vacuum expectation values smaller than the required one. The behaviour of the  $\mathfrak{h}_j$  is the exact opposite: The larger their UV values are chosen, the faster the system is pushed towards the broken phase and hence the larger becomes the IR value of the vacuum expectation value. If their UV values are chosen too small, the system never reaches the spontaneously broken phase.

We tested a cut-off range from  $10^4$  to  $10^8$  (in units of GeV) and bare parameter values  $u_2(\Lambda)$  from zero to 100. According to the explanations above there will be a critical value  $u_2^{crit}$ , where the system remains in the symmetric phase or at least where we no longer can manage to obtain the correct IR physics. In this case, as described in section 5.4, we already have to start in the broken phase, using  $\kappa_k$  and  $\mathfrak{h}_0$  for the fine-tuning procedure. For the current truncation, the critical value is  $u_2^{crit} = 1 \dots 2$ , depending on the cut-off.

The results of these first investigations are shown in figure 5.1 and figure 5.2.

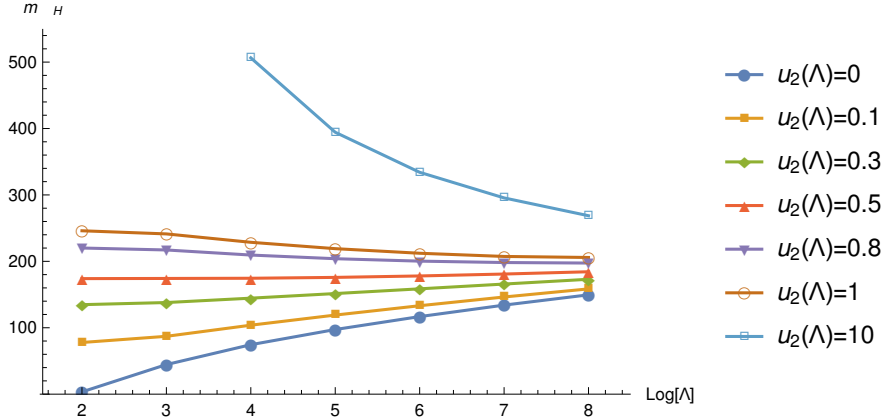


FIGURE 5.1: Higgs mass in dependency on the cut-off for different fixed bare couplings  $u_2$

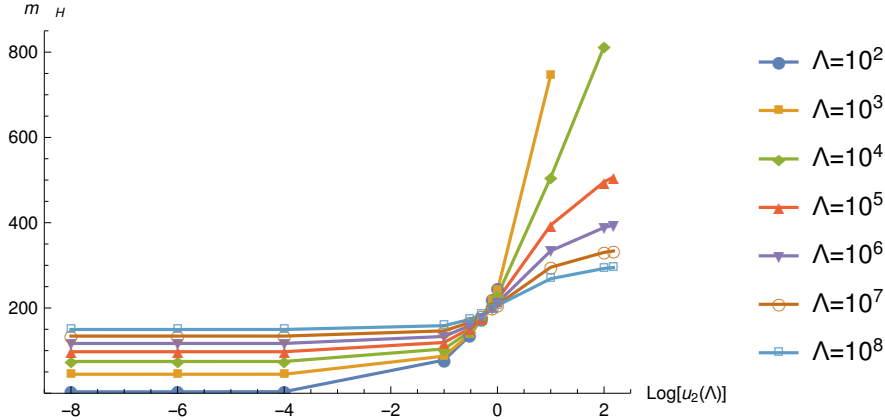


FIGURE 5.2: Higgs mass in dependency on the bare coupling  $u_2$  at different fixed cut-offs

The interpolating lines are drawn just to guide the eye. We can see that for fixed  $u_2(\Lambda)$  the Higgs mass increases with the cut-off. At the same time, when fixing the cut-off, the Higgs mass increases with  $u_2(\Lambda)$ <sup>4</sup>. Because our main interest lies in manipulating the lower Higgs mass bound, we should therefore concentrate on lowering  $u_2(\Lambda)$  as far as possible in our future analysis. The qualitative shape of the plots above agree with the results of [13], [14], [11]. From figure 5.1 we see that for large cut-offs, the actual Higgs mass varies less and less with the actual choice of the bare coupling  $u_2(\Lambda)$ . At the same time, figure 5.2 shows us that for fixed cut-offs, the Higgs mass seems to approach a state of saturation. The larger the cut-off the earlier the Higgs mass becomes saturated.

<sup>4</sup>This is no surprise since the Higgs mass is proportional to the IR value of  $\sqrt{u_2}$ , see equation (5.3.4).

This kind of reminds us on the Landau pole: If the cut-off lies in the vicinity of the Landau pole, an "infinite change" of the bare value of  $u_2$  only translates into a finite change of its IR value [11]. As we mentioned before, we also observed that the lowest Higgs masses are achieved in the case of  $u_2(\Lambda) = 0$ . Furthermore, the results do not only match qualitatively but also quantitatively. If we compare the lower Higgs mass bounds ( $u_2 = 0$ ) at  $\Lambda = 10^4$  and  $\Lambda = 10^8$  with [14] we find

TABLE 5.1: Comparison of lower Higgs mass bounds in GeV

	$\Lambda = 10^4$	$\Lambda = 10^8$
$m_H^{min}$ (our result)	74.50	149.56
$m_H^{min}$ ([14])	73.66	147.52
deviation	1.23%	1.36%

The small deviations can for example be explained by the fact that the fine-tuning precision for the vacuum expectation value and the top mass were different. An indication for this might be that the deviation at the higher cut-off is bigger, since more digits become significant when performing the numerics in dimensionless quantities (at the end, the dimensionless quantities have to be multiplied with powers of the cut-off).

### 5.5.2 Higher truncations

In this subsection we want to analyse the influence of higher truncations. Because the system becomes increasingly complicated when more and more operators are taken into account, we have to state one more criterion to distinguish between physical and non-physical flows. When we considered higher truncations  $m$  and  $n$ , we observed that the effective potential  $U_k$  develops additional (local) minima for some bare parameter combinations, although it is still described by the symmetric equations, see figure 5.3.

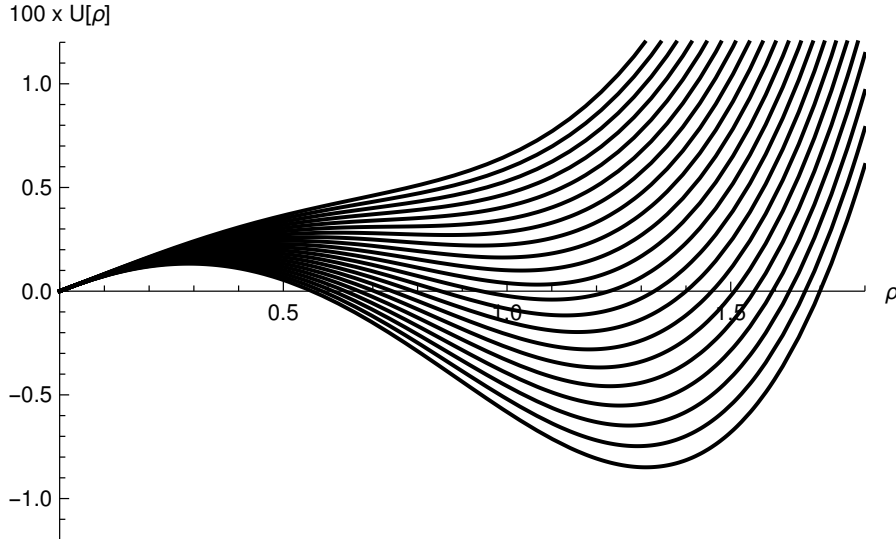


FIGURE 5.3: An inconvenient choice of the start parameters can cause the appearance of additional minima in the symmetric phase. Here we have  $m = 1$  and  $n = 4$  with  $(u_2(\Lambda), u_3(\Lambda), u_4(\Lambda)) = (0.10, 0.00, 0.00)$  and  $\mathfrak{h}_1(\Lambda) = 8$  at  $\Lambda = 10^8$

There are two issues in such a case. The first is that our truncation approach relies on the fact that we expand about the vacuum expectation value. If an additional (local) minimum appears, we are no longer able to decide which minimum the system is situated in and thus we do not know where to expand. This problem can be addressed by solving the full flow of  $U_k(\rho)$ , but this is beyond the scope of this thesis. The second issue is even more crucial: Actually, we are not able to decide whether the additional minima are just artefacts of our truncation or not. It might turn out that if we were able to solve the full equation of the effective potential  $U_k$ , we could observe no additional minima at all. Indeed, according to [11], the radius of convergence of our expansion is typically too small to resolve additional minima. Hence, such bare parameter combinations cannot be used for further argumentations.

Speaking of artefacts of our truncation we should mention another fact. In general we want the effective potential to be bounded from below, which means that the highest order coupling  $u_n$  should remain positive at all scales.

However, it is enough to choose a positive UV value, because if the UV potential is bounded from below, the effective potential will remain bounded from below at all scales. We can see this by considering the flow equation of  $U_k$  (see first equation in (5.2.2)): Up to the dimensional flow caused by introducing dimensionless quantities, the flow is suppressed by the factors  $\frac{1}{\omega_u(\rho)}$  and  $\frac{1}{1+2\rho h_k^2(\rho)}$ , which both tend to zero for  $\rho \rightarrow \infty$ . In other words, for sufficiently large  $\rho$ ,  $U_k$  does not change significantly and thus the property of being bounded from below is preserved. Hence, the leading order coupling  $u_n$  becoming negative during the flow does not cause any problems, it is just an artefact of our truncation as well.

To finally analyse the influence of the different couplings we tested different combinations of  $m$  and  $n$  and computed the Higgs mass. The UV parameters were all set to zero,  $u_i(\Lambda) = 0$  and  $h_j(\Lambda) = 0$ . The cut-off was chosen to be  $10^4$  and  $10^8$ . The corresponding results are shown in table 5.2 and table 5.3.

 TABLE 5.2: Higgs mass in GeV for different truncations at  $\Lambda = 10^4$ 

		n				
		2	3	4	5	6
m	0	74.50	71.93	72.17	72.15	72.15
	1	74.09	71.56	71.80	71.78	71.78
	2	74.12	71.60	71.84	71.81	71.82
	3	74.11	71.60	71.83	71.81	71.81
	4	74.11	71.60	71.83	71.81	71.81
	5	74.11	71.60	71.83	71.81	71.81

 TABLE 5.3: Higgs mass in GeV for different truncations at  $\Lambda = 10^8$ 

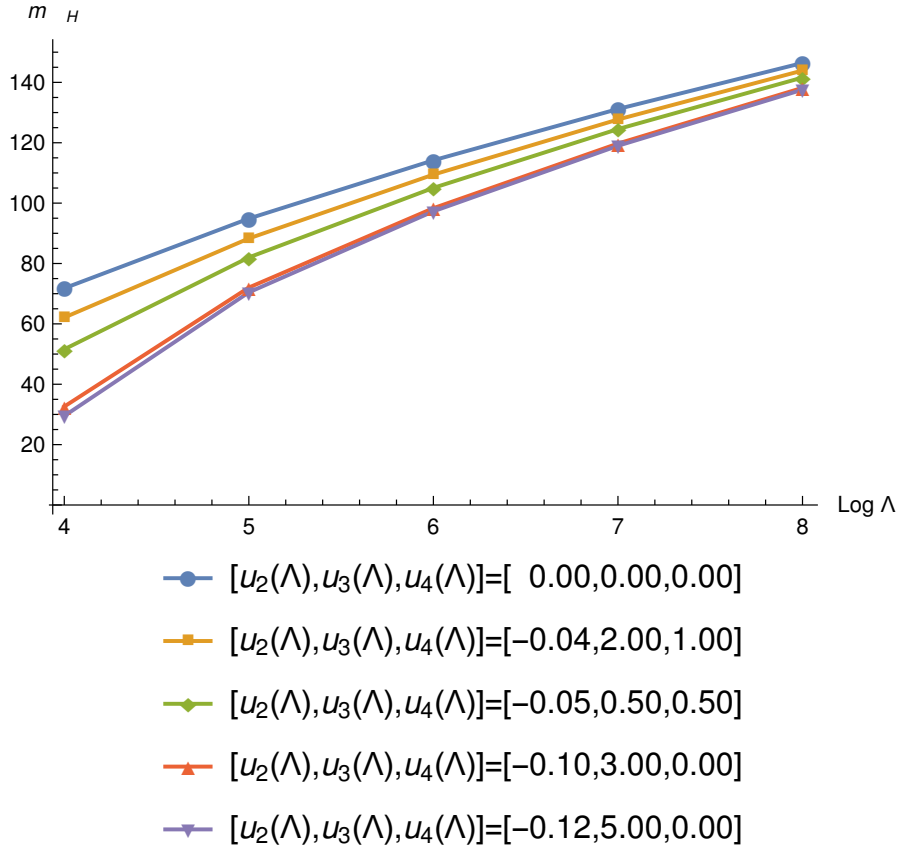
		n				
		2	3	4	5	6
m	0	149.56	147.69	147.70	147.76	147.68
	1	148.18	146.41	146.43	146.47	146.37
	2	148.27	146.40	146.44	146.53	146.39
	3	148.21	146.41	146.43	146.43	146.38
	4	148.22	146.35	146.48	146.39	146.41
	5	148.25	146.33	146.42	146.42	146.43

According to this it will be sufficient to choose  $m = 1$  and  $n = 4$  as our highest truncation. We will use this combination for our further analysis.

### 5.5.3 Lower Higgs mass bound induced by $u_2$

In this subsection we try to lower the Higgs mass bound by varying  $u_2(\Lambda)$ , while  $\mathfrak{h}_1(\Lambda) = 0$  is kept fixed. The difference to subsection 5.5.1 is that due to our new truncation we are now free to allow even negative bare values of  $u_2$ , which are stabilized by the new higher order bosonic couplings  $u_3$  and  $u_4$ . In other words, we investigate the influence of deviations of the effective potential from the  $\varphi^4$ -type bare potential. According to what we have observed so far, this should yield smaller Higgs masses than the ones achieved in the mentioned subsection. To make negative  $u_2$  possible, we have to match some conditions. For example, we have to make sure that  $u_2$  is positive when reaching the broken phase. Otherwise, if  $u_2$  remains negative, it would yield an imaginary Higgs mass (since the vacuum expectation value must be positive). On the other hand, if it was negative but became positive again, it would mean that  $u_2$  somewhere becomes zero, leading to a singularity in our equations according to equation (5.3.3). Both cases imply that we do not reproduce the correct IR physics and thus they are non-physical. The reason for this behaviour is of course the fact that starting with negative  $u_2$  in the spontaneously broken phase corresponds to expanding about a maximum which contradicts our approach to always expand about the minimum of the effective potential. Since we start with positive  $u_4$  (UV potential has to be bounded from below) the UV value of  $u_3$  needs to be positive as well, because otherwise the UV potential would already possess additional minima. To make sure that no additional minima appear during the flow,  $u_3$  has to change its sign before getting to the switching scale determined by  $u_1$  becoming zero. These effects lead to the fact that  $u_2$  cannot be chosen arbitrarily low.

Taking this into account, we can generate flows that reproduce the correct IR physics. The results for the Higgs masses are shown in figure 5.4.


 FIGURE 5.4: Higgs mass for negative bare couplings  $u_2(\Lambda)$ 

We see that indeed a negative bare coupling  $u_2(\Lambda)$  lowers the Higgs mass significantly. The effect becomes less strong when increasing the cut-off. This behaviour has already been observed in [14], [11]. The lowest Higgs masses we achieved are listed in table 5.4.

TABLE 5.4: Lowest achieved Higgs mass at different cut-offs

	$\Lambda = 10^4$	$\Lambda = 10^5$	$\Lambda = 10^6$	$\Lambda = 10^7$	$\Lambda = 10^8$
$m_H^{min}$	29.49	70.44	92.50	114.74	132.22

To compare these results qualitatively with the FRG studies in [14], [11] we have to repeat these calculations for the case  $m = 0$ , since the authors did not include the flow of the  $\mathfrak{h}_1$  operator into their equations. For a  $n = 3$  truncation and a bare value of  $u_3 = 3$  we find for example

 TABLE 5.5: Comparison of Higgs masses in GeV for negative bare values of  $u_2$ 

	$\Lambda = 10^4$		$\Lambda = 10^8$	
	$u_2 = -0.05$	$u_2 = -0.08$	$u_2 = -0.05$	$u_2 = -0.08$
$m_H$ (our result)	61.29	45.73	144.91	141.69
$m_H$ ([14])	60.83	45.67	142.82	139.48
$\Delta m_H/m_H^0$ (our result)	17.73%	37.92%	3.11%	5.26%
$\Delta m_H/m_H^0$ ([14])	17.42%	38.00%	3.19%	5.45%

Here,  $\frac{\Delta m_H}{m_H^0} = \frac{m_H^0 - m_H}{m_H^0}$  is the relative change of the Higgs mass normalized with the former lower Higgs mass bound  $m_H^0$  derived from the  $\varphi^4$ -type bare potentials (see table 5.1). This is the interesting quantity because it characterizes how far we can shift down the Higgs mass when considering deviations from the quartic UV potential. Our results agree with those of [14].

#### 5.5.4 Lower Higgs mass bound induced by $\mathfrak{h}_1$

In the case of  $\mathfrak{h}_1$  we are a priori completely free to assume any bare values, positive or negative. For a fixed cut-off  $\Lambda = 10^5$  and fixed  $(u_2(\Lambda), u_3(\Lambda), u_4(\Lambda)) = (0.50, 0.00, 0.00)$  we thus tested a first set of bare values. The results are shown in table 5.6.

 TABLE 5.6: Higgs mass for different bare parameters  $\mathfrak{h}_1$ 

	$\mathfrak{h}_1 = 0$	$\mathfrak{h}_1 = -5$	$\mathfrak{h}_1 = 5$	$\mathfrak{h}_1 = -10$	$\mathfrak{h}_1 = 10$
$m_H$	175.32	194.65	152.31	211.38	123.47

Negative  $\mathfrak{h}_1$  seem to raise the Higgs mass whereas positive  $\mathfrak{h}_1$  lower it. Since we want to find a lower bound, the latter case is the interesting one. Before we move on, however, let us check whether different relative signs between the  $\mathfrak{h}_j$  have an interesting effect. We therefore temporarily set  $m = 2$  and use different combinations of  $\mathfrak{h}_1(\Lambda)$  and  $\mathfrak{h}_2(\Lambda)$ .

The results are listed in table 5.7<sup>5</sup>.

TABLE 5.7: Higgs mass for different combinations of  $\mathfrak{h}_1$  and  $\mathfrak{h}_2$

	$(\mathfrak{h}_1, \mathfrak{h}_2)$					
	(0,0)	(5,0)	(5,-5)	(-5,5)	(-5,-5)	(5,5)
$m_H$	175.34	152.34	152.44	194.66	194.79	152.24

There are no exceptional effects observable. In the case of fixed  $\mathfrak{h}_1$ , positive  $\mathfrak{h}_2$  still lower the Higgs mass and negative  $\mathfrak{h}_2$  increase it. The same holds the other way around. This is another argument for studying only truncations with  $m = 1$ . The next step in our analysis is to investigate in which ways the Higgs mass behaves if we steadily increase  $\mathfrak{h}_1$ . At the same time, different UV set-ups for the  $u_i$  should be considered. As earlier, we restrict ourselves to positive values of  $u_2$  at the beginning. To find out which set-ups of  $u_3$  and  $u_4$  yield the smallest Higgs masses, we tested some combinations for fixed cut-off and fixed  $u_2$ . For  $\Lambda = 10^5$  and  $u_2 = 0.3$  table 5.8 shows the outcome.

TABLE 5.8: Higgs mass for different combinations of  $u_3$  and  $u_4$

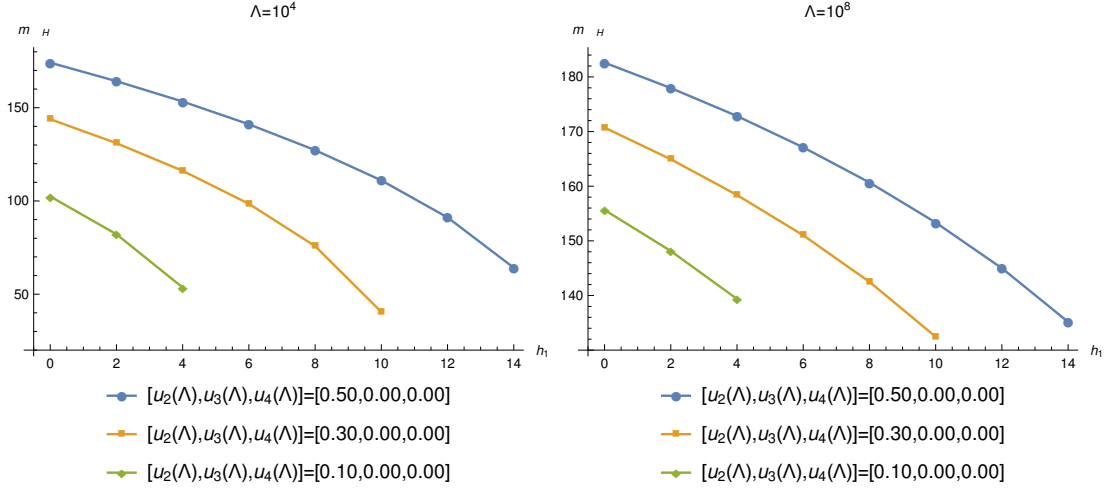
		$\mathfrak{h}_1$		
		0	4	8
$(u_3, u_4)$	(0.0,0.0)	150.36	127.01	94.69
	(0.5,0.5)	150.89	127.68	95.67
	(1.0,0.0)	151.41	128.34	96.62
	(0.0,1.0)	150.36	127.01	94.70
	(1.0,0.2)	151.41	128.35	96.62
	(0.2,1.0)	150.58	127.28	95.09
	(5.0,5.0)	155.54	133.53	103.94

The lowest Higgs masses are achieved when the UV values of  $u_3$  and  $u_4$  are set to zero or in other words when considering a quartic UV potential. In our further analysis we therefore keep them zero and consider different UV values  $u_2 \geq 0$ . For the cut-offs  $\Lambda = 10^4$  and  $\Lambda = 10^8$ , the outcome of this analysis is shown in figure 5.5.

The influence of  $\mathfrak{h}_1$  on the Higgs mass is significant. However, we observed an important fact. Considering a fixed UV set-up of the  $u_i$ ,  $\mathfrak{h}_1$  cannot be arbitrarily increased. There exists a critical value from which on the effective potential develops additional minima. From figure 5.5 we see that these critical values are  $\mathfrak{h}_1 = 4, 10, 14$  for  $u_2 = 0.1, 0.3, 0.5$ . Furthermore,  $u_2$  cannot be chosen arbitrarily low.

---

<sup>5</sup>Note that even for a vanishing bare value of  $\mathfrak{h}_2$  the Higgs masses already differ from those of the  $m = 1$  truncation. However, it changes by less than 0.1%.


 FIGURE 5.5:  $h_1$  dependency of the Higgs mass

If it becomes too small, the fermionic fluctuations heavily dominate, which yields either too large top masses or  $u_2$  becomes negative in the spontaneously broken phase. This can be seen from the flow equation of  $u_2$  in the symmetric phase<sup>6</sup>:

$$\begin{aligned} \partial_t u_2 = & \frac{32\mathfrak{h}_0 (\mathfrak{h}_0^3 - \mathfrak{h}_1) (u_1 + 1)^3 (\mathfrak{h}_0^4 + 80\pi^2\mathfrak{h}_0^2 - 6400\pi^4 (u_1 + 1)^2)}{160\pi^2 (u_1 + 1)^3 (1280\pi^4 (u_1 + 1)^2 - \mathfrak{h}_0^4)} \\ & + \frac{1600\pi^2\mathfrak{h}_0^2 u_2 (u_1 + 1)^3 (64\pi^2(1 + u_1)^2 - \mathfrak{h}_0^2)}{160\pi^2 (u_1 + 1)^3 (1280\pi^4 (u_1 + 1)^2 - \mathfrak{h}_0^4)} \\ & + \frac{15u_2^2 (-320\pi^2\mathfrak{h}_0^2 (u_1 + 1)^2 - \mathfrak{h}_0^4 + 7680\pi^4 (u_1 + 1)^2)}{160\pi^2 (u_1 + 1)^3 (1280\pi^4 (u_1 + 1)^2 - \mathfrak{h}_0^4)} \end{aligned}$$

In the symmetric phase  $u_1$  stays positive (its zero determines the switching scale to the broken phase) while  $\mathfrak{h}_0$  remains positive and smaller than one. Hence the denominator in the equation above is positive and the  $h_1$  contribution comes with a positive sign as well as with a large coefficient in comparison to the other terms. Hence, it is lowering  $u_2$  when integrating out the flow equation ( $t \leq 0$ ).

If the effects mentioned above occur, the correct IR physics cannot be reproduced. In order to make use of the fact that  $h_1$  lowers the Higgs mass we thus have to choose  $u_2$  sufficiently large, which however increases the Higgs mass again, according to subsection 5.5.3. It is of relevance to find out which effect dominates.

<sup>6</sup>For simplicity, we consider the  $n = 2$  and  $m = 1$  truncation.

Figure 5.6 compares the lowest Higgs masses achieved by the variation of  $\mathfrak{h}_1$  (and keeping  $u_2 \geq 0$ ) as well as those achieved by variation of  $u_2$ .

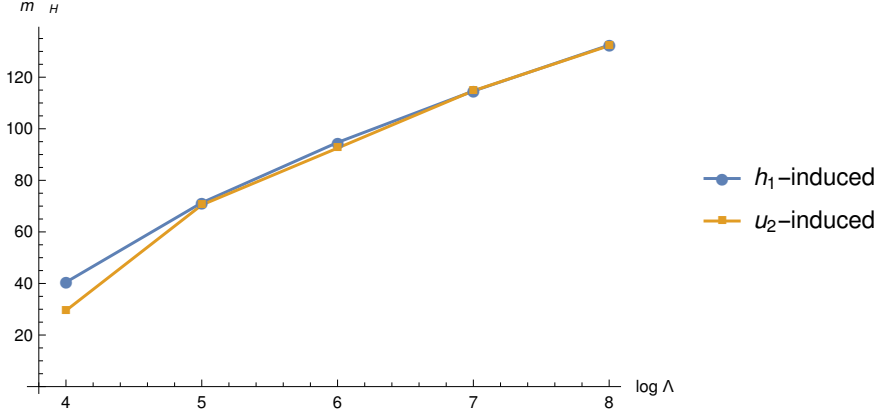
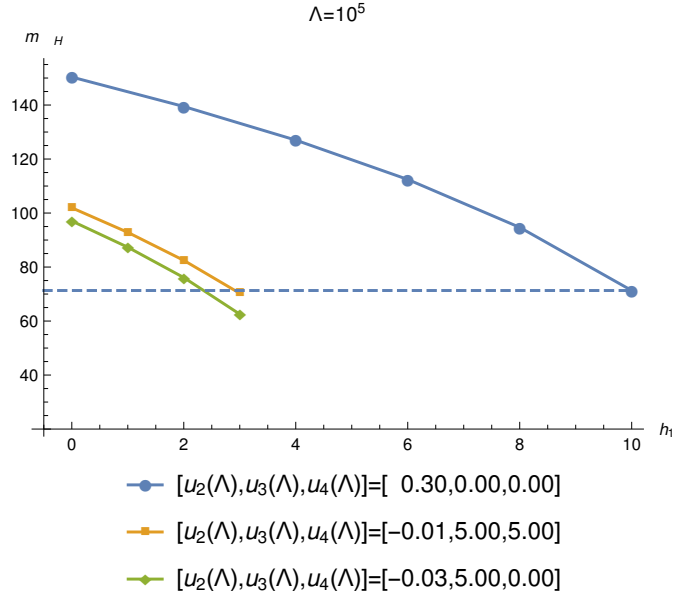


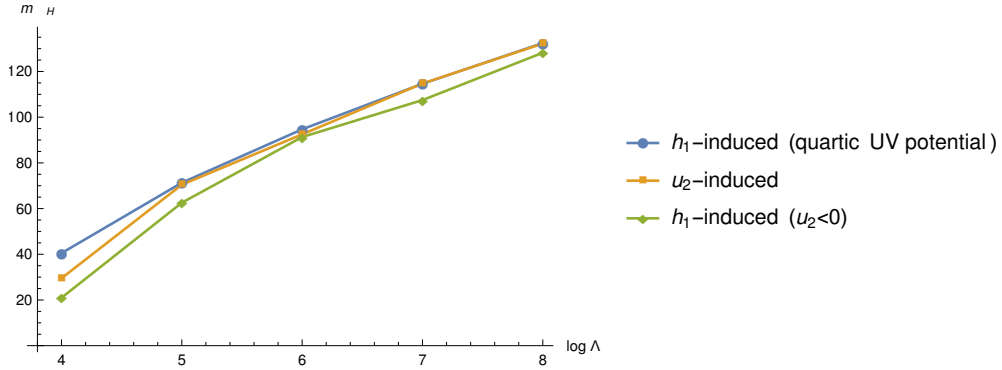
FIGURE 5.6: Comparison between  $\mathfrak{h}_1$ -induced and  $u_2$ -induced lower Higgs mass bound

We find that the answer to the question above is that both effects keep the balance. In the end, the lowest Higgs masses obtained by varying  $\mathfrak{h}_1$  (while keeping  $u_2 \geq 0$ ) are of the same magnitude as the ones obtained by varying  $u_2$ . Most of the time the latter case even yields the smaller Higgs masses.

Similar to the investigations on the  $u_2$ -induced mass bounds we therefore want to allow for negative bare couplings  $u_2$ . This implies that we have to choose non-zero bare values of  $u_3$  and/or  $u_4$  in order to establish a bounded from below UV effective potential. According to what has been observed so far it is also clear that we will not be able to extend the bare value of  $\mathfrak{h}_1$  as far as when considering bare potentials with  $u_2 \geq 0$ . Indeed, we were not able to increase  $\mathfrak{h}_1$  further than  $3 \dots 4$ , as shown in figure 5.7 for the case of  $\Lambda = 10^5$ .


 FIGURE 5.7:  $h_1$  dependency of the Higgs mass for non-quartic UV potentials

However, we find that considering these deviations from the quartic UV potential allows us to further decrease the Higgs mass, although we have to restrict ourselves to smaller UV values of  $h_1$ . Figure 5.8 compares the corresponding new lower Higgs mass bounds with the former result.


 FIGURE 5.8: Comparison between  $u_2$ -induced and  $h_1$ -induced lower Higgs mass bound, where we distinguished the latter one between negative and non-negative bare values of  $u_2$

Hence, we state that it is indeed possible to further decrease the lower Higgs mass bound by considering higher order Yukawa interactions  $\mathfrak{h}_j \varphi^{2j+1} \bar{\psi} \psi$ ,  $j > 0$ , since we managed to beat the bounds we obtained by only considering deviations from the quartic UV potential while taking only the standard Yukawa coupling into account. Table 5.9 shows the relative change of the Higgs mass, normalized with the former  $u_2$  induced lower bound.

TABLE 5.9:  $\mathfrak{h}_1$  induced lower bounds with generalized UV potentials

	$\Lambda = 10^4$	$\Lambda = 10^5$	$\Lambda = 10^6$	$\Lambda = 10^8$	$\Lambda = 10^8$
$m_H^{min}$	20.96	62.56	91.31	107.48	128.20
$\Delta m_H / m_H^0$	28.93%	11.19%	1.29%	6.33%	3.04%

The fact that the value for  $\Lambda = 10^6$  is a bit odd is most likely a numerical issue rather than a physical effect.

## 6 Extending the toy model

In this chapter we want to extend our toy model. Hence, we return to dimensionful and non-renormalized quantities. Our goal is to take the  $SU(N_C)$  structure of the Standard Model into account. We focus on the strong interaction part of the Standard Model unlike [40] where the flow of the non-abelian part of the electroweak sector has been studied. For a phenomenological investigation of lower Higgs mass bounds in a model similar to our approach see [41]. In [32] two-flavour QCD at finite temperature and quark density has been considered, also including a generalized Yukawa interaction.

We start with adding a Yang-Mills term to our effective average action,

$$\Gamma_{YM} = \int_x \frac{1}{2} \text{Tr} (F_{\mu\nu} F^{\mu\nu}), \quad F_{\mu\nu}^I = \partial_\mu A_\nu^I - \partial_\nu A_\mu^I + gf^{IJK} A_\mu^J A_\nu^K.$$

which requires a gauge fixing term, as usual. We choose

$$\Gamma_{gf} = \int_x \frac{Z_{A,k}}{\xi} \text{Tr} ((\partial_\mu A^\mu)^2).$$

In this chapter we will use Roman small letters for the colour indices ( $a, b, \dots = 1, \dots, N_C$ ) and Roman capital letters to label the generators  $T_I$  of the Lie algebra  $\mathfrak{su}(N_C)$ , i.e.  $I, J, \dots = 1, \dots, N_C^2 - 1$ . The generators shall be chosen such that  $\text{Tr}(T_I T_J) = \frac{1}{2} \delta_{IJ}$ . The Yang-Mills term and the gauge fixing term then read

$$\Gamma_{gf} = \int_x \frac{Z_{A,k}}{2\xi} \partial_\mu A_K^\mu \partial_\nu A_K^\nu, \quad \Gamma_{YM} = \int_x \frac{Z_{A,k}}{4} F_{\mu\nu}^I F_I^{\mu\nu}$$

Furthermore, this yields a ghost term

$$\Gamma_{ghost} = - \int_x Z_{c,k} c_a^* \partial_\mu D_{ab}^\mu c_b,$$

with the covariant derivative

$$D_{ab}^\mu = \delta_{ab} \partial^\mu - ig A_I^\mu [T_I]_{ab},$$

where  $g$  is the  $SU(N_C)$  coupling. Our new ansatz for the effective action eventually reads

$$\begin{aligned} \Gamma_k = & \int_x U_k + \int_p \frac{Z_{\varphi,k}}{2} p^2 \varphi(p) \varphi(-p) - \int_p Z_{\psi,k} \bar{\psi}^a(p) \not{p} \psi^a(p) + \int_x \frac{Z_{A,k}}{4} F_{\mu\nu}^I F_I^{\mu\nu} + \int_p Z_{c,k} p^2 c_a^*(p) c_a(p) \\ & + \int_p \frac{Z_{A,k}}{2\xi} p_\mu p_\nu A_I^\mu(p) A_I^\nu(-p) + i \int_x H_k \bar{\psi}^a(x) \psi^a(x) + \int_{p,q} g Z_{\psi,k} \bar{\psi}^a(p) \gamma^\mu A_\mu^I(p-q) [T_I]_{ab} \psi^b(q) \\ & + \int_{p,q} g Z_{c,k} c_a^*(p) (p^\mu - q^\mu) A_\mu^I(p-q) [T_I]^{ab} c_b(q). \end{aligned} \quad (6.0.1)$$

Note that the ghost fields are scalar Grassmann valued fields.

## 6.1 Extended fluctuation matrix

Although we introduced more fields like the gauge field and the ghost fields, the derivation of the flow equation is completely the same as in subsection 2.2.3. The Wetterich equation is still valid, the only thing that changes is that now the super trace has to be taken over the colour indices, the generator indices and the spacetime indices as well. Because the ghost fields are Grassmann valued fields, the contribution from ghost sectors come with a minus sign, just as in the case of the fermion fields. We introduce the new (macroscopic) field vector

$$\phi(p) = \begin{pmatrix} \varphi(p) \\ \psi_a(p) \\ \bar{\psi}_a^T(-p) \\ A_\mu^I(p) \\ c_a(p) \\ c_a^*(-p) \end{pmatrix},$$

which will make the fluctuation matrix a  $6 \times 6$  matrix with respect to the field indices

$$\Gamma_k^{(2)}(p, q) = \begin{pmatrix} \frac{\overrightarrow{\delta}}{\delta\varphi(-p)} \\ \frac{\overrightarrow{\delta}}{\delta\psi_a(-p)} \\ \frac{\overrightarrow{\delta}}{\delta\bar{\psi}_a^T(p)} \\ \frac{\overrightarrow{\delta}}{\delta A_\mu^I(-p)} \\ \frac{\overrightarrow{\delta}}{\delta c_a(-p)} \\ \frac{\overrightarrow{\delta}}{\delta c_a^*(p)} \end{pmatrix} \Gamma_k[\phi] \begin{pmatrix} \overleftarrow{\delta} \\ \overleftarrow{\delta} \\ \overleftarrow{\delta} \\ \overleftarrow{\delta} \\ \overleftarrow{\delta} \\ \overleftarrow{\delta} \end{pmatrix} \begin{pmatrix} \frac{\overleftarrow{\delta}}{\delta\varphi(q)} & \frac{\overleftarrow{\delta}}{\delta\psi(q)} & \frac{\overleftarrow{\delta}}{\delta\bar{\psi}^T(-q)} & \frac{\overleftarrow{\delta}}{\delta A_\nu^J(q)} & \frac{\overleftarrow{\delta}}{\delta c_b(q)} & \frac{\overleftarrow{\delta}}{\delta c_b^*(-q)} \end{pmatrix}.$$

We will focus on the additional terms in the flow equations of the quantities  $U_k$ ,  $H_k$ ,  $Z_{\psi,k}$  and  $Z_{\varphi,k}$ . Because their corresponding projection rules imply setting the gauge field to zero it is sufficient to take only the quadratic part of the Yang-Mills term into account. In momentum space it reads

$$\int_p \frac{Z_{A,k}}{2} (p^2 \delta_{\mu\nu} - p_\mu p_\nu) A_I^\mu(p) A_I^\nu(-p).$$

Together with the gauge fixing term this yields

$$\begin{aligned} & \int_p \frac{Z_{A,k}}{2} p^2 \left( \delta_{\mu\nu} - \frac{p_\mu p_\nu}{p^2} + \frac{1}{\xi} \frac{p_\mu p_\nu}{p^2} \right) A_I^\mu(p) A_I^\nu(-p) \\ & =: \int_p \frac{Z_{A,k}}{2} p^2 \left( \pi_{\mu\nu}^T + \frac{1}{\xi} \pi_{\mu\nu}^L \right) A_I^\mu(p) A_I^\nu(-p), \end{aligned}$$

where we introduced the transversal projector  $\pi_{\mu\nu}^T = \delta_{\mu\nu} - \frac{p_\mu p_\nu}{p^2}$  and the longitudinal projector  $\pi_{\mu\nu}^L = \frac{p_\mu p_\nu}{p^2}$ . They satisfy the relations

$$\begin{aligned} \pi_{\mu\nu}^T + \pi_{\mu\nu}^L &= \delta_{\mu\nu} \\ \pi_{\mu\nu}^T \pi_L^{\nu\sigma} &= 0 \\ \pi_{\mu\nu}^T \pi_T^{\nu\sigma} &= \pi_\mu^{T\sigma} \\ \pi_{\mu\nu}^L \pi_L^{\nu\sigma} &= \pi_\mu^{L\sigma}. \end{aligned} \tag{6.1.1}$$

The structure of the new regulator is given by

$$R_k(p, q) = \delta_{p,q} \begin{pmatrix} R_\varphi(p) & 0 & 0 & 0 & 0 & 0 \\ 0 & 0 & -R_\psi^T(-p) & 0 & 0 & 0 \\ 0 & R_\psi(p) & 0 & 0 & 0 & 0 \\ 0 & 0 & 0 & R_A(p) & 0 & 0 \\ 0 & 0 & 0 & 0 & 0 & -R_c(-p) \\ 0 & 0 & 0 & 0 & R_c(p) & 0 \end{pmatrix},$$

where we choose the following convenient form of the regulators

$$\begin{aligned} R_\varphi &= Z_{\varphi,k} p^2 r_{\varphi,k} \\ R_\psi &= -\delta_{ab} Z_{\psi,k} \not{p} r_{\psi,k} \\ R_A &= \delta_{IJ} Z_{A,k} p^2 \left( r_{A,k}^T \pi_{\mu\nu}^T + \frac{1}{\xi} r_{A,k}^L \pi_{\mu\nu}^L \right) \\ R_c &= \delta_{ab} Z_{c,k} p^2 r_{c,k}. \end{aligned}$$

This leads to the familiar abbreviations

$$\begin{aligned} P_\varphi &= p^2 (1 + r_{\varphi,k}) \\ P_\psi &= p^2 (1 + r_{\psi,k})^2 \\ P_A^{T/L} &= p^2 (1 + r_{k,A}^{T/L}) \\ P_c &= p^2 (1 + r_{c,k}) \end{aligned}$$

and

$$\xi_\varphi(q) = Z_{\varphi,k} P_\varphi(q) + U_k''(\varphi^2), \quad \xi_\psi(q) = Z_{\psi,k}^2 P_\psi(q) + H_k^2(\varphi).$$

## 6.1 Extended fluctuation matrix

---

Finally, we can write down  $\Gamma_k^{(2)} + R_k$  for our extended toy model. We will label the entries of the matrix with the fields, so for example the (2, 4) entry will be denoted by  $(\psi, A)$ . Then the non-vanishing entries (the gauge field and the ghost fields have already been set to zero, as mentioned above) read

$$\begin{aligned}
(\varphi, \varphi) &: Z_{\varphi,k} P_\varphi \delta_{p,q} + \int_x U_k''(\varphi^2) e^{-i(p-q)x} + i \int_x H_k''(\varphi) e^{-i(p-q)x} \bar{\psi}^l(x) \psi^l(x) \\
(\varphi, \psi) &: i \int_x H_k'(\varphi) \bar{\psi}^b(x) e^{-i(p-q)x} \\
(\varphi, \bar{\psi}) &: -i \int_x H_k'(\varphi) \psi^{T,b}(x) e^{-i(p-q)x} \\
(\psi, \varphi) &: -i \int_x H_k'(\varphi) \bar{\psi}^{T,a}(x) e^{-i(p-q)x} \\
(\bar{\psi}, \varphi) &: i \int_x H_k'(\varphi) \psi^a(x) e^{-i(p-q)x} \\
(\psi, \bar{\psi}) &: \delta_{ab} \delta_{p,q} (-Z_{\psi,k} (1 + r_{\psi,k}) \not{p}^T) - i \delta_{ab} \int_x H_k e^{-i(p-q)x} \\
(\bar{\psi}, \psi) &: \delta_{ab} \delta_{p,q} Z_{\psi,k} (1 + r_{\psi,k}) \not{p} + i \delta_{ab} \int_x H_k e^{-i(p-q)x} \\
(\psi, A) &: -g Z_{\psi,k} \gamma_\nu^T \bar{\psi}^{T,e} (q-p) [TJ]_{ea} \\
(\bar{\psi}, A) &: g Z_{\psi,k} [TJ]_{ae} \gamma_\nu \psi^e (p-q) \\
(A, \psi) &: g Z_{\psi,k} \bar{\psi}^e (q-p) \gamma_\mu [TI]_{eb} \\
(A, \bar{\psi}) &: -g Z_{\psi,k} [TI]_{be} \psi^{T,e} (p-q) \gamma_\mu^T \\
(A, A) &: \delta_{IJ} \delta_{p,q} Z_{A,k} \left( P_A^T \pi_{\mu\nu}^T + \frac{1}{\xi} P_A^L \pi_{\mu\nu}^L \right) \\
(c, c^*) &: -\delta_{ab} Z_{c,k} P_c \\
(c^*, c) &: \delta_{ab} Z_{c,k} P_c.
\end{aligned} \tag{6.1.2}$$

The first six terms are the same as in our old truncation (4.1.2), up to the new colour indices.

## 6.2 Extended flow equations

### 6.2.1 Extended flow of the generalized Yukawa coupling

The modified projection rule reads

$$\delta_0 \partial_t H_k(\varphi) \mathbb{1}_{d_\gamma} = \frac{1}{iN_C} \frac{\overrightarrow{\delta}}{\delta \bar{\psi}^f} \frac{1}{2} \text{STr} \left[ \frac{\partial_t R_k}{\Gamma_k^{(2)} + R_k} \right] \frac{\overleftarrow{\delta}}{\delta \psi^f} \Bigg|_{\substack{\varphi = \text{const} \\ \psi = \bar{\psi} = 0 \\ A_\mu = 0 \\ c = c^* = 0}}. \quad (6.2.1)$$

In principle, we can perform exactly the same steps as in section 4.2. First, we can set all fields to constants again, which yields factors  $\delta_{p,q}$  as earlier. Then we decompose

$$\Gamma_k^{(2)} + R_k = \left( \Gamma_{k,A,\varphi,c}^{(2)} + R_k \right) + \Delta \Gamma_k^{(2)},$$

so that  $\Delta \Gamma_k^{(2)}$  contains all fermionic fluctuations, i.e. the "old" entries  $(\varphi, \psi)$ ,  $(\varphi, \bar{\psi})$ ,  $(\psi, \varphi)$ ,  $(\bar{\psi}, \varphi)$  and the Yukawa part of the  $(\varphi, \varphi)$  entry, as well as the new terms  $(\psi, A)$ ,  $(\bar{\psi}, A)$ ,  $(A, \psi)$  and  $(A, \bar{\psi})$ . The remaining matrix  $\Gamma_{k,A,\varphi,c}^{(2)} + R_k$  is block-diagonal. According to section 4.2, the rewritten flow equation reads

$$\delta_0 \partial_t H_k(\varphi) \mathbb{1}_{d_\gamma} = \frac{1}{iN_C} \frac{\overrightarrow{\delta}}{\delta \bar{\psi}^f} \frac{1}{2} \text{STr} \left[ \tilde{\partial}_t \log \left( 1 + \frac{\Delta \Gamma_k^{(2)}}{\Gamma_{k,\varphi,A,c}^{(2)} + R_k} \right) \right] \frac{\overleftarrow{\delta}}{\delta \psi^f} \Bigg|_{\substack{\varphi = \text{const} \\ \psi = \bar{\psi} = 0 \\ A_\mu = 0 \\ c = c^* = 0}}. \quad (6.2.2)$$

Hence, we have to compute the inverse of  $\Gamma_{k,A,\varphi,c}^{(2)} + R_k$ . As mentioned before, it is block-diagonal,  $\Gamma_{k,A,\varphi,c}^{(2)} + R_k = A \oplus B$ . The matrix  $A$  contains the same entries as in our former truncation up to the new colour indices (see (4.2.6)). However, as we can see from (6.1.2), these entries are diagonal in the colour indices. Thus, we can immediately invert it, using the former results up to a factor  $\delta_{ab}$ . The inverse of  $B$  can be computed easily as well, because the entries  $(c, c^*)$  and  $(c^*, c)$  are just scalars (and diagonal in the colour indices) and to invert the  $(A, A)$  element we can make use of the properties (6.1.1) of the projectors. The inverse of  $B$  is then given by

$$\delta_{p,q} \times \begin{pmatrix} \delta_{IJ} \frac{1}{Z_{A,k}} \left( \frac{\pi_{\mu\nu}^T}{P_A^T} + \xi \frac{\pi_{\mu\nu}^L}{P_A^L} \right) & 0 & 0 \\ 0 & 0 & \frac{\delta_{ab}}{Z_{c,k} P_c} \\ 0 & -\frac{\delta_{ab}}{Z_{c,k} P_c} & 0 \end{pmatrix}$$

## 6.2 Extended flow equations

and we eventually have  $(\Gamma_{k,A,\varphi,c}^{(2)} + R_k)^{-1} = A^{-1} \oplus B^{-1}$ . Consequently, the product  $\frac{\Delta\Gamma_k^{(2)}}{\Gamma_{k,\varphi,A,c}^{(2)} + R_k}$  has the following non-vanishing entries:

$$\begin{aligned}
(\varphi, \varphi) &: i\delta_{p,q} H_k'' \bar{\psi}^l \psi^l \frac{1}{\xi_\varphi} \\
(\varphi, \psi) &: i\delta_{p,q} H_k' \bar{\psi}^b \frac{1}{\xi_\varphi} \\
(\varphi, \bar{\psi}) &: -i\delta_{p,q} H_k' \psi^{T,b} \frac{1}{\xi_\varphi} \\
(\psi, \varphi) &: -i\delta_{p,q} H_k' \frac{Z_{\psi,k}(1+r_{\psi,k})\not{p} + iH_k}{\xi_\psi} \psi^a \\
(\bar{\psi}, \varphi) &: i\delta_{p,q} H_k' \frac{Z_{\psi,k}(1+r_{\psi,k})\not{p}^T - iH_k}{\xi_\psi} \bar{\psi}^{T,a} \\
(\psi, A) &: -\delta_{p,q} g Z_{\psi,k} \frac{Z_{\psi,k}(1+r_{\psi,k})\not{p} + iH_k}{\xi_\psi} [T_J]_{ae} \gamma_\nu \psi^e \\
(\bar{\psi}, A) &: -\delta_{p,q} g Z_{\psi,k} \frac{-Z_{\psi,k}(1+r_{\psi,k})\not{p}^T + iH_k}{\xi_\psi} \gamma_\nu^T \bar{\psi}^{T,e} [T_J]_{ea} \\
(A, \psi) &: \delta_{p,q} \frac{g Z_{\psi,k}}{Z_{A,k}} \left( \frac{\pi_{\mu\lambda}^T}{P_A^T} + \xi \frac{\pi_{\mu\lambda}^L}{P_A^L} \right) \bar{\psi}^e \gamma^\lambda [T_I]_{eb} \\
(A, \bar{\psi}) &: -\delta_{p,q} \frac{g Z_{\psi,k}}{Z_{A,k}} \left( \frac{\pi_{\mu\lambda}^T}{P_A^T} + \xi \frac{\pi_{\mu\lambda}^L}{P_A^L} \right) [T_I]_{be} \psi^{T,e} \gamma^{T,\lambda}. \tag{6.2.3}
\end{aligned}$$

Now it is time to perform the log-expansion again. From (6.2.3) we see that concerning the first order, only the  $(\varphi, \varphi)$  entry is relevant. Indeed, it yields exactly the same contribution as in our former truncation. The same way, the old contributions coming from the second order are reproduced. However, there appear some new terms in the entries  $(\psi, \psi)$ ,  $(\bar{\psi}, \bar{\psi})$  and  $(A, A)$  of  $\left( \frac{\Delta\Gamma_k^{(2)}}{\Gamma_{k,\varphi,A,c}^{(2)} + R_k} \right)^2$ . They read

$$\begin{aligned}
(\psi, \psi) &: -\delta_{p,q} \frac{g^2 Z_{\psi,k}^2}{Z_{A,k}} \frac{Z_{\psi,k}(1+r_{\psi,k})\not{p} + iH_k}{\xi_\psi} \left( \frac{\pi_{\sigma\lambda}^T}{P_A^T} + \xi \frac{\pi_{\sigma\lambda}^L}{P_A^L} \right) [T_K]_{ae} \gamma^\lambda \psi^e \bar{\psi}^f \gamma^\sigma [T_K]_{fb} \\
(\bar{\psi}, \bar{\psi}) &: \delta_{p,q} \frac{g^2 Z_{\psi,k}^2}{Z_{A,k}} \frac{-Z_{\psi,k}(1+r_{\psi,k})\not{p}^T + iH_k}{\xi_\psi} \left( \frac{\pi_{\sigma\lambda}^T}{P_A^T} + \xi \frac{\pi_{\sigma\lambda}^L}{P_A^L} \right) \gamma^{T,\lambda} \bar{\psi}^{T,f} [T_K]_{fa} [T_K]_{be} \psi^{T,e} \gamma^{T,\sigma} \\
(A, A) &: -\delta_{p,q} \frac{g^2 Z_{\psi,k}^2}{Z_{A,k}} \left( \frac{\pi_{\mu\sigma}^T}{P_A^T} + \xi \frac{\pi_{\mu\sigma}^L}{P_A^L} \right) \bar{\psi}^e \gamma^\sigma [T_I]_{ed} \frac{Z_{\psi,k}(1+r_{\psi,k})\not{p} + iH_k}{\xi_\psi} [T_J]_{df} \gamma^\nu \psi^f \\
&+ \frac{g^2 Z_{\psi,k}^2}{Z_{A,k}} \left( \frac{\pi_{\mu\sigma}^T}{P_A^T} + \xi \frac{\pi_{\mu\sigma}^L}{P_A^L} \right) [T_I]_{de} \psi^{T,e} \gamma^{T,\sigma} \frac{-Z_{\psi,k}(1+r_{\psi,k})\not{p}^T + iH_k}{\xi_\psi} \gamma^{T,\nu} \bar{\psi}^{T,f} [T_J]_{fd}. \tag{6.2.4}
\end{aligned}$$

The next step is to analyse the super trace. We start with the analysis of the Dirac structure. We explain the calculations in detail for the fermionic sectors, the calculations for the  $(A, A)$  entry are similar.

The first observation is that we can neglect the  $\not{p}$  terms since the trace over the product of an odd number of  $\gamma$ -matrices always vanishes. Because taking the super trace also implies setting  $a = b$  and summing over  $a$ , the coefficients of  $(\bar{\psi}, \bar{\psi})$  and  $(\psi, \psi)$  are the same and we are left with

$$\begin{aligned} \text{Tr}_\gamma(-\gamma^\lambda \psi^e \bar{\psi}^f \gamma^\sigma + \gamma^{T,\lambda} \bar{\psi}^{T,f} \psi^{T,e} \gamma^{T,\sigma}) &= \text{Tr}_\gamma(-\gamma^\lambda \psi^e \bar{\psi}^f \gamma^\sigma - \gamma^\sigma \psi^e \bar{\psi}^f \gamma^\lambda) \\ &= \bar{\psi}^f \gamma^\sigma \gamma^\lambda \psi^e + \bar{\psi}^f \gamma^\lambda \gamma^\sigma \psi^e. \end{aligned}$$

Note that both the terms are contracted with the projectors  $\pi_{\lambda\sigma}$ , which are symmetric in the spacetime indices. Hence, both terms together yield the contribution

$$2 \bar{\psi}^f \gamma^\sigma \gamma^\lambda \psi^e.$$

By performing the field derivatives of the projection rule (which yield a factor  $\delta_{ef}$ ) and using

$$\pi_{\lambda\sigma}(\gamma^\sigma \gamma^\lambda) = \frac{1}{2} \pi_{\lambda\sigma}(\gamma^\sigma \gamma^\lambda + \gamma^\lambda \gamma^\sigma) = \pi_{\lambda\sigma} \delta^{\sigma\lambda} \mathbb{1}_{d_\gamma}$$

we finally get<sup>1</sup>

$$2i \delta_{p,q} \frac{g^2 Z_{\psi,k}^2}{Z_{A,k}} \frac{H_k}{\xi_\psi} \left( \frac{\pi_\lambda^{T\lambda}}{P_A^T} + \xi \frac{\pi_\lambda^{L\lambda}}{P_A^L} \right) [T_I]_{ae} [T_J]_{ea}.$$

Due to the super trace we also have to set  $I = J$ , which enables us to simplify the expression above once more

$$[T_I]_{ae} [T_I]_{ea} = \text{Tr}(T_I T_I) = \frac{1}{2} \delta_{II} = \frac{1}{2} (N_C^2 - 1).$$

Furthermore, we can use

$$\begin{aligned} \pi_\lambda^{T\lambda} &= (d-1) \\ \pi_\lambda^{L\lambda} &= 1. \end{aligned}$$

After taking the trace over the momentum indices and collecting all missing pre-factors from the Wetterich equation, the projection rule and the log-expansion as well as a factor  $(-1)$ , since we operate in fermionic sectors, we finally end up with<sup>2</sup>

$$\frac{1}{4} \delta_0 H_k \frac{N_C^2 - 1}{N_C} \frac{g^2 Z_{\psi,k}^2}{Z_{A,k}} \tilde{\partial}_t \int_p \frac{1}{\xi_\psi} \left( \frac{d-1}{P_A^T} + \xi \frac{1}{P_A^L} \right). \quad (6.2.5)$$

Similar calculations for the  $(A, A)$  entry yield exactly the same term.

The factor  $\delta_0$  cancels with the one on the left hand side of the flow equation as always.

<sup>1</sup>The  $\mathbb{1}_{d_\gamma}$  can be skipped, because it also appears on the left hand side of the flow equation.

<sup>2</sup>Note that in this chapter, the modified scale derivative  $\tilde{\partial}_t = \sum_i \int_x Z_{i,k}^{-1} \partial_t (Z_{i,k} r_i(x)) \frac{\delta}{\delta r_i(x)}$  includes terms  $i = \varphi, \psi, A^T, A^L, c$ .

Hence, the additional contribution to the flow equation of  $H_k$  reads

$$\frac{1}{2}H_k \frac{N_C^2 - 1}{N_C} \frac{g^2 Z_{\psi,k}^2}{Z_{A,k}} \tilde{\partial}_t \int_p \frac{1}{\xi_{\psi}} \left( \frac{d-1}{P_A^T} + \xi \frac{1}{P_A^L} \right) \quad (6.2.6)$$

and in terms of the threshold functions

$$\begin{aligned} -2g^2 Z_{A,k}^{-1} H_k \frac{N_C^2 - 1}{N_C} v_d k^{d-4} \left\{ (d-1) l_{1,1}^{(FB)d} \left[ k^{-2} Z_{\psi,k}^{-2} H_k^2, 0; \eta_{\psi}, \eta_A^T \right] \right. \\ \left. + \xi l_{1,1}^{(FB)d} \left[ k^{-2} Z_{\psi,k}^{-2} H_k^2, 0; \eta_{\psi}, \eta_A^L \right] \right\}. \end{aligned} \quad (6.2.7)$$

### 6.2.2 Extended flow of the effective potential

The projection rule reads

$$\delta_0 \partial_t U_k(\varphi) = \frac{1}{2} \text{STr} \left[ \frac{\partial_t R_k}{\Gamma_k^{(2)} + R_k} \right] \Bigg|_{\substack{\varphi = \varphi_0 = \text{const} \\ \psi = \bar{\psi} = 0 \\ A_{\mu} = 0 \\ c = c^* = 0}}. \quad (6.2.8)$$

Due to the fact that except  $\varphi$  all fields are set to zero, the new fluctuation terms disappear. Hence, it is clear that no additional terms emerge, but just like in case of the Yukawa coupling, the former terms are reproduced. However, there will be two differences. The first is the additional colour structure in the fermionic sector. Although it is diagonal in the colour indices (see  $(\bar{\psi}, \psi)$  and  $(\psi, \bar{\psi})$  entries in (6.1.2)), we will get an additional factor  $N_C$  when taking the super trace<sup>3</sup>. This holds for all former terms with a  $d_{\gamma}$  in front. The second difference is the new structure of the regulator term  $R_k$ . It will lead to additional terms in the  $(A, A)$ ,  $(c, c^*)$  and  $(c^*, c)$  entries of  $\frac{\partial_t R_k}{\Gamma_k^{(2)} + R_k}$ . The corresponding contributions to the flow equation of  $U_k$  read

$$\frac{1}{2} (N_C^2 - 1) \int_p p^2 \left( (d-1) \frac{\partial_t(Z_{A,k} r_{A,k}^T)}{Z_{A,k} P_A^T} + \xi \frac{\partial_t(Z_{A,k} r_{A,k}^L)}{Z_{A,k} P_A^L} \right)$$

and

$$N_C \int_p p^2 \frac{\partial_t(Z_{c,k} r_{c,k})}{Z_{c,k} P_c}.$$

However, we see that both contributions are independent of  $\varphi$ . Hence, they only result in a scale dependent shift of the effective potential (and thus contribute to the cosmological constant, see chapter 3). If we were interested in an analysis as performed in chapter 5, we could neglect these terms. Then the flow equation reads

$$\partial_t U_k(\varphi) = 2v_d k^d l_0^d \left[ Z_{\varphi,k}^{-1} k^{-2} U_k''(\varphi); \eta_{\varphi} \right] - 2d_{\gamma} N_C v_d k^d l_0^{(F)d} \left[ Z_{\psi,k}^{-2} k^{-2} H_k^2; \eta_{\psi} \right]. \quad (6.2.9)$$

<sup>3</sup>In the case of the Yukawa coupling it was cancelled due to the modified projection rule.

## 6.2.3 Extended flow of the anomalous dimensions

We focus only on the anomalous dimensions of  $\varphi$  and  $\psi$ , respectively  $\bar{\psi}$ . Let us start with  $Z_{\varphi,k}$ . The projection rule reads

$$\delta_0 Z_{\varphi,k} = \frac{1}{2d} \eta^{\rho\sigma} \partial_{q\rho} \partial_{q\sigma} \frac{\delta}{\delta\sigma(q)} \frac{\delta}{\delta\sigma(p')} \Gamma_k \left| \begin{array}{l} \sigma = 0 \\ \psi = \bar{\psi} = 0 \\ A_\mu = 0 \\ c = c^* = 0 \\ p' = -q \\ p' = -q = 0 \end{array} \right. . \quad (6.2.10)$$

We immediately see that all new fluctuation terms that appeared in the extended fluctuation matrix (6.1.2) will vanish again, since we set the fermionic fields to zero. In contrast to the case of the effective potential however, we have to apply the trick involving the rewriting of the super trace and using the log-expansion. It turns out that as a consequence even the entries  $(A, A)$ ,  $(c, c^*)$  and  $(c^*, c)$  will yield no additional terms so that we obtain the same result as in our former truncation. The only thing we have to be aware of is the colour structure of the fermionic sector again, which simply yields a factor  $N_C$  in front of former terms that contained a factor  $d_\gamma$ . Thus, the flow equation reads

$$\begin{aligned} \partial_t Z_{\varphi,k} = & -\frac{4}{d} v_d k^{d-6} \left( U_k^{(3)} \right)^2 Z_{\varphi,k}^{-2} m_{2,2}^d \left[ Z_{\varphi,k}^{-1} k^{-2} U_k''(v_k), Z_{\varphi,k}^{-1} k^{-2} U_k''(v_k); \eta_\varphi \right] \\ & -\frac{8}{d} d_\gamma N_C v_d k^{d-4} H_k'^2(v_k) Z_{\psi,k}^{-2} m_4^{(F)d} \left[ Z_{\psi,k}^{-2} k^{-2} H_k^2(v_k); \eta_\varphi \right] \\ & +\frac{8}{d} d_\gamma N_C v_d k^{d-6} H_k'^2(v_k) H_k^2(v_k) Z_{\psi,k}^{-4} m_2^{(F)d} \left[ Z_{\psi,k}^{-2} k^{-2} H_k^2(v_k); \eta_\psi \right]. \end{aligned} \quad (6.2.11)$$

The projection rule for  $Z_{\psi,k}$  is given by

$$\delta_0 Z_{\psi,k} = -\frac{1}{dd_\gamma} \frac{1}{N_C} \text{Tr}_\gamma \gamma^\mu \partial_{p'\mu} \frac{\overrightarrow{\delta}}{\delta\bar{\psi}^l(p')} \Gamma_k \frac{\overleftarrow{\delta}}{\delta\psi^l(q)} \left| \begin{array}{l} \sigma = 0 \\ \psi = \bar{\psi} = 0 \\ A_\mu = 0 \\ c = c^* = 0 \\ q = p' \\ q = p' = 0 \end{array} \right. . \quad (6.2.12)$$

It is clear that in this case we have to work a little more, because we cannot set the fermionic fields to zero from the beginning. The calculations are similar to those in the case of  $H_k$ . We perform the decomposition of  $\Gamma_k + R_k$  as well as the rewriting of the super trace. However, we have to take into consideration that the fermionic fields carry momentum.

The usual calculation of  $\frac{\Delta\Gamma_k^{(2)}}{\Gamma_{k,A,\phi,c}^{(2)}+R_k}$  and its square shows that all former terms of the flow equation are reproduced, but there appear new terms in the  $(A, A)$ ,  $(\psi, \psi)$  and  $(\bar{\psi}, \bar{\psi})$  entry of  $\left(\frac{\Delta\Gamma_k^{(2)}}{\Gamma_{k,A,\phi,c}^{(2)}+R_k}\right)^2$ . Introducing the abbreviations<sup>4</sup>

$$\begin{aligned} K_{\mu\sigma}(q) &= \frac{\pi_{\mu\sigma}^T(q)}{P_A^T(q)} + \xi \frac{\pi_{\mu\sigma}^L(q)}{P_A^L(q)} \\ R(q) &= \frac{Z_{\psi,k}(1+r_{\psi,k}(q))\not{q} + iH_k}{\xi_{\psi}(q)} \\ \tilde{R}(q) &= \frac{-Z_{\psi,k}(1+r_{\psi,k}(q))\not{q}^T + iH_k}{\xi_{\psi}(q)} \end{aligned}$$

they read

$$\begin{aligned} (\psi, \psi) : & \quad -\frac{g^2 Z_{\psi,k}^2}{Z_{A,k}} \int_{p,s} R(p) [T_K]_{ae} \gamma_{\lambda} \psi^e(p-s) K^{\lambda\sigma}(s) \bar{\psi}^f(p-s) \gamma_{\sigma} [T_K]_{fb} \\ (\bar{\psi}, \bar{\psi}) : & \quad \frac{g^2 Z_{\psi,k}^2}{Z_{A,k}} \int_{p,s} \tilde{R}(p) K^{\lambda\sigma}(s) \gamma_{\lambda}^T \bar{\psi}^{T,f}(s-p) [T_K]_{fa} [T_K]_{be} \psi^{T,e}(s-p) \gamma_{\sigma}^T \\ (A, A) : & \quad -\frac{g^2 Z_{\psi,k}^2}{Z_{A,k}} \int_{p,s} K^{\mu\lambda}(p) \bar{\psi}^e(s-p) \gamma_{\lambda} [T_I]_{ed} R(s) [T_J]_{df} \gamma_{\nu} \psi^f(s-p) \\ & \quad + \frac{g^2 Z_{\psi,k}^2}{Z_{A,k}} \int_{p,s} K^{\mu\lambda}(p) [T_I]_{de} \psi^{T,e}(p-s) \gamma_{\lambda}^T \tilde{R}(s) \gamma_{\nu}^T \bar{\psi}^{T,f}(p-s) [T_J]_{fd}, \end{aligned} \tag{6.2.13}$$

where we already set  $p = q$  and integrated with respect to  $p$ , due to the super trace. We are still left with two momentum integrals, because the fermionic fields carry momentum and thus  $\frac{\Delta\Gamma_k^{(2)}}{\Gamma_{k,A,\phi,c}^{(2)}+R_k}$  is not diagonal in the momentum indices. Therefore, we have

$$\int_p \left( \frac{\Delta\Gamma_k^{(2)}}{\Gamma_{k,A,\phi,c}^{(2)}+R_k} \right)^2 (p, p) = \int_{p,s} \left( \frac{\Delta\Gamma_k^{(2)}}{\Gamma_{k,A,\phi,c}^{(2)}+R_k} \right) (p, s) \left( \frac{\Delta\Gamma_k^{(2)}}{\Gamma_{k,A,\phi,c}^{(2)}+R_k} \right) (s, p),$$

which corresponds to the two momentum integrals appearing in equation (6.2.13). The next step is to perform the trace over the remaining index structures. We will explain the calculations in detail for the fermionic contributions, the calculations for the  $(A, A)$  entry are similar.

<sup>4</sup>Note that  $R(q)$  and  $\tilde{R}(q)$  are matrix-valued.

Let us start with the Dirac trace. In the  $(\psi, \psi)$  entry we have

$$\begin{aligned}\mathrm{Tr}_\gamma(-R(p)\gamma_\lambda\psi^e(p-s)\bar{\psi}^f(p-s)\gamma_\sigma) &= \mathrm{Tr}_\gamma(\bar{\psi}^f(p-s)\gamma_\sigma R(p)\gamma_\lambda\psi^e(p-s)) \\ &= \bar{\psi}^f(p-s)\gamma_\sigma R(p)\gamma_\lambda\psi^e(p-s).\end{aligned}$$

Performing the field derivatives  $\frac{\overrightarrow{\delta}}{\delta\psi^l(p')}$  and  $\frac{\overleftarrow{\delta}}{\delta\psi^l(q)}$  creates factors  $\delta_{ef}$ ,  $\delta_{p-s,p'}$  and  $\delta_{p-s,q}$ . Concerning the  $(\bar{\psi}, \bar{\psi})$  entry we obtain

$$\begin{aligned}\mathrm{Tr}_\gamma(\tilde{R}(p)\gamma_\lambda^T\bar{\psi}^{T,f}(s-p)\psi^{T,e}(s-p)\gamma_\sigma^T) &= -\mathrm{Tr}_\gamma(\gamma_\sigma\psi^e(s-p)\bar{\psi}^f(s-p)\gamma_\lambda\tilde{R}^T(p)) \\ &= \mathrm{Tr}_\gamma(\bar{\psi}^f(s-p)\gamma_\lambda\tilde{R}^T(p)\gamma_\sigma\psi^e(s-p)) \\ &= \bar{\psi}^f(s-p)\gamma_\lambda\tilde{R}^T(p)\gamma_\sigma\psi^e(s-p).\end{aligned}$$

In this case the field derivatives create factors  $\delta_{ef}$ ,  $\delta_{s-p,p'}$  and  $\delta_{s-p,q}$ . By setting  $a = b$  due to the super trace and using the  $\delta_{ef}$  we obtain  $\mathrm{Tr}(T_I T_I) = \frac{1}{2}(N_C^2 - 1)$  in front of both terms, just like in case of  $H_k$ . Carrying out the  $s$ -integration enables us to summarize both terms, which yields

$$\frac{1}{2}\delta_{p',q}\frac{g^2 Z_{\psi,k}^2}{Z_{A,k}}(N_C^2 - 1)\int_p\left(K^{\lambda\sigma}(p-p')\gamma_\sigma R(p)\gamma_\lambda + K^{\lambda\sigma}(p+p')\gamma_\lambda\tilde{R}^T(p)\gamma_\sigma\right).$$

According to the projection rule we have to set  $p' = q$ , which yields a factor  $\delta_0$ . The last part of the projection rule reads  $\mathrm{Tr}_\gamma\gamma^\nu\partial_{p'\nu}$ . Hence, the  $iH_k$  terms of  $R(q)$  and  $\tilde{R}^T(q)$  vanish, because the trace over an odd number of  $\gamma$ -matrices vanishes. By defining

$$f(p)\not{p} = \frac{Z_{\psi,k}(1+r_{\psi,k}(p))}{\xi_\psi(p)}\not{p}$$

we obtain

$$\frac{1}{2}\delta_0\mathrm{Tr}_\gamma\gamma^\nu\partial_{p'\nu}\frac{g^2 Z_{\psi,k}^2}{Z_{A,k}}(N_C^2 - 1)\int_p\left(K^{\lambda\sigma}(p-p')\gamma_\sigma f(p)\not{p}\gamma_\lambda - K^{\lambda\sigma}(p+p')\gamma_\lambda f(p)\not{p}\gamma_\sigma\right).$$

Because  $K^{\lambda\sigma}$  is symmetric and by writing  $\not{p} = p_\mu\gamma^\mu$  we find

$$\frac{1}{2}\delta_0\frac{g^2 Z_{\psi,k}^2}{Z_{A,k}}(N_C^2 - 1)\int_p\mathrm{Tr}_\gamma\left(\gamma^\nu\gamma^\sigma\gamma^\mu\gamma^\lambda\right)f(p)p_\mu\partial_{p'\nu}(K_{\lambda\sigma}(p-p') - K_{\lambda\sigma}(p+p'))\tag{6.2.14}$$

Accomplishing the  $p'$ -derivative and setting  $p' = 0$  due to the projection rule gives

$$\begin{aligned}\partial_{p'\nu}K_{\lambda\sigma}(p\mp p')\Big|_{p'=0} &= \pm 2\xi\frac{p_\lambda p_\sigma p_\nu}{p^4 P_A^L(p)} \mp 2\xi\frac{p_\lambda p_\sigma p_\nu}{p^2}\partial_{p^2}\frac{1}{P_A^L(p)} \mp \xi\frac{\delta_{\lambda\nu}p_\sigma + \delta_{\nu\sigma}p_\lambda}{p^2 P_A^L(p)} \mp 2\delta_{\lambda\sigma}p_\nu\partial_{p^2}\frac{1}{P_A^T(p)} \\ &\mp 2\frac{p_\lambda p_\sigma p_\nu}{p^4 P_A^T(p)} \pm 2\frac{p_\lambda p_\sigma p_\nu}{p^2}\partial_{p^2}\frac{1}{P_A^T(p)} \pm \frac{\delta_{\lambda\nu}p_\sigma + \delta_{\nu\sigma}p_\lambda}{p^2 P_A^T(p)}.\end{aligned}$$

Eventually, the new contribution reads

$$\begin{aligned}
 & 2\delta_0 \frac{g^2 Z_{\psi,k}^2}{Z_{A,k}} (N_C^2 - 1) \int_p \text{Tr}_\gamma \left( \gamma^\nu \gamma^\sigma \gamma^\mu \gamma^\lambda \right) f(p) p_\mu \\
 & \times \left( \xi \frac{p_\lambda p_\sigma p_\nu}{p^4 P_A^L(p)} - \xi \frac{p_\lambda p_\sigma p_\nu}{p^2} \partial_{p^2} \frac{1}{P_A^L(p)} + \frac{1}{2} \xi \frac{\delta_{\lambda\nu} p_\sigma + \delta_{\nu\sigma} p_\lambda}{p^2 P_A^L(p)} - \delta_{\lambda\sigma} p_\nu \partial_{p^2} \frac{1}{P_A^T(p)} \right. \\
 & \quad \left. - \frac{p_\lambda p_\sigma p_\nu}{p^4 P_A^T(p)} + \frac{p_\lambda p_\sigma p_\nu}{p^2} \partial_{p^2} \frac{1}{P_A^T(p)} + \frac{1}{2} \frac{\delta_{\lambda\nu} p_\sigma + \delta_{\nu\sigma} p_\lambda}{p^2 P_A^T(p)} \right). \tag{6.2.15}
 \end{aligned}$$

After using the identity

$$\text{Tr}_\gamma \left( \gamma^\nu \gamma^\sigma \gamma^\mu \gamma^\lambda \right) = d_\gamma \left( \delta^{\nu\sigma} \delta^{\mu\lambda} - \delta^{\nu\mu} \delta^{\sigma\lambda} + \delta^{\nu\lambda} \delta^{\sigma\mu} \right)$$

and some index algebra we find

$$2\delta_0 d_\gamma \frac{g^2 Z_{\psi,k}^2}{Z_{A,k}} (N_C^2 - 1) \int_p f(p) \left\{ p^2 \partial_{p^2} \left( \frac{d-1}{P_A^T(p)} - \frac{\xi}{P_A^L(p)} \right) + \frac{\xi(1-d)}{P_A^L(p)} - \frac{(1-d)}{P_A^T(p)} \right\}. \tag{6.2.16}$$

The final step is to collect all remaining pre-factors, i.e. from the Wetterich equation, the projection rule and the log-expansion as well as a factor  $(-1)$ , since we operate in fermionic sectors. Therefore, we obtain

$$-\frac{1}{d} \frac{g^2 Z_{\psi,k}^2}{Z_{A,k}} \frac{N_C^2 - 1}{2N_C} \tilde{\partial}_t \int_p \frac{Z_{\psi,k}(1+r_\psi)}{\xi_\psi} \left\{ p^2 \partial_{p^2} \left( \frac{d-1}{P_A^T(p)} - \frac{\xi}{P_A^L(p)} \right) + \frac{\xi(1-d)}{P_A^L(p)} - \frac{(1-d)}{P_A^T(p)} \right\}.$$

The  $(A, A)$  entry yields exactly the same term, so the final result for the additional contribution to the flow equation of  $Z_{\psi,k}$  reads

$$-\frac{2}{d} \frac{g^2 Z_{\psi,k}^2}{Z_{A,k}} \frac{N_C^2 - 1}{2N_C} \tilde{\partial}_t \int_p \frac{Z_{\psi,k}(1+r_\psi)}{\xi_\psi} \left\{ p^2 \partial_{p^2} \left( \frac{d-1}{P_A^T(p)} - \frac{\xi}{P_A^L(p)} \right) + \frac{\xi(1-d)}{P_A^L(p)} - \frac{(1-d)}{P_A^T(p)} \right\}, \tag{6.2.17}$$

and in terms of the threshold functions

$$\begin{aligned}
 & Z_{\psi,k} \frac{8v_d}{d} \frac{g^2}{Z_{A,k}} \frac{N_C^2 - 1}{2N_C} k^{d-4} \left\{ (1-d) m_{1,2}^{(FB)d} \left[ k^{-2} Z_{\psi,k}^{-2} H_k^2, 0; \eta_\psi, \eta_A^T \right] \right. \\
 & \quad + \xi m_{1,2}^{(FB)d} \left[ k^{-2} Z_{\psi,k}^{-2} H_k^2, 0; \eta_\psi, \eta_A^L \right] - (1-d) M_{1,1}^{(FB)d} \left[ k^{-2} Z_{\psi,k}^{-2} H_k^2, 0; \eta_\psi, \eta_A^T \right] \\
 & \quad \left. + \xi(1-d) M_{1,1}^{(FB)d} \left[ k^{-2} Z_{\psi,k}^{-2} H_k^2, 0; \eta_\psi, \eta_A^L \right] \right\}. \tag{6.2.18}
 \end{aligned}$$

## 6.2 Extended flow equations

It is convenient to choose the same regulator for the transversal and longitudinal part,  $P_A^L = P_A^T$ . Our new set of flow equations in dimensionless and renormalized quantities then reads<sup>5</sup>

$$\begin{aligned}
\partial_t \tilde{U}_k(\tilde{\rho}) &= -d\tilde{U}_k + (d-2 + \eta_{\varphi,k})\tilde{\rho}\tilde{U}'_k(\tilde{\rho}) + 2v_d l_0^d [\omega_u(\tilde{\rho}); \eta_\varphi] - 2d_\gamma N_C v_d l_0^{(F)d} [\tilde{H}_k^2(\tilde{\varphi}); \eta_\psi] \\
\partial_t \tilde{H}_k(\tilde{\varphi}) &= (\eta_{\psi,k} - 1)\tilde{H}_k + \left(\frac{d}{2} - 1 + \frac{\eta_{\varphi,k}}{2}\right) \tilde{\varphi}\tilde{H}'_k(\tilde{\varphi}) - 2\tilde{H}_k''(\tilde{\varphi})v_d l_1^d [\omega_u(\tilde{\rho}); \eta_\varphi] \\
&\quad + 4v_d \tilde{H}_k(\tilde{\varphi})\tilde{H}_k'^2(\tilde{\varphi})l_{1,1}^{(FB)d} [\tilde{H}_k^2(\tilde{\varphi}), \omega_u(\tilde{\rho}); \eta_\psi, \eta_\phi] \\
&\quad - 4\tilde{g}^2 \tilde{H}_k \frac{N_C^2 - 1}{2N_C} v_d \left\{ (d-1 + \xi) l_{1,1}^{(FB)d} [\tilde{H}_k^2(\tilde{\varphi}), 0; \eta_\psi, \eta_A] \right\} \\
\eta_{\psi,k} &= \frac{8}{d} \tilde{H}_k'^2(\tilde{v}_k) v_d m_{1,2}^{(FB)d} [\tilde{H}_k^2(\tilde{v}_k), \omega_u(\tilde{\kappa}_k); \eta_\psi, \eta_\varphi] \\
&\quad - \frac{8v_d \tilde{g}^2 N_C^2 - 1}{d} \left\{ (1-d + \xi) m_{1,2}^{(FB)d} [\tilde{H}_k^2(\tilde{v}_k), 0; \eta_\psi, \eta_A] \right. \\
&\quad \quad \left. + (1-d)(\xi-1) M_{1,1}^{(FB)d} [\tilde{H}_k^2(\tilde{v}_k), 0; \eta_\psi, \eta_A] \right\} \\
\eta_{\varphi,k} &= \frac{4}{d} v_d \mathcal{D}[\tilde{U}_k](\tilde{\kappa}_k) m_{2,2}^d [\omega_u(\tilde{\kappa}_k), \omega_u(\tilde{\kappa}_k); \eta_\varphi] \\
&\quad + \frac{8}{d} d_\gamma N_C v_d \tilde{H}_k'^2(\tilde{v}_k) m_4^{(F)d} [\tilde{H}_k^2(\tilde{v}_k); \eta_\varphi] \\
&\quad - \frac{8}{d} d_\gamma N_C v_d \tilde{H}_k'^2(\tilde{v}_k) \tilde{H}_k^2(\tilde{v}_k) m_2^{(F)d} [\tilde{H}_k^2(\tilde{v}_k); \eta_\psi], \tag{6.2.19}
\end{aligned}$$

where  $\mathcal{D}[\tilde{U}_k](\tilde{\rho}) = \tilde{\rho} \left( 3\tilde{U}_k''(\tilde{\rho}) + 2\tilde{\rho}\tilde{U}_k'''(\tilde{\rho}) \right)^2$  and  $\omega_u(\tilde{\rho}) = 2\tilde{\rho}\tilde{U}_k''(\tilde{\rho}) + \tilde{U}_k'(\tilde{\rho})$ .

By these equations we take the full impact of the strong sector on the flow of the generalized Yukawa coupling into account. This set of equations is to be completed by the flow of  $\tilde{g}$  and  $\eta_A$ . As a first simple approach we can use the perturbation theory one-loop  $\beta$ -function to test the qualitative impact of the newly derived terms.

<sup>5</sup>For the strong coupling we have  $\tilde{g}^2 = k^{d-4} \frac{g^2}{Z_A}$ .

## 7 Summary and Outlook

In this thesis we considered a simple Higgs-Yukawa system to investigate the impact of certain operators on lower Higgs mass bounds, applying techniques of the functional renormalization group. Therefore, the main focus lay on the flow of the effective potential since the Higgs mass is determined by the curvature of the potential evaluated at the ground state. After presenting some basics about the FRG including the derivation of the central equation of this thesis, the Wetterich equation, we initially derived the flow equations of the quantities appearing in our toy model. Unlike former works ([13], [14]) that dealt with lower Higgs mass bounds in a Higgs-Yukawa system in the FRG framework we included a generalized Yukawa coupling  $H(\varphi)\bar{\psi}\psi$  and computed changes in the old versions of the flow equations. While the equations of the effective potential  $U_k$  and the field renormalizations  $Z_{\varphi,k}$  and  $Z_{\psi,k}$  were basically the same, up to some natural substitutions, the flow equation of the generalized Yukawa coupling exhibited an additional term. Our results matched with the flow equations of [33], who considered the same model but under a different point of view.

Using the derived flow equations as a starting point, we subsequently solved the flow of the couplings numerically. In the course of the numerical treatment we performed a polynomial expansion of the effective potential and the generalized Yukawa coupling about the vacuum expectation value in order to simplify the set of differential equations. Solving the equation system we reproduced established results of [14], i.e. we showed that deviations from the quartic UV effective potential indeed allows us to find bare coupling combinations that decrease the lower Higgs mass bound. The next step was to investigate the influence of the new operators encoded in the generalized Yukawa coupling  $H(\varphi)$ . We observed that the new operators affect the flow significantly, for a fixed UV potential the Higgs mass could be lowered by several GeV, just by taking the simplest new interaction term  $\mathfrak{h}_1\varphi^3\bar{\psi}\psi$  into account. Its impact on the Higgs mass was much bigger than the one of other higher dimensional operators  $\mathfrak{h}_j\varphi^{2j+1}\bar{\psi}\psi$  with  $j > 1$ , thus we restricted ourselves to the case  $j = 1$  in our further analysis. It turned out that to guarantee the correct IR physics, we have to choose a sufficiently large UV value of the quartic coupling of the effective potential. At first we restricted ourselves to quartic UV potentials and thus we were able to choose relatively large bare values of  $\mathfrak{h}_1$  since in the case of quartic UV potentials  $u_2 \geq 0$  has to hold anyway. However, to compensate the large  $\mathfrak{h}_1$  bare values the bare value of  $u_2$  had to be increased as well and as a consequence the lowering of the Higgs mass due to increasing  $\mathfrak{h}_1$  and the increasing of the Higgs mass due to increasing  $u_2$  nearly compensated each other. The derived mass bounds were at the same order of magnitude as those derived when considering deviations from the quartic UV potential but taking only the standard Yukawa interaction into account.

---

Thus, we extended our analysis to more general UV potentials up to  $\rho^4$ , especially investigating the case  $u_2 < 0$  again. Although this restricted us to much smaller bare values of  $\mathfrak{h}_1$  we were able to generate flows that yielded smaller Higgs masses. Hence, the combination of negative  $u_2$  and comparatively small  $\mathfrak{h}_1$  lead to a notable lowering of the former Higgs mass bound.

Nevertheless, as already mentioned in section 3, the Higgs-Yukawa Model in its current version completely neglects contributions from the strong interaction sector of the Standard Model. However, since we know from perturbative calculations that the flow of the top Yukawa coupling is influenced significantly by strong interaction terms, we decided to further extend our toy model by introducing the  $SU(N_C)$  structure of the Standard Model. We derived the new flow equations of this system, at least the equations of the effective potential  $U_k$ , the generalized Yukawa coupling  $H_k$  and the field renormalizations  $Z_{\psi,k}$  and  $Z_{\varphi,k}$ . The flow equations of  $H_k$  and the field renormalization  $Z_{\psi,k}$  acquired qualitatively new terms. The new set of equations opens the door for a further numerical analysis. The flow equations of the remaining quantities, e.g. the equation of the strong coupling, can be adopted from perturbative results, since the location of the Landau pole lies sufficiently far beyond the scale where the interesting quantities freeze out. Thus, a future task is to investigate whether the new operators of the generalized Yukawa coupling can achieve a further lowering of the Higgs mass bound in this more accurate model (with reference to the Standard Model). The new terms in the flow equations might enable this.

# Appendices

# A Threshold functions

The definition of the threshold functions is taken from [21]. Together with the introduced abbreviations

$$\begin{aligned} P_B(q) &= q^2(1 + r_{k,B}(q)) \\ P_F(q) &= q^2(1 + r_{k,F}(q))^2 \\ v_d^{-1} &= 2^{d+1}\pi^{\frac{d}{2}}\Gamma\left(\frac{d}{2}\right) \end{aligned}$$

the threshold functions read

$$\begin{aligned} l_n^d[\omega; \eta_B] &= \frac{n + \delta_{n,0}}{4} v_d^{-1} k^{2n-d} \int_q \left[ \left( \frac{1}{Z_{B,k}} \partial_t R_{k,B}(q) \right) (P_B(q) + \omega k^2)^{-(n+1)} \right] \\ l_n^{(F)d}[\omega; \eta_F] &= \frac{n + \delta_{n,0}}{2} v_d^{-1} k^{2n-d} \int_q \left[ \frac{P_F(q)}{1 + r_{k,F}} \left( \frac{1}{Z_{F,k}} \partial_t (Z_{F,k} r_{F,k}(q)) \right) (P_F(q) + \omega k^2)^{-(n+1)} \right] \\ l_{n_1, n_2}^{(FB)d}[\omega_1, \omega_2; \eta_F, \eta_B] &= -\frac{1}{4} v_d^{-1} k^{2(n_1+n_2)-d} \int_q \tilde{\partial}_t \left[ \frac{1}{(P_F(q) + k^2\omega_1)^{n_1} (P_B(q) + k^2\omega_2)^{n_2}} \right] \\ m_4^{(F)d}[\omega; \eta_B] &= -\frac{1}{4} v_d^{-1} k^{4-d} \int_q q^4 \tilde{\partial}_t \left[ \frac{\partial}{\partial q^2} \frac{1 + r_{F,k}(q)}{P_F(q) + k^2\omega} \right]^2 \\ m_2^{(F)d}[\omega; \eta_F] &= -\frac{1}{4} v_d^{-1} k^{6-d} \int_q q^2 \tilde{\partial}_t \left[ \frac{\left( \frac{\partial}{\partial q^2} P_F(q) \right)}{P_F(q) + k^2\omega} \right]^2 \\ m_{n_1, n_2}^d[\omega_1, \omega_2; \eta_B] &= -\frac{1}{4} v_d^{-1} k^{2(n_1+n_2-1)-d} \int_q q^2 \tilde{\partial}_t \left[ \frac{\left( \frac{\partial}{\partial q^2} P_B(q) \right)}{(P_B(q) + k^2\omega_1)^{n_1}} \frac{\left( \frac{\partial}{\partial q^2} P_B(q) \right)}{(P_B(q) + k^2\omega_2)^{n_2}} \right] \\ m_{n_1, n_2}^{(FB)d}[\omega_1, \omega_2; \eta_F, \eta_B] &= -\frac{1}{4} v_d^{-1} k^{2(n_1+n_2-1)-d} \int_q q^2 \tilde{\partial}_t \left[ \frac{1 + r_{F,k}(q)}{(P_F(q) + k^2\omega_1)^{n_1}} \frac{\left( \frac{\partial}{\partial q^2} P_B(q) \right)}{(P_B(q) + k^2\omega_2)^{n_2}} \right] \\ M_{n_1, n_2}^{(FB)d}[\omega_1, \omega_2; \eta_F, \eta_B] &= -\frac{1}{4} v_d^{-1} k^{2(n_1+n_2)-d} \int_q \tilde{\partial}_t \left[ \frac{1 + r_{F,k}(q)}{(P_F(q) + k^2\omega_1)^{n_1}} \frac{1}{(P_B(q) + k^2\omega_2)^{n_2}} \right]. \end{aligned}$$

## B Threshold functions for the Litim regulator

After application of the regulator

$$r_{B,k}(q) = \left( \frac{k^2}{q^2} - 1 \right) \Theta(k^2 - p^2)$$

$$(1 + r_{F,k}(q))^2 = (1 + r_{B,k}(q))$$

the threshold functions defined in appendix A read

$$l_n^d[\omega; \eta_B] = \frac{2(n + \delta_{n,0})}{d} \left( 1 - \frac{\eta_{B,k}}{d+2} \right) \frac{1}{(1 + \omega)^{n+1}}$$

$$l_n^{(F)d}[\omega; \eta_F] = \frac{2(n + \delta_{n,0})}{d} \left( 1 - \frac{\eta_{F,k}}{d+1} \right) \frac{1}{(1 + \omega)^{n+1}}$$

$$l_{n_1, n_2}^{(FB)d}[\omega_1, \omega_2; \eta_F, \eta_B] = \frac{2}{d} \frac{1}{(1 + \omega_1)^{n_1} (1 + \omega_2)^{n_2}} \left[ \frac{n_1}{1 + \omega_1} \left( 1 - \frac{\eta_{F,k}}{d+1} \right) + \frac{n_2}{1 + \omega_2} \left( 1 - \frac{\eta_{B,k}}{d+2} \right) \right]$$

$$m_4^{(F)d}[\omega; \eta_B] = \frac{1}{(1 + \omega)^4} + \frac{1 - \eta_{F,k}}{d-2} \frac{1}{(1 + \omega)^3} - \left( \frac{1 - \eta_{F,k}}{2d-4} + \frac{1}{4} \right) \frac{1}{(1 + \omega)^2}$$

$$m_2^{(F)d}[\omega; \eta_F] = \frac{1}{(1 + \omega)^4}$$

$$m_{n_1, n_2}^d[\omega_1, \omega_2; \eta_B] = \frac{1}{(1 + \omega_1)^{n_1} (1 + \omega_2)^{n_2}}$$

$$m_{n_1, n_2}^{(FB)d}[\omega_1, \omega_2; \eta_F, \eta_B] = \left( 1 - \frac{\eta_{B,k}}{d+1} \right) \frac{1}{(1 + \omega_1)^{n_1} (1 + \omega_2)^{n_2}}$$

$$M_{n_1, n_2}^{(FB)d}[\omega_1, \omega_2; \eta_F, \eta_B] = \frac{2n_2}{(d-1)} \left( 1 - \frac{\eta_{F,k}}{d-1} \right) \frac{1}{(1 + \omega_1)^{n_1} (1 + \omega_2)^{n_2+1}}$$

$$- \frac{1 + \omega_1 - 2n_1}{d-1} \left( 1 - \frac{\eta_{F,k}}{d} \right) \frac{1}{(1 + \omega_1)^{n_1+1} (1 + \omega_2)^{n_2}}.$$

These results match with those of [36] (apart from the newly introduced  $M_{n_1, n_2}^{(FB)d}$ ).

# List of Figures

2.1	Typical shape of the regulator . . . . .	22
2.2	Illustration of spontaneous symmetry breaking . . . . .	23
5.1	Higgs mass in dependency on the cut-off . . . . .	52
5.2	Higgs mass in dependency on the bare coupling $u_2$ . . . . .	52
5.3	Inconvenient flow of potential . . . . .	54
5.4	Negative bare couplings $u_2(\Lambda)$ . . . . .	57
5.5	$\mathfrak{h}_1$ dependency of the Higgs mass . . . . .	60
5.6	Comparison between $\mathfrak{h}_1$ -induced and $u_2$ -induced lower Higgs mass bound .	61
5.7	$\mathfrak{h}_1$ dependency of the Higgs mass II . . . . .	62
5.8	Comparison between $\mathfrak{h}_1$ -induced and $u_2$ -induced lower Higgs mass bound II	62

# Bibliography

- [1] F. Englert and R. Brout. Broken Symmetry and the Mass of Gauge Vector Mesons. *Phys.Rev.Lett.*, 13:321-323, 1964.
- [2] G.S. Guralnik, C.R. Hagen, and T.W.B. Kibble. Global Conservation Laws and Massless Particles. *Phys.Rev.Lett.*, 13:585-587, 1964.
- [3] P.W. Higgs. Broken symmetries, massless particles and gauge fields. *Phys.Lett.*, 12:132-133, 1964.
- [4] P.W. Higgs. Broken Symmetries and the Masses of Gauge Bosons. *Phys.Rev.Lett.*, 13:508-509, 1964.
- [5] The CMS Collaboration. Observation of a new boson at a mass of 125 GeV with the CMS experiment at the LHC. *Phys. Lett. B*716:30-61, 2012. arXiv:1207.7235v2 [hep-ex]
- [6] M. Sher. Electroweak Higgs Potentials and Vacuum Stability. *Phys.Rept.*, 179:273-418, 1989.
- [7] J.A. Casas, J.R. Espinosa, and M. Quiros. Standard model stability bounds for new physics within LHC reach. *Phys.Lett.*, B382:374-382, 1996. arXiv:hep-ph/9603227.
- [8] G. Isidori, G. Ridolfi, A. Strumia. On the metastability of the standard model vacuum. *Nucl.Phys.*, B609:387-409, 2001. arXiv:hep-ph/0104016.
- [9] K. Holland. Triviality and the Higgs mass lower bound. *Nucl.Phys.Proc.Suppl.*, 140:155-161, 2005. arXiv:hep-lat/0409112.
- [10] V. Branchina, H. Faivre. Effective potential (in)stability and lower bounds on the scalar (Higgs) mass. *Phys.Rev.*, D72:065017, 2005. arXiv:hep-th/0503188.
- [11] H. Gies, C. Gneiting, R. Sondenheimer. Higgs Mass Bounds from Renormalization Flow for a simple Yukawa model  
*Phys. Rev. D* 89, 045012, 2014. arXiv:1308.5075v1 [hep-ph]
- [12] C. Wetterich. Exact evolution equation for the effective potential. *Phys. Lett. B*301:90-94, 1993.
- [13] C. Gneiting. Higgs mass bounds from renormalization flow. Diploma Thesis, 2005.
- [14] R. Sondenheimer. Renormierungsflüsse von Higgsmassenschranken in einfachen Yukawa-Systemen. Master's Thesis, 2012.

- [15] M.E. Peskin, D. Schroeder. An introduction to Quantum Field Theory. Westview Press Inc (11 Sept. 1995)
- [16] M. Böhm, A. Denner, H. Joos. Gauge Theories of the Strong and Electroweak Interaction. Vieweg+Teubner Verlag, 2001
- [17] P. Kopietz, L. Bartosch, F. Schütz: Introduction to the Functional Renormalization Group. Springer-Verlag Berlin Heidelberg, 2010.
- [18] H. Gies. Introduction to the functional RG and applications to gauge theories. arXiv:hep-ph/0611146 (2006).
- [19] K. G. Wilson. Renormalization Group and Critical Phenomena. II. Phase-Space Cell Analysis of Critical Behavior. Phys. Rev. B 4, 3174 (1971); *ibid.*, 3184-3205, 1971.
- [20] K. G. Wilson, J. B. Kogut. The renormalization group and the  $\epsilon$ -expansion. Phys. Rept. 12:75-199, 1974.
- [21] J. Berges, N. Tetradis, and C. Wetterich. Nonperturbative renormalization flow in quantum field theory and statistical physics. Phys.Rept., 363:223-386, 2002. arXiv:hep-ph/0005122.
- [22] J.M. Pawłowski. Aspects of the Functional Renormalisation Group. Annals Phys.322:2831-2915, 2007. arXiv:hep-th/0512261
- [23] S. Weinberg. A model of leptons. Phys. Rev. Lett. 19: 1264-1266, 1967.
- [24] A. Salam. Weak and Electromagnetic Interactions. Conf.Proc. C680519: 367-377, 1968.
- [25] K. Holland, J. Kuti. How light can the Higgs be? Nucl. Phys. (Proc. Suppl.) 129 765, 2004 [hep-lat/0308020]
- [26] [HTTP://PDG.LBL.GOV](http://pdg.lbl.gov) (last access: 3. September 2015 14:06 CEST)
- [27] C. Ford, D.R.T. Jones, P.W. Stephenson, and M.B. Einhorn. The effective potential and the renormalization group. Nucl.Phys., B395:17-34, 1993. arXiv:hep-lat/9210033.
- [28] J.A. Casas, J.R. Espinosa, and M. Quiros. Improved Higgs mass stability bound in the standard model and implications for supersymmetry. Phys.Lett., B342:171-179, 1995. arXiv:hep-ph/9409458.
- [29] J.A. Casas, J.R. Espinosa, and M. Quiros. Standard model stability bounds for new physics within LHC reach. Phys.Lett., B382:374-382, 1996. arXiv:hep-ph/9603227.
- [30] G. P. Vacca, O. Zanusso. Asymptotic Safety in Einstein Gravity and Scalar-Fermion Matter. Phys.Rev.Lett.105:231601,2010. arXiv:1009.1735 [hep-th]
- [31] O. Zanusso *et al.* Gravitational corrections to Yukawa systems. Phys.Lett.B689:90-94,2010. arXiv:0904.0938 [hep-th]

- [32] J. M. Pawłowski, F. Rennecke. Higher order quark-mesonic scattering processes and the phase structure of QCD. Phys. Rev. D 90, 076002, 2014. arXiv:1403.1179 [hep-ph]
- [33] G.P. Vacca, L. Zambelli. Multi-meson Yukawa interactions at criticality Phys. Rev. D 91, 125003, 2015. arXiv:1503.09136 [hep-th]
- [34] D.F. Litim. Optimised Renormalisation Group Flows. Phys.Rev. D64 105007, 2001. arXiv:hep-th/0103195
- [35] D.F. Litim. Critical exponents from optimised renormalisation group flows. Nucl.Phys.B631:128-158, 2002. arXiv:hep-th/0203006
- [36] F. Höfling, C. Nowak, C. Wetterich. Phase transition and critical behaviour of the  $d=3$  Gross-Neveu model. Phys.Rev. B66 205111, 2002. arXiv:cond-mat/0203588v4
- [37] Z. Fodor *et al.* New Higgs physics from the lattice. PoSLAT2007:056,2007. arXiv:0710.3151 [hep-lat]
- [38] P. Gerhold and K. Jansen. Lower Higgs boson mass bounds from a chirally invariant lattice Higgs-Yukawa model with overlap fermions. JHEP 0907:025,2009. arXiv:0902.4135 [hep-lat]
- [39] P. Gerhold, K. Jansen, J. Kallarackal. Higgs boson mass bounds in the presence of a very heavy fourth quark generation. JHEP 1101:143,2011. arXiv:1011.1648 [hep-lat]
- [40] H. Gies *et al.* An asymptotic safety scenario for gauged chiral Higgs-Yukawa models. Eur.Phys.J. C73 (2013) 2652 arXiv:1306.6508 [hep-th]
- [41] A. Eichhorn *et al.* The Higgs Mass and the Scale of New Physics. JHEP April 2015, 2015:22. arXiv:1501.02812 [hep-ph]

# Selbstständigkeitserklärung

Hiermit erkläre ich an Eides statt, dass ich die vorliegende Arbeit eigenständig verfasst, keine anderen als die angegebenen Quellen und Hilfsmittel verwendet sowie Zitate und gedankliche Übernahmen kenntlich gemacht habe. Seitens des Verfassers bestehen keine Einwände, die vorliegende Masterarbeit für die öffentliche Nutzung in der Thüringer Universitäts- und Landesbibliothek zur Verfügung zu stellen.

---

Ort, Datum

Matthias Warschinke

# Danksagung

Zunächst möchte ich mich herzlich bei Professor Gies für die Betreuung dieser Arbeit bedanken und insbesondere auch für seine Unterstützung bezüglich meines Promotionsvorhabens. Weiterhin danke ich René Sondenheimer für die vielen aufschlussreichen Gespräche und interessanten Ausblicke auf das Themengebiet dieser Arbeit. Bei meinem Kommilitonen Andreas Schoepe bedanke ich mich nicht nur für das stundenlange gemeinsame Bearbeiten von Übungsserien, Protokollen und Problemstellungen aus diversen Vorlesungen und die gemeinsame Vorbereitung auf allerlei Testate, Vorträge und Klausuren, sondern auch ganz allgemein dafür, dass er das ganze Studium über eine große moralische Stütze war.

Meiner Schwester Maria Warschinke, meinen Großeltern Renate und Günter Dennstedt sowie Helga und Erhard Warschinke danke ich für die mahnenden Worte, das Studium hin und wieder auch mal Studium sein zu lassen.

Mein größter Dank gilt jedoch meinen Eltern Birgit und Mario Warschinke. Eure Unterstützung beschränkte sich bei weitem nicht nur auf das Finanzielle. Ich bin Euch dankbar für Eure Geduld mit mir, besonders in den nicht ganz so einfachen Phasen meines Studiums und für die Aufmunterungen in diesen Zeiten. Ohne Eure Rückendeckung wäre weder das Erstellen dieser Arbeit, noch das erfolgreiche Bestehen meines Studiums insgesamt möglich gewesen. Danke dafür!